In-Theatre Infrared Audio Broadcasting

by
Mohammad R. Paiam, B.Eng.

A thesis submitted to the
School of Graduate Studies and Research
in partial fulfilment of the requirements
for the degree of
Master of Applied Science

Ottawa-Carleton Institute for Electrical Engineering
Department of Electrical Engineering
Faculty of Engineering
University of Ottawa

September 1993

ISBN 0-315-89703-1

UNIVERSITÉ D'OTTAWA
UNIVERSITY OF OTTAWA

ABSTRACT

Several factors have to be analyzed before designing an appropriate communication system for in-theatre IR multi-channel audio broadcasting. The infrared channel characteristics for the in-theatre propagation environment are examined and a suitable IR transmission configuration is suggested. The free-space IR transmission has a simple channel model which simplifies the analysis. The CD digital audio technology which provides advanced digital signal processing techniques at a relatively low cost is a strong candidate for use in the system. However, the channel coding used in the CD system (known as EFM) has a high redundancy which results in a performance degradation. A more suitable channel coding scheme (which is a version of 8B10B channel modulation) is designed and simple implementations for the corresponding coder and decoder are given.

The receiver design for an indoor non-directional IR communication system requires an approach different from that commonly employed in optical fibre communications. A signal-to-noise ratio analysis is carried out and a simple strategy for the receiver design is proposed. A link power budget calculation is performed to find the required transmitted optical power. Also, it is shown analog FM requires much higher transmitted optical power to provide the performance achieved by the CD-based digital audio system in the in-theatre IR audio broadcasting. Finally, a simulation is carried out to investigate the effects of the multipath dispersion on the performance of the system.

Acknowledgements

I would like to express my gratitude to Dr. Peter Galko for his constant guidance throughout the work. I am particularly thankful to Dr. Gang Yun for his unselfish help through many valuable discussions. Also, I want to thank my family for their sacrifice and patience during my studies at the University of Ottawa.

Table of Contents

List of Figures

List of Tables

List of Abbreviations

8B10B - eight (data bits) to ten (channel bits) modulation

ADC - analog-to-digital converter

APD - avalanche photodiode

BER - bit error rate

BPF - band pass filter

CD - compact disc

CIRC - cross-interleaved Reed-Solomon code

DAC - digital-to-analog converter

DBC - directive beam configuration

DC - direct current

DEC_1 - first part of the CIRC error correction coding scheme

DEC_2 - second part of the CIRC error correction coding scheme

DIC - diffuse infrared configuration

DSV - digital sum value

EFM - eight (data bits) to fourteen (channel bits) modulation

FCC - Federal Communication Commission

FET - field-effect transistor

JFET - junction field-effect transistor

FM - frequency modulation

ID - integrate and dump filter

IR - infrared

LED - light emitting diode

LPF - low pass filter

NRZ - nonreturn-to-zero

NRZI - nonreturn-to-zero inverted

OOK - on-off keying

PCM - pulse code modulation

pin - positive-intrinsic-negative

RDS - running digital sum

RF - radio frequency

rms - root mean square

SMC - spot-diffusing multi-line-of-sight configuration

SNR - signal-to-noise ratio

$(SNR)_D$ - signal-to-noise ratio after the FM detector

$(SNR)_{opt}$ - optimum value of the SNR for a pin-based receiver in a free-space optical communication system (this SNR value is obtained when the photodetector area is at its optimum value)

List of Symbols

a - eye-height

A_0 - transimpedance preamplifier open-loop voltage gain

A_d - photodetector surface area

$A_{xx}(k)$ - discrete time-average autocovariance function

$\hat{A}_{xx}(k)$ - estimate of the discrete time-average autocovariance function

B_c - channel bit rate

B_d - data bit rate

B_T - the total bandwidth of four multiplexed FM signals

c - velocity of light (3×10^8 m/s)

c_d - photodetector capacitance per unit area

C_a - input capacitance of the preamplifier

C_d - photodetector capacitance

C_t - total input capacitance at the input of the receiver

d_m - the minimum distance in a linear block error correction coding scheme

D - deviation ratio in FM

E_b - received energy per data bit

f_{3dB} - the 3-dB bandwidth of the low-pass filter at the input of a transimpedance receiver

f_c - FET 1/f-noise corner frequency

f_{cut} - cut-off frequency of the optical channel of the CD system

f_d - data bit rate in the CD system

f_m - the highest fundamental frequency of a channel modulation scheme

g_m - FET transconductance

i_{bg} - the photocurrent due to the received background radiation

i_{fet} - input-referred noise current due to the FET channel noise

i_R - input-referred noise current due to the feedback resistor

i_s - the photocurrent due to the average received optical signal

i_{shot} - input-referred noise current due to shot noise

i_{tot} - total input-referred noise current

I_2 - noise bandwidth factor (0.564)

I_{bg} - received background irradiance (after optical filter)

I_s - average received optical signal irradiance (after optical filter)

k - Boltzmann's constant (1.38×10^{-23} J/K)

L_f - the loss due to optical filters

n - the number, describing the shape of the reflected radiation characteristics for a generalized Lambert law reflector

NA - numerical aperture of the objective lens in the CD player

N_0 - one-sided noise power spectral density

P_r - average received optical power

P_{rA} - average received optical power at a position close to the edge of the audience area of a theatre

P_{rO} - average received optical power at the centre of the dome-shaped screen in a theatre

P_t - average transmitted optical power

q - electron charge (1.602×10^{-19} C)

r_c - redundancy of the channel modulation

R - photodetector responsivity

R_c - code rate of an error correction coding scheme

R_f - feedback resistor of the transimpedance preamplifier

S_r - received electrical power of the FM signal

T - absolute temperature

T_c - channel bit period

T_d - data bit period

T_f - transmittance of the receiver optical filter (= 0.75)

T_{max} - maximum run-length for a channel modulation scheme

T_{min} - minimum run-length for a channel modulation scheme

v - the track velocity in the CD player

W - the bandwidth of the standard stereo audio signal (W = 53 KHz)

Z_{in} - input impedance of the transimpedance receiver

Γ - FET channel noise factor

η - photodetector quantum efficiency

θ_{fov} - field-of-view angle of the photodetector

θ_{hp} - the half-power angle of a Lambert-law reflection characteristics

λ - optical wavelength

μ - the modulation index for intensity modulation of an optical source

π - 3.14159

ρ - optical reflection coefficient

σ - linear information density of the compact disc (the number of data bits per unit length of the track)

τ_e - eye-width

Chapter 1

Introduction

Traditionally, wires and cables have been used to carry multiple audio signals to the audience in a theatre. The cost of maintaining and reconfiguring a wired network such as this could be high. To avoid these costs, there has been a recent interest in developing a wireless in-theatre audio broadcasting system. In this system, multiple high quality audio signals are to be transmitted inside a theatre by an appropriate free-space transmission means so that anybody in a theatre can receive the transmitted signal with a small, light, portable receiver. The intent of the audio system is as an augmentation of the existing audio system in the theatre in conjunction with a system to provide three dimensional images to the audience through projection of images on a dome-shaped screen. The three dimensional imagery is provided via a system where the audience wear special glasses whose lenses for the right and left eye are switched on and off in concert with images projected on the screen intended for the right and left eye. The audio receiving system is to be included in the glasses assembly.

A wide range of problems are involved in designing a communication system for

broadcasting multi-channel high quality audio signals in an indoor theatre environment. The issues which have to be dealt with are: the choice of the transmission medium (radio frequency or infrared), the modulation technique (digital or analog), interference with other communication systems, bandwidth and transmitted power requirements, distortions and multipath effects, multiplexing arrangements for the different audio signals, power consumption at the portable receiver, cost, size and availability of technology. It is particularly important for receivers to be of small size, low cost and low power consumption since they are battery-powered and produced in moderate volumes for use by the audience of a theatre. Transmitters, on the other hand, are much fewer compared with receivers (one transmitter per theatre) and their cost and power consumption are not as critical.

Among the above issues, the first two are the key ones and all others are basically dependent on the choices that we make for the transmission medium and the modulation technique. Infrared (IR) and Radio frequency (RF) are the two possible means of free-space transmission, each with its own advantages and drawbacks. Also, the audio signal can be modulated using analog methods like frequency modulation, or it can be digitized by pulse code modulation (PCM) and transmitted using digital modulation techniques. The merits and the weak points of these choices are examined in the following two sections.

1.1 Infrared vs Radio Frequency

For a free-space indoor communication system, infrared (IR) transmission has several advantages over radio frequency (RF) transmission. The most important one is

that IR has an extremely large available bandwidth, and is outside the frequency range that most regulatory agencies (e.g., the DOC, FCC, etc) control. For example, in the US, the FCC regulates all uses of the frequency range from 10 KHz to 300 GHz [1]. RF radiation is very penetrating and can cause interference with other RF systems used in the neighbouring areas, whereas infrared light does not penetrate walls and remains totally confined within the window-less indoor environment of a theatre. Systems employing RF may also suffer from interference generated by nearby electrical equipment, while systems based on IR transmission are immune to interference from such sources.

IR components are mostly relatively inexpensive, small and their power consumption is low. Highly efficient, low-cost, large-area silicon pin photodiodes and high-power GaAs-based laser diodes and LEDs are available within the wavelength range of 780 nm to 830 nm [2].

Figure 1.1 shows an IR transmission system with intensity modulation and direct detection which is by far the simplest optical transmission system. In this scheme, the light intensity (most specifically, the power) of the optical source (laser or LED) is modulated linearly with respect to the input electrical signal voltage. The transmitted

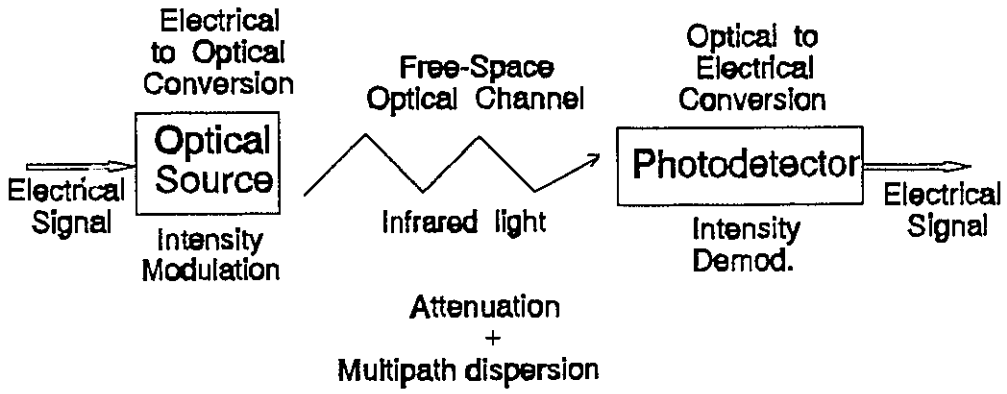

Figure 1.1 Optical intensity modulation with direct detection.

optical signal undergoes attenuation and multipath dispersion in the free-space optical channel. On the receiving side, the photodetector reconverts the optical signal into an electrical signal. The frequency and phase of the optical carrier has no effect on this system because a photodetector only responds to the changes in the power level (the intensity) of the received optical signal not its frequency or phase content; this results in a simple channel model for the IR transmission system with intensity modulation and direct detection [11]. We will look at this channel model in the next chapter.

Shadowing and eye safety are two potential problems associated with an indoor free-space infrared transmission system which have to be considered in the design of such a system. An IR link is susceptible to shadowing caused by objects positioned between the transmitter and receiver. Also, safety considerations impose limits on the IR transmitted power. These safety concerns apply mainly to laser diodes which have a narrow beam and their transmitted light can be easily focused by the human eye. LEDs are Lambertian sources and do not usually cause safety hazards. But, laser diodes have higher speeds and larger power capabilities compared with LEDs; this makes laser diodes the preferable optical sources for in-theatre infrared transmission where the transmitted power requirements is high. Safety can be improved by using a large-area lens in front of the transmitter to produce a wide angle beam. In the system which we will discuss in this thesis, the transmitted infrared is directed towards a number of spots located on the dome-shaped screen, and from there, it is diffusively reflected back towards the audience area. Fortunately, with this configuration, safety is not a major concern and the problem of shadowing is improved greatly by creating multiple paths between the transmitter and receiver. Considering all the advantages of IR transmission as discussed above, we choose IR system with intensity modulation and direct detection for the in-theatre audio

broadcasting.

1.2 Digital vs Analog

Having chosen infrared as the medium of transmission based on the above considerations, we can now look for a suitable modulation technique capable of handling multiple high quality stereo audio signals. The members of an audience in a theatre expect to hear high quality audio signals. Two well-known modulation techniques which can deliver audio signals with high fidelity are pulse code modulation (PCM) and stereo FM.

PCM is a digital scheme for the transmission of analog signals in which the analog signal is first sampled and then each sample is quantized and represented by a number of binary digits. Quantization can be uniform or non-uniform. The resolution of the system is determined by the number of bits used to represent each sample and the quantization method. For example, the compact disc system employs uniform quantization with 16-bit resolution. The PCM data from several digital audio sources can be simply time-division multiplexed and transmitted using nonreturn-to-zero (NRZ) on-off keying (OOK). For NRZ OOK, the optical source (laser or LED) is turned on to transmit a "1" or turned off to transmit a "0". This two level transmission is simple and is not affected by any non-linearity in the optical source. Another feature of digital audio is that we can use advanced error correction coding schemes to overcome the degradations imposed on the transmitted signal in the channel and, therefore, improve the performance and decrease the transmitted power requirements of the system.

Frequency modulation which is an analog method has been used in commercial

FM radio broadcasting for years and it has a well-developed technology. Frequency-division multiplexing could be used to transmit several audio signals. One possible approach to achieve this is via the optical multisubcarrier modulation scheme shown in Fig. 1.2. Each stereo source is frequency modulated on a separate carrier and all FM signals are combined using frequency-division multiplexing. Then the resultant signal is used to intensity modulate the optical source. On the receiving side, the optical detector converts the received optical power variations into the electrical signal. The desired FM signal is selected by an adjustable band-pass filter and demodulated to recover the stereo signal. This multisubcarrier system will be adversely affected by any nonlinearity in the optical channel. The distortions due to the nonlinearity have been considered in [31], [33]. Here, we just say that a nonlinear device will create frequency components in the output signal which were not present in the input signal and this results in two important nonlinear effects known as harmonic and intermodulation distortions. Fortunately, the effects of nonlinearity on FM are not as severe as those on amplitude modulation. Also,

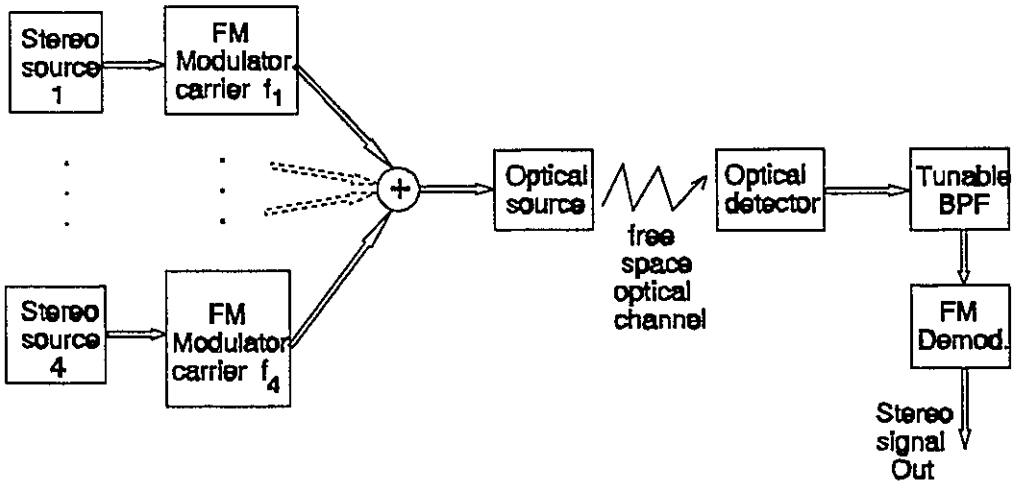

Figure 1.2 Optical multisubcarrier modulation of FM signals using a single optical source.

several compensation schemes for linearization of optical sources in analog communication systems have been reported [13]-[16]; one of the most successful techniques is the quasi-feedforward method, with which a 30 to 40 dB reduction in total harmonic distortion has been achieved [13]. Furthermore, as shown in Fig. 1.3, the problem of the optical source nonlinearity can be easily reduced to a considerable extent by using multiple optical sources, each modulated by only one FM signal; in this way the cross-talk between different FM signals is avoided. In fact, multiple optical sources will likely be required to meet the high transmitted power requirements.

Multisubcarrier modulation has another drawback in its inherent power penalty when compared to baseband OOK. An FM single-subcarrier modulation suffers a 3 dB electrical power penalty compared to baseband OOK and the power penalty gets larger as the number of subcarriers increases. This penalty is due to the difference of the peak-

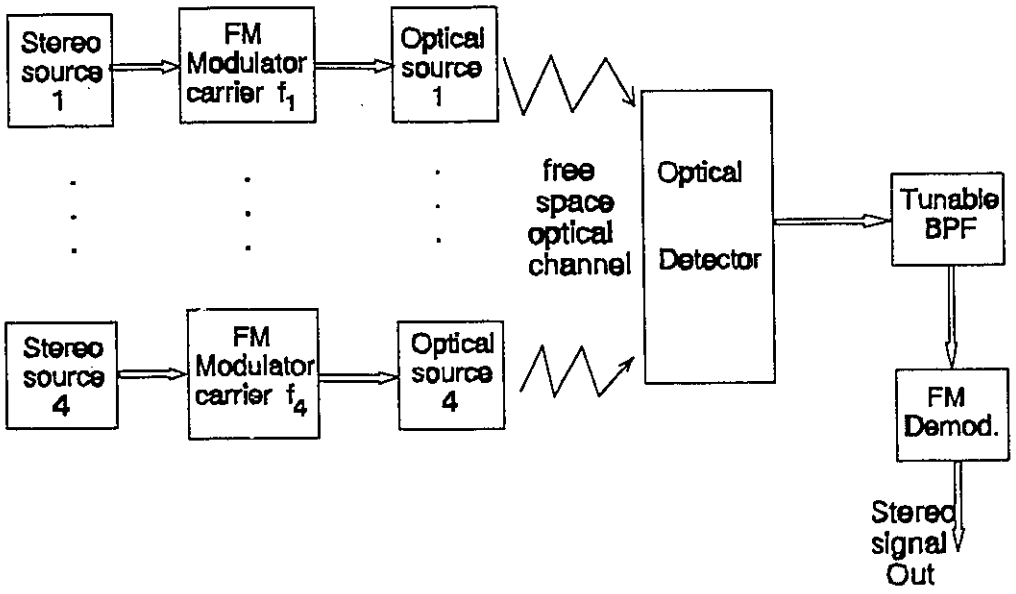

Figure 1.3 Optical multisubcarrier modulation of FM signals using multiple optical sources.

to-rms ratios between the two systems. The peak-to-rms ratio for the NRZ signal is equal to 1 while it is equal to $\sqrt{2}$ for an FM single-subcarrier modulation. To explain this, consider an optical source operating at some bias point. Then the average and the peak transmitted optical power for transmission of an NRZ OOK signal would be the same as those for transmission of an FM signal, while at the receiver side after removing the electrical DC bias, both NRZ and FM signals have the same peak amplitude and the electrical power of the NRZ signal is obviously 3 dB higher than that of the FM signal.

In defence of frequency modulation, it must be said that, first, FM transmission requires a lower bandwidth than comparable digital ones (which do not use data compression techniques). Second, FM components may be cheaper than their digital counterparts. But, with every new generation of more highly integrated and, consequently, lower cost digital components, this factor becomes less important. Moreover, the mass production of compact disc (CD) player has helped to lower the price of digital audio technology. The quality of the commercial stereo FM broadcasting may not satisfy the most demanding listeners' criteria in terms of dynamic range and signal-to-noise ratio. This has been the driving force behind the introduction of digital audio and the CD technology. The signal-to-noise ratio and the dynamic range provided by the CD system are both more than 90 dB which satisfies even the most sensitive listeners. We are, of course, not bounded by the performance characteristics of the commercial stereo FM broadcasting and we can certainly have FM systems which deliver an audio signal with a quality comparable to that of the CD system. The two systems have to be compared on the basis of the bandwidth and power requirements for a given delivered audio quality. Such a comparison shall be carried out in Chapter 4.

As the digital audio system is much more complex than an analog FM system,

there is much more to consider for these systems and thus most of this thesis will concern multi-channel in-theatre digital audio broadcasting. Another point to mention is that we have deliberately shown four stereo sources in Figures 1.2 and 1.3 as it is likely that only four audio signals are used in a multi-channel in-theatre broadcasting. In the rest of this thesis we have considered the same number (four) of audio signals; this does not affect the generality of our work except that, of course, the bandwidth and power requirements derived in our analysis will change if a different number of audio sources are considered.

1.3 Thesis Objectives

As becomes evident from the above discussion, several factors have to be analyzed before an appropriate communication system for in-theatre infrared digital audio broadcasting is designed. To begin with, the IR channel characteristics for the in-theatre propagation environment have to be investigated and a suitable IR transmission configuration suggested to provide a suitable basic channel. While keeping the strong features of the CD system, some of its aspects have to be modified to adapt well into the in-theatre IR transmission system. The channel modulation used in the CD system has been particularly designed to perform well in the CD channel. This modulation known as EFM (eight-to-fourteen "modulation") has a high redundancy (the ratio of channel bit rate to data bit rate). We will show in Chapter 4 that this high redundancy results in a performance degradation of EFM in terms of power and bandwidth requirements when compared with other possibilities. A suitable low-redundant channel modulation scheme has to be found for in-theatre IR transmission. The spectral shaping provided by the new channel modulation should be comparable to that of EFM. In particular, the low

frequency components of the transmitted signal have to be well-suppressed, so that by using an electrical high-pass filter, we can remove most of the noise due to the background radiation which is concentrated at the low frequency region.

The noise sources in the system have to be examined and a suitable receiver design has to be carried out so that the signal-to-noise ratio is maximized. A link power budget analysis has to be performed and the required power and bandwidth be found; a comparison between digital audio scheme and analog FM has to be made. Finally, the effects of multipath dispersion on the performance of the system have to be studied. In summary the objectives of this thesis are:

(i) to find the in-theatre IR channel model and to arrive at a suitable IR transmission configuration;

(ii) to adapt the CD system into the in-theatre IR transmission by finding an appropriate channel modulation technique;

(iii) to examine the noise sources in the system and carry out a performance evaluation of the overall system; and

(iv) to find out how the performance of the system is affected by the multipath dispersion.

1.4 Thesis Organization

The remainder of this thesis is organized in four chapters.

In Chapter 2, we look at different possible IR transmission configurations and suggest a suitable configuration for the in-theatre IR audio broadcasting system. The physical and optical characteristics of the dome-shaped screen are considered. The IR channel model is derived and some actual in-theatre IR propagation measurements are discussed.

In Chapter 3, the CD digital audio system is discussed and its different constituent parts are explained. Some modifications which improve the performance of the CD digital audio, when used in the in-theatre IR audio broadcasting system, are suggested. A suitable channel modulation scheme is proposed and its characteristics is compared with the channel modulation technique used in the CD system.

We carry out a performance evaluation of the overall system in Chapter 4. Noise sources in the in-theatre environment are discussed. After performing a signal-to-noise ratio analysis, a simple strategy for designing the receiver is obtained. The parameters of the design are optimized in the sense of maximizing the received signal-to-noise ratio. The required transmitted optical power for a given bit error rate in the in-theatre audio broadcasting system is computed. With respect to power requirements, a comparison is made between the CD-based digital system and the analog FM. Finally, a simulation is performed to examine the effects of the multipath dispersion on the performance of the system.

Chapter 5 contains a brief review of all material presented and summarizes the results.

Chapter 2

In-Theatre Infrared Transmission

No previous work on an indoor IR audio broadcasting system has been reported in the available literature. However, various aspects of a free-space IR transmission system for establishing a wireless access to a local-area network have been covered in [1]-[12]. Different IR transmission configurations, appropriate for varied applications, have been examined [1], [3], [7], [8], [9], [12]. The feasibility of an indoor IR link at high bit rates up to 100 Mb/s using diffusively propagating radiation has been studied [2], [4], [5]. Also, issues such as background radiation, optical filtering, sources of noise, receiver design and other related subjects have been investigated. All of these works have considered a two-way communication link between the network and a number of fixed or mobile terminals. But, most of them have concentrated on the high-speed downlink since it presents a much greater technical challenge than the low-speed uplink. This makes a similarity between some of these works and the indoor IR audio broadcasting system which is, of course, a one-way link.

In an indoor environment, infrared transmission has many advantages over RF

transmission. To fully exploit all these advantages, we have to know the IR propagation characteristics. Infrared light is close in wavelength to visible light and behaves similarly in many respects; IR light passes through most transparent materials, is absorbed by dark objects, is diffusively scattered from rough surfaces and is directionally reflected by mirrors and shiny objects. However, there are optical filters which block visible light and allow only infrared light to pass through, or vice versa. These filters need to be used in our system to minimize the visible part of the background radiation which can sometimes have high frequency components (especially from fluorescent lighting fixtures).

Also, a channel model for the in-theatre IR transmission has to be found. The channel model depends on how the infrared light is transmitted in a theatre. So, first, we have to find a suitable in-theatre IR transmission configuration.

2.1 IR Transmission Configuration

Before discussing the different possible IR transmission configurations, we have to remind ourselves of some of the required physical characteristics of the portable receiver which is going to be used in our in-theatre audio broadcasting system. The receiver components, including the photodetector, are going to be mounted on special glasses which the audience are going to wear and, therefore, the receiver has to be small and light. The angular direction of the photodetector is not fixed and it varies as the members of the audience turn their heads while looking from one place to another. Light concentrators like lenses are bulky and heavy compared with photodetectors, and as we will see in Chapter 4, the required area of the photodetector will be relatively large. This precludes the use of a lens in the receiver.

There are, basically, two possible configurations for an indoor infrared transmission system. They are known as the diffuse infrared configuration (DIC) and the directive beam configuration (DBC). Consider a room, in which, we want to establish an IR link. In the DIC shown in Fig 2.1a, the infrared light is uniformly transmitted in all directions and is diffusively reflected back from the internal surfaces (i.e., the ceiling and the walls) of the room, and is received by a portable photodetector with a wide field-of-view angle (θ_{fov}). Any radiation arriving at an angle greater than θ_{fov} will not be received by the photodetector. With this configuration, the received optical power is almost independent of the position and the angular orientation of the photodetector [1], and no alignment between the photodetector and the transmitter are required. The DIC, however, is power inefficient and suffers from multipath effects. Under the DBC scheme shown in Fig. 2.1b, the optical transmitter sends a narrow IR beam directly towards the receiver; the photodetector has a narrow field-of-view angle and must be aligned with the optical source. The DBC employs a directional transmission and, therefore, it has a higher gain, resulting in higher obtainable data transmission rates and lower power requirements. But, the single path (which is the line-of-sight path) between the transmitter and the receiver can be easily obstructed. More importantly, the DBC is only suitable when receivers can be fixed in both position and angular orientation. This feature of DBC makes it unfit for use in the in-theatre audio broadcasting system where the receiver is frequently changing directions. Only the DIC is suitable for applications where the receiver is mobile and changes its direction continually.

A third IR transmission configuration, which is a compromise between the DIC and the DBC, has been proposed [12]; this is known as spot-diffusing multi-line-of-sight configuration (SMC). In the SMC method, the optical transmitter directs a collimated or

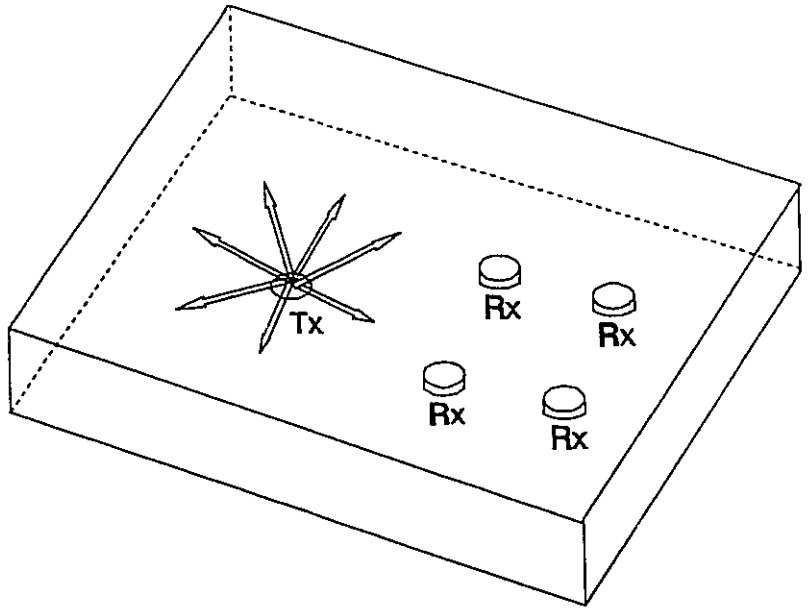

(a)

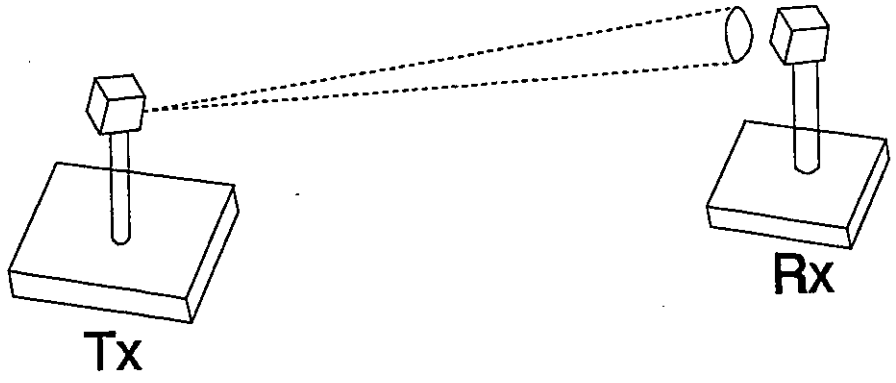

(b)

Figure 2.1 *IR transmission configurations; (a) the DIC, (b) the DBC. The field-of-view of the receiver (Rx) in the DIC is wide, while it is narrow in the DBC.*

slightly diverted IR beam to a small surface area on the ceiling or the walls. The small area illuminated by the IR beam is called a diffusing spot, and the IR light is diffusively reflected back from the diffusing spot to cover all the receivers placed in a room. The size of a diffusing spot is much less than the dimensions of the room (or the theatre in our system). By creating multiple diffusing spots, multiple paths between the transmitter and receiver are produced, and this reduces the chances of all the paths being, simultaneously, obstructed by shadowing. We will show in the next section that if only one diffusing spot is created on the dome-shaped screen of the theatre, then, it is possible that some members of audience, while looking at certain directions, will not see the spot and will not receive any optical signal. So a number of diffusing spots have to be, carefully, positioned on the dome to cover all the blind angles. The multipath distortion in this case will not be as severe as that in the DIC because there are an infinite number of paths between the transmitter and the receiver in the DIC. Also, the optical part of the transmitter is simpler for the SMC compared with that of the DIC; for example, a laser with a small lens (or no lens at all) can be used to create a diffusing spot, whereas, illuminating the whole dome, as in the DIC, would require a more complex optical set-up at the transmitter.

The SMC was originally proposed for use in indoor wireless connection of computer terminals to a local area network. In that application, each photodetector has a narrow field-of-view (θ_{fov}) and a fixed angular orientation; therefore, lenses can be utilized to enhance the received optical power, and this results in relatively high gain for the SMC compared with DIC [12]. But that advantage is not applicable to our system where the photodiode is changing direction frequently and lenses cannot be used.

Based on the above discussions, the IR transmission configuration that we choose

for the in-theatre audio broadcasting system, is that a number of diffusing spots are created on the dome; the IR light is diffusively reflected back from these spots towards the audience who are watching the movie projected on the dome. We, now, find an expression for the average received optical power by the photodetector of the receiver. Consider the case, where there is only a single diffusing spot on the dome, and assume that the reflectivity of the screen of the dome can be modelled with a generalized Lambert law. The power radiated from the diffusing spot into a solid angle $d\Omega$, positioned at an angle x from the normal to the diffusing spot, is then given by

$$dP_r = \rho P_t \frac{n+1}{2\pi} \cos^n x \, d\Omega \ , \qquad (2.1)$$

where P_t is the average transmitted optical power by the optical source, ρ is the reflection coefficient of the screen of the dome (the ratio of the diffusively reflected power to the incident power), and n is the number describing the shape of the radiation characteristics. We explain more about n in the next section. To determine the received optical power, consider the geometry of the situation as described by Fig. 2.2, where

r = the distance between the diffusing spot and the photodetector,
A_d = the surface area of the photodetector,
A_s = the surface area of the diffusing spot,
y = the angle between the normal to the photodetector and the line connecting the photodetector to the diffusing spot, and
x = the angle between the normal to the diffusing spot and the line connecting the photodetector to the diffusing spot (as before).

Assuming that r^2 is much greater than both A_d and A_s, the solid angle subtended by the photodiode from the diffusing spot will be

$$d\Omega = \frac{A_d \cos y}{r^2} \ . \qquad (2.2)$$

Assuming that the secondary reflections from the dome are insignificant, and ignoring any

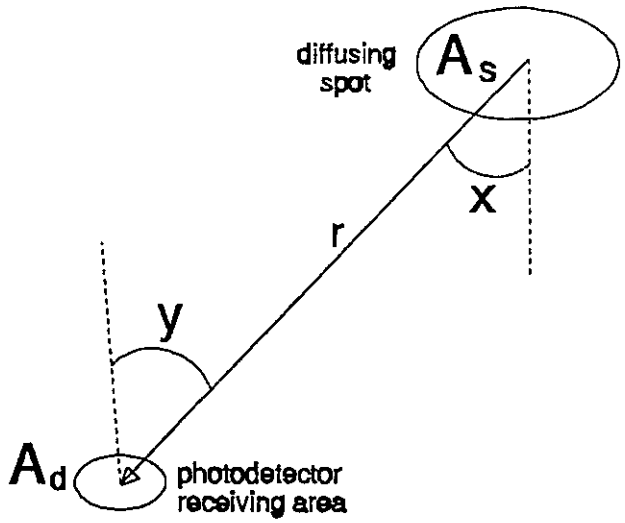

Figure 2.2 The geometry of an IR transmission configuration with a single diffusing spot.

reflections[1] from the audience area for the present time, the average received power by the photodetector is obtained by combining (2.1) and (2.2) to give

$$P_r = \begin{cases} \rho A_d P_t \frac{n+1}{2\pi r^2} \cos^n x \cos y , & \text{if } |y| \le \theta_{fov} ; \\ 0 , & \text{otherwise} . \end{cases} \qquad (2.3)$$

In our system, we assume that the θ_{fov} of the photodetector is 90 degrees and, therefore, the received power will be zero if $y \ge 90°$. The losses due to the optical filters have not been included in the expression given by (2.3); these losses are constant and can be easily taken into account by a penalty factor in the link power budget calculations.

Equation (2.3) can be easily extended to the case of multiple diffusing spots. For k diffusing spots, and assuming that the transmitted power is divided, equally, between different spots, the received power is given by

[1]In reality, there might be some weak reflections from the audience area.

$$P_r = \frac{P_t}{k}\rho A_d \frac{n+1}{2\pi}\sum_{\substack{i=1 \\ y_i<90}}^{k}\left(\frac{\cos^n x_i \cos y_i}{r_i^2}\right), \qquad (2.4)$$

where r_i, x_i and y_i are the r, x, y quantities above for the ith spot. Note that, only positive terms have to be included in (2.4) and the negative terms with $y_i > 90°$ are not included in the sum in (2.4). The received power, in this case, will be zero only if all y_i (i=1,...,k) are, simultaneously, greater than 90°; the probability of this happening will diminish as the number of spots increases. However, the higher the number of spots, the worse will be the multipath dispersion, so a compromise has to be made. The number and the location of the diffusing spots on the dome have to be, carefully, chosen for each particular theatre. This choice depends, mainly, on the physical and optical characteristics of the theatre and the dome, the position of the dome with respect to the audience area, the data rate and the effect of the multipath dispersion on the performance of the system.

2.2 Characteristics of the Dome-Shaped Screen

In a theatre, as was explained before, a movie is projected on a dome-shaped screen which is placed above and to the front of the audience area. This dome plays a major role in the in-theatre IR transmission because the diffusing spots are formed on this dome. To be able to perform a link power budget calculation, we need to know the size of the dome and the optical characteristics of the screen.

The reflectivity of the screen is modelled with a generalized Lambert law as given previously by (2.1) where n describes the shape of the radiation characteristics. The angular spread of the reflected beam is indicated by the half-power angle, θ_{hp}, at which

the intensity decreases to half of its maximum value, and is given by

$$\theta_{hp} = \arccos(0.5^{1/n}) \ . \tag{2.5}$$

So, by finding the half-power angle, we can obtain n.

As far as the optical reflectivity is concerned, two types of screens are presently used; they can be described as high gain and low gain. The high gain screen has a larger reflection coefficient and a narrower angular spread. Table 2.1 shows the corresponding values of n, the half-power angle, and the reflection coefficient, ρ. These numbers are based on the measurements[2] made on these screens. The diffuse reflection polar diagram of the two screens are shown in Fig. 2.3.

The number of the diffusing spots and their location on the dome is important, as well. Consider a 160 degrees dome used by the IMAX company. This dome has a radius of 12 meters. The audience area lies along the base plane of an imaginary hemisphere containing the dome; a cross section of the dome is shown in Fig. 2.4a,b. The centre of the dome (or the centre of the imaginary hemisphere) is point O, and the audience area is along the line AA`. In Fig. 2.4a, only one diffusing spot has been formed at point C, while in Fig. 2.4b, two diffusing spots have been placed, symmetrically and 90° apart, at points D and E. In Fig. 2.4a, consider a photodetector positioned at point O and looking towards the diffusing spot at point C (OC = 12 m). The received power by the photodetector, using (2.3), is given by

$$P_{rO} = \rho A_d P_t \frac{n+1}{2\pi(12)^2} \cos^n x_O \cos y_O \ , \tag{2.6}$$

---

[2]These measurements were made by Dr. Gang Yun who is, presently, a research associate at the Department of Electrical Engineering, University of Ottawa.

Table 2.1 The optical characteristics of the two reflecting screens.

	θ_{hp}	n	ρ
Low Gain	45°	1	0.4
High Gain	19.3°	12	0.8

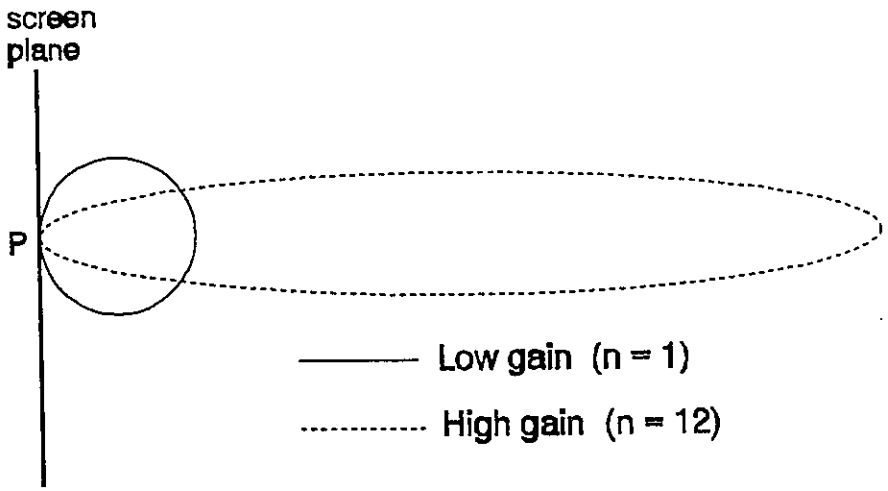

***Figure 2.3** Diffuse reflection polar diagram of the two types of screens. The value of the gain is the radial distance away from point P.*

where $x_O = y_O = 0°$. Note that P_{rO} is a special case of P_r. Assuming a low gain screen, and substituting for $n = 1$, $\rho = 0.4$, x_O and y_O in (2.6), a simplified expression for P_{rO} will be obtained which is

$$P_{rO} = \frac{0.4 A_d P_t}{144\pi}. \qquad (2.7)$$

We use P_{rO}, given by (2.7), as a reference and we compare the received power in other situations with this particular case.

Now consider a photodetector placed at point A where OA = 9 m. We want to

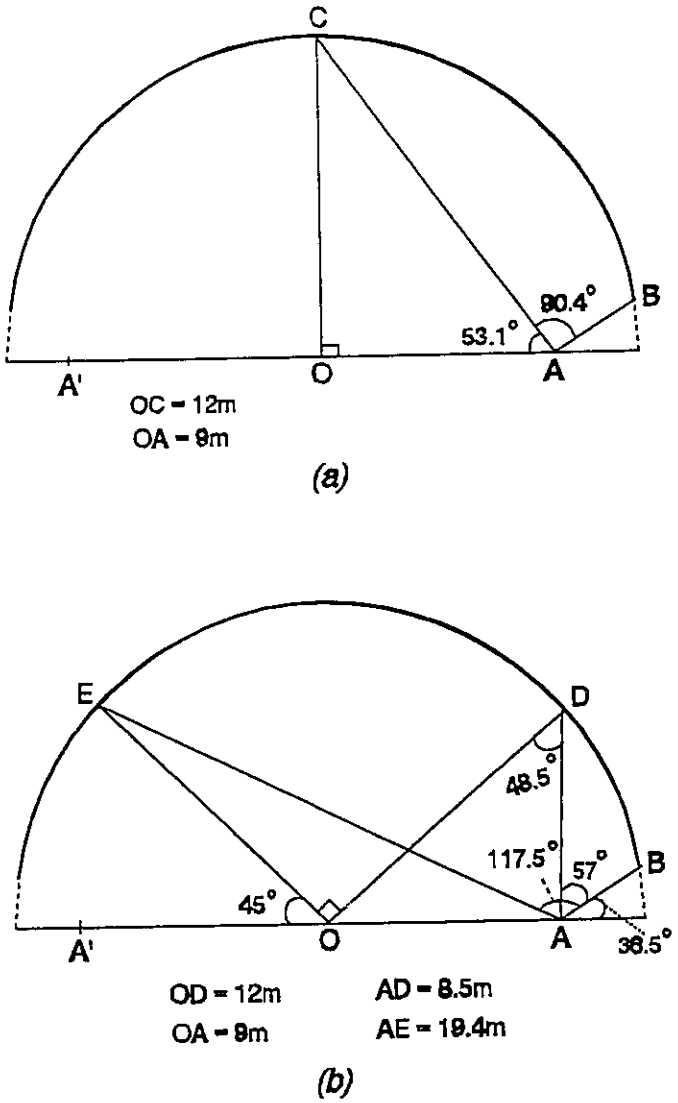

Figure 2.4 160° dome with a diameter of 12 m (a) only one diffusing spot at point C (b) two spots placed 90° apart at points D and E.

evaluate the power received by this photodetector when it is looking at the nearest edge of the dome which is point B. In the one-spot case (Fig. 2.4a), the angle between the normal to the photodetector (line AB) and the line connecting the spot to the photodetector (line AC) is found using simple geometry; this angle is equal to 90.4°

which is greater than 90°. So, the photodetector does not see the spot and the received optical signal will be zero. In the two-spot case (Fig. 2.4b), however, that photodetector with the same angular direction is able to see one of the spots (point D) and the received signal will certainly not be zero. The received optical power in this case is given by (2.4) with $k = 2$. But, since the photodetector cannot see the spot E, the term corresponding to that spot is ignored and the received power can be written as

$$P_{rA} = \frac{P_t}{2}\rho A_d \frac{n+1}{2\pi(AD)^2}\cos^n x_D \cos y_D \ , \tag{2.8}$$

where AD = 8.5 m, $x_D = 48.5°$ and $y_D = 57°$. Substituting for AD, x_D and y_D in (2.8), we obtain

$$P_{rA} = (1.885\times10^{-3})\rho A_d P_t \frac{n+1}{\pi}\cos^n(48.5°) \ . \tag{2.9}$$

Let us, compare P_{rA} with the reference case, p_{rO}, given by (2.7). Their ratio is

$$\frac{P_{rA}}{P_{rO}} = (0.271)(n+1)\cos^n(48.5°) \ . \tag{2.10}$$

Equation (2.10) shows that P_{rA}/P_{rO} depends on n, i.e., it depends on whether the screen is high gain or low gain. Substituting for the two values of n from Table 2.1 in (2.10), numerical values for P_{rA}/P_{rO} are obtained which are shown in Table 2.2. We repeated the above analysis for the case where the two spots are 120° apart; the results of this case are shown in Table 2.2, as well.

A comparison of these numerical values shows that P_{rA} is much smaller for the high gain screen compared with that of the low gain one. Consequently, for the high gain screen, a higher number of spots, which have to be placed further apart, are required to

Table 2.2 Numerical values (in dB) of P_{rA}/P_{r0} for two different angles of separation between the two spots.

	90°	120°
Low Gain	-4.4	-0.05
High Gain	-16	-10.1

increase the power received by the receivers which are close to the edge of the audience area. Also, these results indicate that P_{rA} has improved for the second case, compared with the first case where the spots are separated by 90°. But, we know that, the multipath distortion becomes more severe as the spots move further away; so, the distance between the spots cannot be increased without considering the degradations imposed on the system performance by the multipath effects.

The above examples were given to show the impact of the different numbers of spots and their locations on the received optical power. The optimum number of spots and their best positions depend on the particular characteristics of the dome, the audience area and the effects of multipath dispersion on the performance of the system. That optimization has to be made separately for each theatre and we do not intend to do it in this thesis.

These examples, also, show us the large variations of the received optical power for photodetectors placed at different positions and having different angular directions. This is a characteristic of the IR transmission that the received power is dependent on the direction of the photodetector. But, in RF applications, the received power will be relatively insensitive to direction if an omnidirectional antenna is used. The sensitivity of the received optical power to angular direction can be reduced if multiple (i.e., two or

three) photodetectors are used in the receiver. These photodetectors are installed in the receiver so that, they face different directions. Then, the received signal is derived by applying an appropriate combining technique on the output signals of the individual photodetectors. The price that we have to pay for employing multiple photodetectors, is that the receiver becomes more complex, bulkier and heavier.

2.3 IR Channel Model

The wavelength of infrared light is approximately 800 nm, and the surface area of a typical photodetector used in an indoor wireless IR communication system may be around 1 cm^2 which is several orders of magnitude greater than the IR wavelength. This is in contrast with RF applications where the antenna size is smaller than or comparable with the carrier wavelength. In this section, we show that the fact that the photodetector area is much greater than IR wavelength, results in a simple baseband channel model for the IR transmission.

To derive the channel model for the indoor IR transmission, we follow a routine similar to what is given in [11]. Note that the intensity of the optical source is modulated around a bias point and at the receiving side an electrical high-pass filter is used to remove the DC bias term. Let the normalized electrical message signal be denoted by $u(t)$, where $|u(t)| \leq 1$. After adding the appropriate DC bias to $u(t)$, the positive signal, $B[1 + \mu u(t)]$, is used to modulate the light intensity of the optical source, where B is a constant and μ is the modulation index, $0 < \mu < 1$. The transmitted optical power is proportional to $B[1 + \mu u(t)]$, and the complex field of the transmitted optical signal can be characterized by the signal

$$F_t(t) = \sqrt{A[1 + \mu u(t)]}\, e^{j\omega_o t} \quad , \tag{2.11}$$

where A is a constant, $\omega_o = 2\pi f_o$ and f_o is the frequency of the IR light, $f_o = 3\times10^{14}$ Hz.

Since the surface area of the photodetector is much greater than the IR wavelength, the received optical field varies with position on the surface of the photodetector. Assume that due to multiple diffusing spots or because of the reflections from the audience area, there are effectively N distinct paths between the transmitter and the receiver. Consider an arbitrary position with coordinates (x,y) on the surface of the photodetector; at this position, the complex field of the received signal from the component arriving on path k (k = 1,...,N), can be expressed as

$$F_k(t;x,y) = \sqrt{\alpha_k A[1 + \mu u(t - t_{k;x,y})]}\, e^{[j\omega_o(t - t_{k;x,y}) + \gamma_k]} \quad , \tag{2.12}$$

where $t_{k;x,y}$ is the time delay, α_k is the attenuation factor and γ_k represents the phase shift of the optical carrier at the reflection point on the k-th path. The attenuation factor, α_k, is assumed to be independent of the position coordinates (x,y) because its variations with position on the photodetector surface area are negligibly small. Also, assume that α_k includes all the losses in the transmission path such as the inverse square distance-dependent path loss, the reflection loss and the loss due to the optical filters. The complex field of the total received signal is

$$F_r(t;x,y) = \sum_{k=1}^{N} F_k(t;x,y) \quad . \tag{2.13}$$

The intensity of the received signal, $I_r(t;x,y)$, is just the magnitude-squared of $F_r(t;x,y)$,

$$I_r(t;x,y) = |F_r(t;x,y)|^2 \quad . \tag{2.14}$$

Combining (2.12), (2.13) and (2.14), we find that

$$I_r(t;x,y) = \sum_{k=1}^{N}\sum_{i=1}^{N} \beta_{ki}(t;x,y)\, e^{j\theta_{ki;x,y}} \ , \tag{2.15}$$

where

$$\beta_{ki}(t;x,y) = A\sqrt{\alpha_k \alpha_i [1+\mu u(t-t_{k;x,y})][1+\mu u(t-t_{i;x,y})]} \tag{2.16}$$

and

$$\theta_{ki;x,y} = \omega_o(t_{k;x,y} - t_{i;x,y}) + \gamma_i - \gamma_k \ . \tag{2.17}$$

Observing that, $\theta_{ki;x,y} = 0$ when $k = i$, we divide the N^2 terms of (2.15) into N terms with $k = i$ and $N(N - 1)$ terms with $k \neq i$;

$$I_r(t;x,y) = A\sum_{k=1}^{N} \alpha_k [1+\mu u(t-t_{k;x,y})] + \sum_{\substack{k=1 \\ k\neq i}}^{N}\sum_{i=1}^{N} \beta_{ki}(t;x,y)\, e^{j\theta_{ki;x,y}} \ . \tag{2.18}$$

The quantity $I_r(t;x,y)$, is the intensity of the received optical signal at only one point on the photodetector surface; it has to be integrated over the entire surface area of the photodetector to give the total received optical power, $P_r(t)$:

$$\begin{aligned} P_r(t) &= \int\int_{A_d} I_r(t;x,y)\, dx\, dy \\ &= A_d A \sum_{k=1}^{N} \alpha_k [1+\mu u(t-t_k)] \ + \ \sum_{\substack{k=1 \\ k\neq i}}^{N}\sum_{i=1}^{N} \beta_{ki}(t) \int\int_{A_d} e^{j\theta_{ki;x,y}}\, dx\, dy \ , \end{aligned} \tag{2.19}$$

where A_d is the surface area of the photodetector. The time delay, $t_{k;x,y}$, varies by a very small amount as the position (x,y) changes; so, the first term of (2.18) can be taken as a constant (i.e., it is independent of the position). However, $\theta_{ki;x,y}$ varies by large amounts with the change in position on the photodetector surface area; to show this, we rewrite (2.17) in an alternative form,

$$\theta_{ki;x,y} = 2\pi \frac{c(t_{k;x,y} - t_{i;x,y})}{\lambda} + \gamma_i - \gamma_k \ , \tag{2.20}$$

where c is the velocity of light and λ is the wavelength of the optical carrier. Equation (2.20) indicates that, $\theta_{ki;x,y}$ varies by 2π when the excess path length, $c(t_{k;x,y} - t_{i;x,y})$, changes by one wavelength ($\approx$ 800 nm). Since the area of the photodetector is much greater than the optical wavelength, the excess path length would change by several thousands of wavelengths from one edge of the photodetector to the other. So, we can, safely, assume that for all k, i ($k \neq i$), the integral in the second term of (2.19) would become an insignificant quantity, i.e.,

$$\iint_{A_d} e^{j\theta_{ki;x,y}} dx\,dy = 0 \ . \tag{2.21}$$

Using (2.21), we can neglect the second term of (2.19). Now, $P_r(t)$ can be written as

$$P_r(t) = A_d A \sum_{k=1}^{N} \alpha_k [1 + \mu u(t - t_k)] \ . \tag{2.22}$$

The electrical signal, $y(t)$, produced by the photodetector is directly proportional to $P_r(t)$. Ignoring the constant of proportionality and removing the DC term, $y(t)$ will be

$$y(t) = \sum_{k=1}^{N} a_k u(t - t_k), \tag{2.23}$$

where $a_k \propto A_d A \alpha_k \mu$ is a constant for each path. Equation (2.23) shows that the IR transmission channel can be simply replaced by an equivalent baseband transmission channel as shown in Fig. 2.5. An obvious consequence of this channel model is that the destructive (or constructive) additions of the multipath components, for the IR transmission, appear to occur at the baseband level. This is in contrast with the RF channel where the cancellations occur at the carrier frequency.

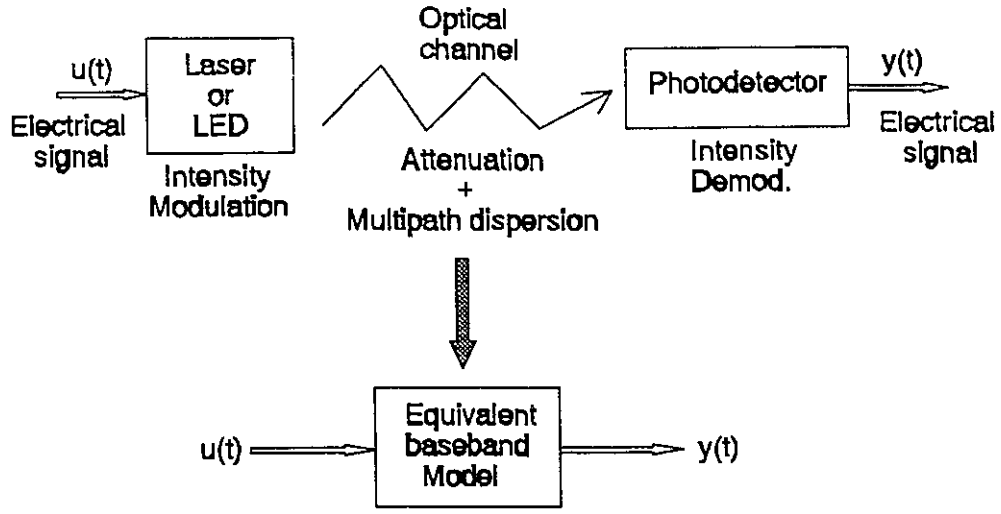

Figure 2.5 Free-space IR transmission with optical intensity modulation and its linear channel model.

2.4 In-Theatre IR Propagation Measurements

In this section, we, briefly, refer to the IR propagation measurements[3] which were performed at the Cineplus Theatre in Hull using the dome screen there. The measurements were made on a low gain screen with the optical characteristics as described before, and the IR transmission configuration employed, was the case of a single diffusing-spot as previously shown in Fig. 2.4a. The diffusing-spot was placed at point C and the optical transmitter was at point O. The frequency response of the IR channel was measured up to 30 MHz. The measurements were made at two different positions (close to point O and, also, at the edge of the audience area), and for several angular orientations of the photodetector at each position. All the measurements showed

[3]Refer to the footnote at page 20.

that the IR channel has approximately a flat response, at least, up to 30 MHz. As expected, they revealed that the received optical power changes with angular direction of the photodetector. Also, two different sizes of diffusing spots were used (one with a diameter of a few centimetres and the other with a diameter of a few metres), and no significant change in the channel response were observed for the two cases. As an example, Fig. 2.6 shows two of the measured frequency responses. These two correspond to two different locations for the photodetector (close to the centre and at the edge location). The photodetector is looking directly toward the diffusing-spot in both cases and the diffusing-spot is a few metres in diameter. The bottom curve represents the noise in the system.

The measured flat response indicates that, there are not any significant multipath effects for the single-spot IR transmission configuration. However, in a more real theatre environment, there might be reflections from the audience. Also, a high gain screen increases the possibility of reflections from the surrounding area. In addition, more practical configurations which employ multiple diffusing spots will, inherently, suffer from multipath distortions. So, the performance degradations due to multipath effects, have to be considered; we will do this in Chapter 4.

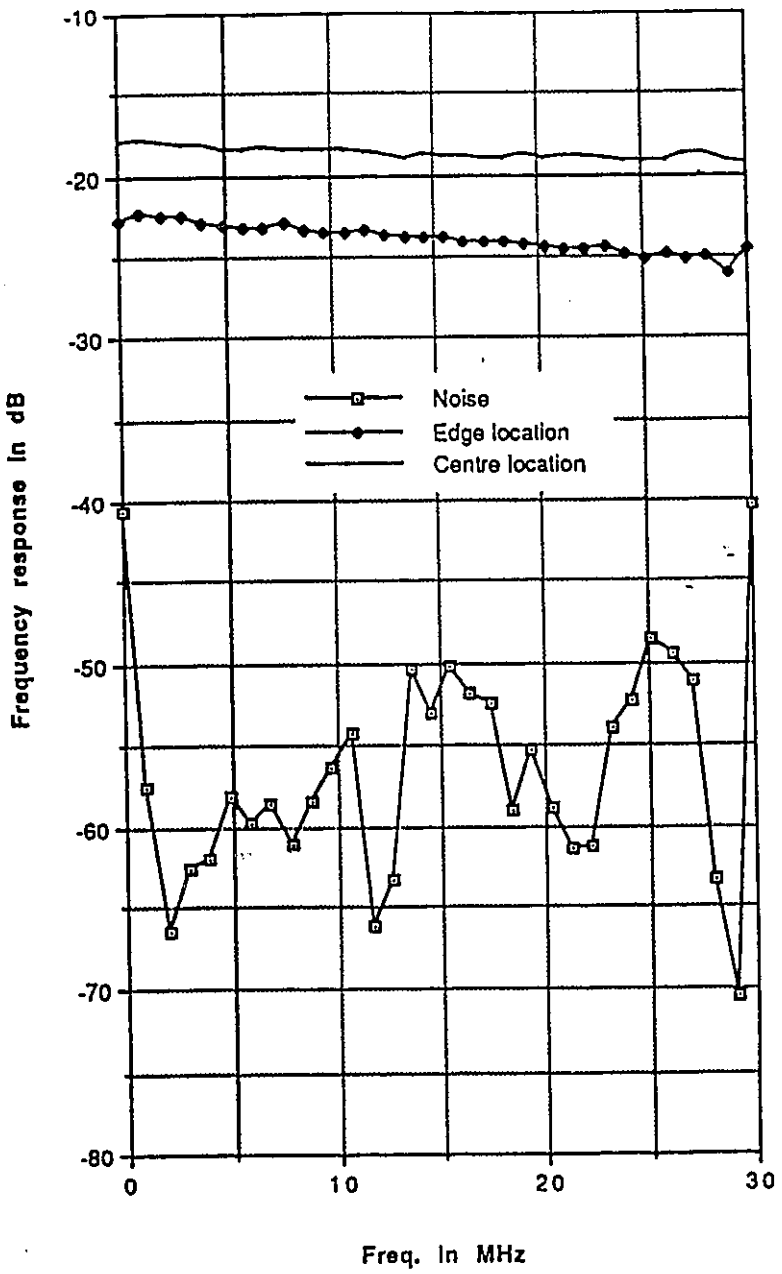

Figure 2.6 The measured frequency response of the in-theatre optical channel for the case of single diffusing-spot.

Chapter 3

Digital Audio

We compared the digital audio with the analog FM audio broadcasting system, in Section 1.2. A great advantage of digital audio is that since it is in the digital domain, all variety of available digital signal processing techniques can be utilized to improve the performance of the system. Digital audio is, of course, more complex than analog FM. Sophisticated communications coding and signal processing methods have been used in the compact disc (CD) system which is a mass-marketed consumer product and is thus relatively cheap. As a result, the CD digital audio is a strong candidate for the in-theatre multichannel audio broadcasting system. In this chapter, we look at the different features of the CD system. Also, the suitability of the CD digital audio for use in the in-theatre audio broadcasting system is examined, and some modifications which improve the performance of the system are suggested. In particular, the channel modulation scheme known as EFM which has been used in the CD system, fits the characteristics of the CD transmission channel very well but, is far from ideal for the in-theatre IR transmission system which has a different channel characteristics. EFM has a high redundancy (the

ratio of channel bit rate to the data bit rate), and we will show in Chapter 4 that modulation methods with a lower redundancy have a superior performance to EFM when used in the in-theatre IR transmission system. At a later part of this chapter, we propose a suitable channel modulation method for the in-theatre audio broadcasting system.

3.1 Compact Disc System

The idea of the compact disc digital audio was first announced in 1980; since then, various aspects of the system have been described in the literature and standards documents [17]-[25]. The CD digital audio was introduced to overcome the shortcomings of the conventional analog recording. The single-sided 12 cm diameter disc used in the CD audio system stores up to 54 minutes of high quality stereo sound. It has no surface grooves and the digitally encoded audio information lies beneath the disc surface, relatively invulnerable to dirt and damage. The digital audio information are in the form of pits impressed onto the surface of a substrate which is covered by a protective layer. The intervals between the pits are known as lands. The recording is read using a non-contacting laser pick-up which imposes no wear on the disc and suffers none itself. The light from the CD player laser is focused on the surface of the disc, and from there, it is reflected back towards the optical pick-up of the player. The light reflected back from the pits undergoes destructive interference and, therefore, its intensity is weaker than that of the light reflected back from the lands. The digital signal recovered from the disc is then used to accurately reconstruct the original sound recorded. The laser pick-up is mounted on a servo-controlled arm which tracks radially from the inside to the outside of the disc. Tracking, decoding and disc drive are all controlled by a central timing

generator in the CD player. Signal-to-noise ratio, channel separation and dynamic range are all more than 90 dB.

3.1.1 Description of the CD System

From a system point of view, the CD system was designed on the basis of communications concepts. The concepts applied in the CD system include modulation, error correction and detection, interpolation, and bandwidth expansion to ease the requirements on the D/A conversion [17].

The block diagram of the encoding process at the recording end of the CD system is shown in Fig. 3.1. The audio signal is, first, converted into PCM format. Two analog-to-digital converters (ADC) are used to perform the sampling and quantization on the left (L) and the right (R) constituent parts of the stereo audio signal. The Nyquist sampling theorem requires that the sampling rate be, at least, twice the highest frequency component of the signal to be sampled. In the CD system, the audio signal contains frequency components up to 20 KHz (the limits of the normal hearing range), and the chosen sampling rate is 44.1 KHz. Each sample is uniformly quantized and is represented by 16 binary digits. The PCM data bits are grouped into frames made up of six 32-bit "sampling periods". Each sampling period consists of 16 left- channel bits and 16 right-channel bits. Each corresponding 16 bit sample is divided into two 8-bit words called symbols; so, a frame contains 24 audio symbols. The audio data bit rate is thus

$$44.1\ \textit{Ksamples/s} \times 32\ \textit{bits/sample} = 1.4112\ \textit{Mb/s}\ . \qquad (3.1)$$

To ensure proper decoding of the data from the disc, an error correction coding scheme, called cross-interleaved Reed-Solomon coding (CIRC) is applied to the PCM data. This

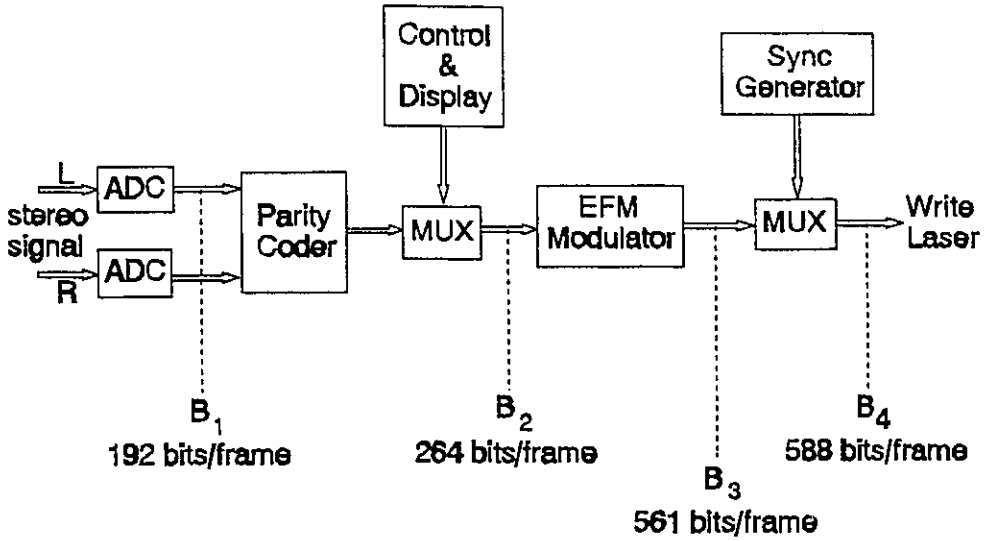

Figure 3.1 Block diagram of the encoding process at the recording end of the CD system.

coding is based on symbols corresponding to bytes of data. Eight parity symbols (each symbol a byte) are added to the successive blocks of the 24 PCM audio symbols; due to this operation the number of bits increases by a ratio of 4/3. After that, an additional byte is added to each frame. This additional symbol, which is known as the control and display byte, contains information about the recording (e.g., the "track" number, etc). The data bit stream is then modulated; i.e., the data bits are translated into channel bits, which are suitable for storage on the disc and later play back. This channel modulation (or channel code) is necessary for several reasons as will be explained in the next sub-section. The modulation scheme used in the CD system is called EFM (eight-to-fourteen modulation). In EFM, symbols of eight bits are translated into blocks of fourteen bits. The successive blocks of fourteen bits are linked by three merging bits so that it appears each 8-bit symbol produces 17 bits of channel data. The modulation increases the number of bits by a ratio of 17/8. Finally, for the synchronization of the bit stream, a

synchronization pattern consisting of 27 channel bits is added to each frame. The number of bits per frame at the successive stages of the CD encoding process are shown in Fig. 3.1, and a summary of these values together with their corresponding bit rates are given in Table 3.1. Different points along the encoding process have been denoted by $B_1,...,B_4$.

Table 3.1 *The bit rates and the associated number of bits per frame for the successive operations of the CD encoding process.*

Operation	Point along the encoding process	Number of bits per frame	Bit Rate (Mb/s)
PCM	B_1	192	1.4112
CIRC + C&D	B_2	264	1.9404
EFM	B_3	561	4.12335
Addition of the Sync pattern	B_4	588	4.3218

The bit stream before the EFM modulation is called the data bit stream; the data bit rate, f_d, is

$$f_d = 1.9404 \ Mb/s \ . \qquad (3.2)$$

The block diagram of the signal processing at the CD player is shown in Fig. 3.2. The data is read from the disc by a pick-up laser and demodulated/decoded. The demodulated data is stored in a temporary buffer memory before entering the error-detection and correction circuit (ERCO). The ERCO decodes the signal correcting for some channel errors and detecting others; those errors which cannot be corrected by ERCO are masked in the CIM block (concealment: interpolation and muting). After passing the data through an interpolation digital filter, two digital-to-analog converters are

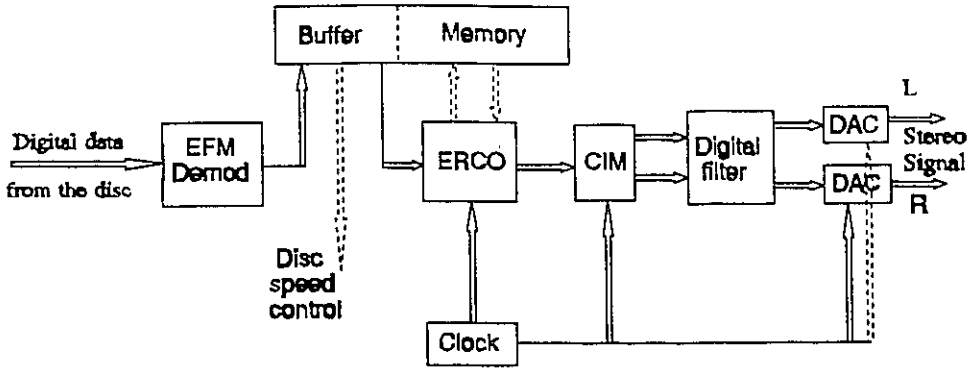

Figure 3.2 Block diagram of the signal processing in the CD player.

used to reconstruct the original audio signal. A quartz crystal clock is used to synchronize the different blocks. The speed of the disc is controlled by the degree of fullness of the buffer memory; the speed is adjusted so that the memory is maintained at the half-full state.

As a final point, we should note that the CD system taken as a whole can be considered as a transmission system. That part of the system, which lies between the write laser in Fig. 3.1 and the optical pick-up in the CD player, is the transmission channel. Signal degradation occur in the transmission channel; these degradation must be remedied by the signal processing elements of the CD player. The operations and the characteristics of the important parts of the CD system are explained in the following sub-sections.

3.1.2 EFM Channel Modulation

The purpose of employing a channel code in the CD system is:

(i) to allow an increased density of information stored on the disc;

(ii) to facilitate the clock recovery by limiting the number of consecutive zeros or ones and, hence, increasing the number of transitions in the bit stream; and

(iii) to suppress the low frequency content of the signal to avoid baseline wandering and to prevent interference with the low frequency signal used by the servo system. (the low frequency noise in the system can also be rejected if the modulated signal does not have any significant components at the low frequency region).

As said before, in EFM, a group of 8 data bits is converted into a 14-bit codeword. The EFM codewords are in the nonreturn-to-zero inverted (NRZI) form. In NRZI format, each transition from a pit to a land or vice versa represents a 1 and the absence of a transition represents a 0. In this way, the information is stored only in the position of transitions in the recorded signal. It should be noted that the channel bit stream is, of course, in the NRZ OOK form, i.e., it simply changes polarity with each 1 in an EFM codeword. To decrease the bandwidth requirements of EFM, the minimum run-length, T_{min}, has been limited to three channel bits. Also, there is an upper limit on the maximum run-length, T_{max}, to ease the clock regeneration; T_{max} = 11 channel bits. So the number of consecutive 0's can be as high as 10 or as low as 2. There are 267 distinct 14-bit sequences that meet the run-length requirements. Eleven of these sequences are discarded since for a unique mapping of 8 bits only 256 sequences are needed. In the CD player, a table look-up is used to convert the 14-bit blocks into 8-bit data symbols. This table was compiled with the aid of computer optimization in such a way that translation in the player can be carried out with the simplest possible logic circuitry [19]. To give a sample, part of the EFM conversion table has been shown in Table 3.2. The left column shows the decimal representation of the 8-bit data word.

The run-length requirements, however, may be violated when combining the 14-bit symbols. Three properly chosen bits termed "merging bits" are inserted between 14-bit

Table 3.2 Part of the conversion table of the EFM channel code.

data symbol	14-bit codeword	data symbol	14-bit codeword
100	01000100100010	107	10001001000010
101	00000000100010	108	01000001000010
102	01000000100100	109	00000001000010
103	00100100100010	110	00010001000010
104	01001001000010	111	00100001000010
105	10000001000010	112	10000000100010
106	10010001000010	113	10000010000010

blocks to continue to satisfy the run length requirements while at the same time suppress the low frequency components. The merging bits are chosen such that the run length constraints is not violated and when there is some choice, such that the running digital sum (RDS) at the end of each channel symbol is minimized. RDS is the accumulated difference between the number of 1's and 0's in a bit sequence. The lower the variations of the RDS, the smaller will be the low frequency content of a digital signal [28]. Also, the 27-bit synchronization pattern consists of a 24-bit unique sync word plus three merging bits. The sync word contains two consecutive 11-bit run-lengths which do not occur any where else in the bit stream; the sync word is: 100000000001000000000010. So, a further constraint on the choice of the merging bits is that the occurrence of the sync pattern at unwanted positions have to be avoided.

EFM fits well with the CIRC error correction scheme because they both operate on 8-bit symbols. This has the effect of avoiding the error propagation; one channel bit error that occurs in the transmission, spoils one and only one data symbol. But, for a different modulation scheme which does not operate on groups of 8 bits (e.g., 5B6B),

a channel bit error might spoil two of the original 8-bit data symbols.

Now, to explain the suitability of EFM scheme for the CD system, we have to consider the frequency characteristics of the CD transmission channel. The amplitude-frequency characteristics of the CD optical channel can be approximated by a form of low-pass filter [22], with the frequency response as shown in Fig. 3.3. In the ideal case the cut-off frequency, f_{cut}, is given by

$$f_{cut} = v\frac{2NA}{\lambda} , \tag{3.3}$$

where λ is the wavelength of the laser light, NA is the numerical aperture of the objective lens and v is the track velocity in the CD player (the speed at which the laser spot travels over the track). But, the optical system of the CD player is not ideal and f_{cut} is, effectively, lower than its ideal value. Usually, it is considered to be smaller by a factor of 0.8, i.e.,

$$f_{cut} = 0.8(v\frac{2NA}{\lambda}) , \tag{3.4}$$

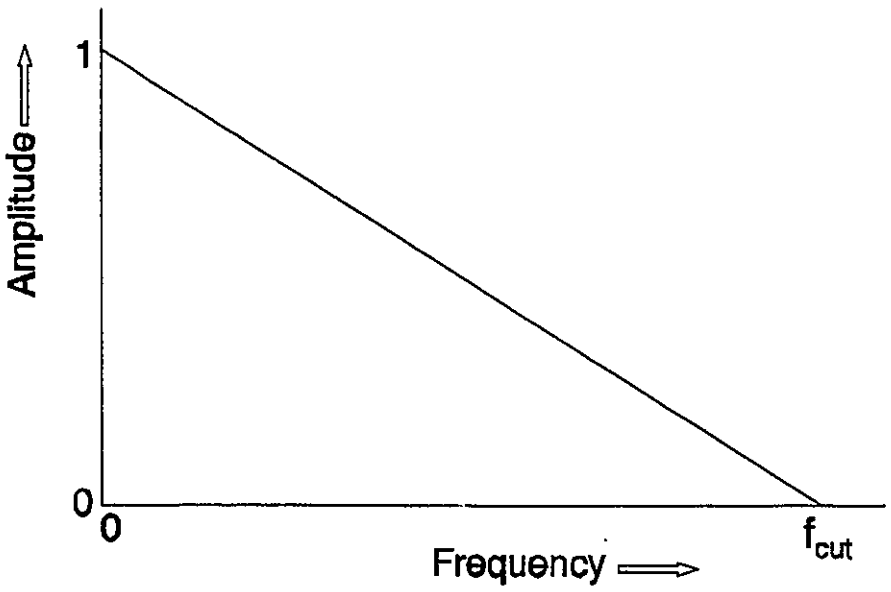

Figure 3.3 Amplitude-frequency characteristics of the CD optical channel.

where v and λ are fixed; v = 1.25 m/s and λ = 0.8 μm. To increase the cut-off frequency, we have to increase *NA*. But, unfortunately certain manufacturing tolerances of the player and the disc are proportional to NA^{-2}, NA^{-3}, and NA^{-4} [19]; i.e., these tolerances become rapidly smaller by increasing *NA*. Therefore, a trade-off has to be made; a value of 0.45 has been chosen for *NA* [19]. The numerical value of f_{cut} is obtained by substituting the values of v, λ and *NA* in (3.4); f_{cut} = 1.125 MHz.

Eye-height is an important parameter in measuring the performance of different channel modulation methods. For a given modulation scheme, the eye-height, a, can be expressed as

$$a = A\sin\left(\frac{\pi T_c}{2T_{min}}\right) , \tag{3.5}$$

where T_c is the channel bit period, T_{min} is the minimum run-length and an integer multiple of T_c, and A is the normalized amplitude of the highest fundamental frequency signal corresponding to the fastest transition of bits (change from a pit to a land or vice versa). Considering the linear amplitude-frequency characteristics of the CD optical channel as shown in Fig. 3.3, A can be written as

$$A = 1 - \frac{f_m}{f_{cut}} , \tag{3.6}$$

where f_m is the highest fundamental frequency and is given by

$$f_m = \frac{1}{2T_{min}} . \tag{3.7}$$

As an example, the eye pattern produced by the highest fundamental frequency signal of EFM is shown in Fig. 3.4. The eye-height is half the value of A, i.e., $a = A/2$. Also, as

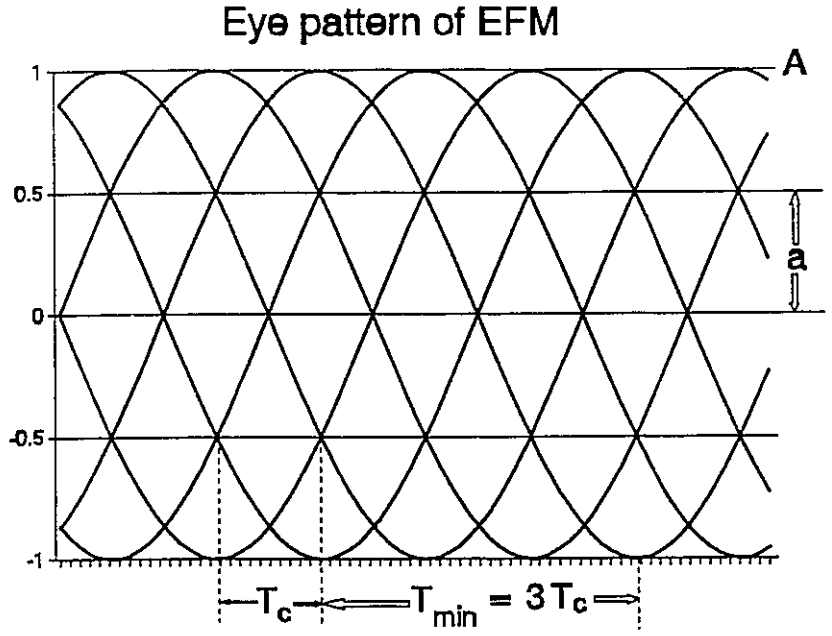

Figure 3.4 Eye pattern produced by the highest fundamental frequency signal in the EFM modulation.

we said previously that $T_{min} = 3T_c$, and therefore using (3.7) we get: $f_m = 1/2T_{min} = 1/6T_c$.

Now, we obtain an alternative expression for the eye-height by combining (3.4), (3.5) and (3.6):

$$a = (1 - \frac{\lambda f_m}{0.8(2\nu NA)}) \sin(\frac{\pi T_c}{2T_{min}}) \ . \tag{3.8}$$

Moreover, the track velocity can be expressed as

$$\nu = \frac{f_d}{\sigma} \ , \tag{3.9}$$

where f_d is the data bit rate in the CD system as given, before, by (3.2), and σ is the linear information density (the number of data bits per unit length of the track on the disc). Substituting for $NA = 0.45$ and $\lambda = 0.8$ μm in (3.8) and, also, substituting for ν from (3.9) in (3.8), we get

$$a = (1 - \frac{\sigma f_m}{0.9 f_d}) \sin(\frac{\pi T_c}{2T_{min}}) \ , \qquad (3.10)$$

where σ is in data bits/μm. The performance of different modulation schemes can be compared on the basis of their associated eye-heights, as given by (3.10). Apart from EFM, we consider two other channel coding methods, labelled 8B24B and 8B10B. In 8B24B modulation, 8 data bits are converted into 24 channel bits; it has a higher redundancy (the ratio of the channel bit rate to the data bit rate) than EFM. Similarly, in 8B10B modulation, 8 data bits are translated into 10 channel bits. The 8B10B scheme has a lower redundancy than that of EFM. We will show, in Chapter 4, that the low redundancy of 8B10B modulation results in a much better performance compared to EFM when used in the in-theatre audio broadcasting system. We have compiled a particular version of 8B10B modulation code, for which the bandwidth requirements has been minimized; we will explain the characteristics of this 8B10B code in a later section of this chapter. Here, we just say that we are referring to this particular version wherever we are talking about the 8B10B modulation in this thesis.

The parameters T_c, T_{min}, a, and f_m for EFM, 8B24B and 8B10B modulations have been tabulated in Table 3.3. The case with no modulation has, also, been included in this table. By substituting for f_m and T_{min} in (3.10), the associated eye-height for each modulation has been expressed as a function of σ. These expressions have been plotted in Fig. 3.5. The disc size is inversely proportional to σ. So, for a given desired eye-height, a modulation method which corresponds to the largest σ has to be chosen to reduce the required disc size. The nature of noise and perturbations in the CD system is such that the eye-height can be smaller than that at point p in Fig. 3.5, but it becomes too small at point q [19]. The fact that EFM performs best at this region explains why EFM

Table 3.3 Corresponding parameters of different channel modulation schemes when used in the CD system.

	Unmodulated	8B10B	EFM	8B24B
T_c	T_d	$(384/496)T_d$	$(264/588)T_d$	$(1/3)T_d$
T_{min}	T_c	T_c	$3T_c$	$6T_c$
f_m	$(1/2)f_d$	$(496/768)f_d$	$(588/1484)f_d$	$(1/4)f_d$
a	1 - σ/1.8	1 - σ/1.39	0.5 - σ/4.85	0.26 - σ/13.85

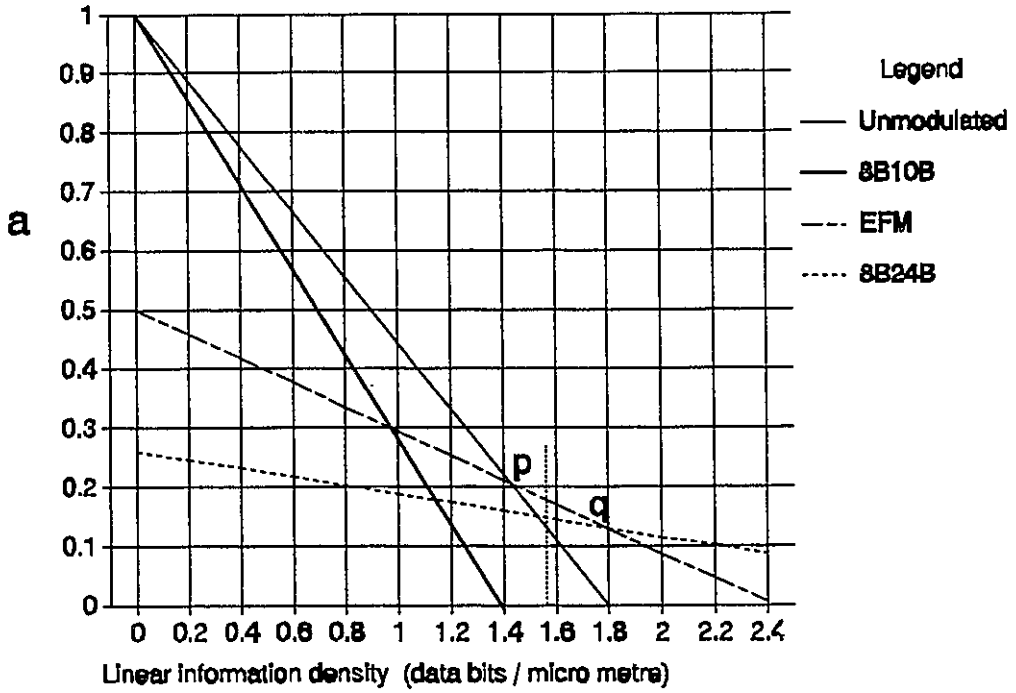

Figure 3.5 Corresponding eye-height of different modulation methods as a function of the linear information density.

has been chosen for the CD system.

Now, by rearranging (3.9), σ can be written as

$$\sigma = \frac{f_d}{v} \quad . \tag{3.11}$$

Substituting for f_d = 1.94 Mb/s and v = 1.25 m/s in (3.11), the numerical value of σ is obtained; i.e., the CD system operates at σ = 1.55 data bits/μm. This operating point has been represented by the thin vertical dotted line shown in Fig. 3.5.

Finally, Fig. 3.6 shows the amplitude spectrum of the EFM modulated bit stream in the CD system. This amplitude spectrum was estimated using the method which will be described later in Section 3.3. It is seen that the DC content has been suppressed and nearly most of the significant frequency components lie below 1 MHz. At the CD player,

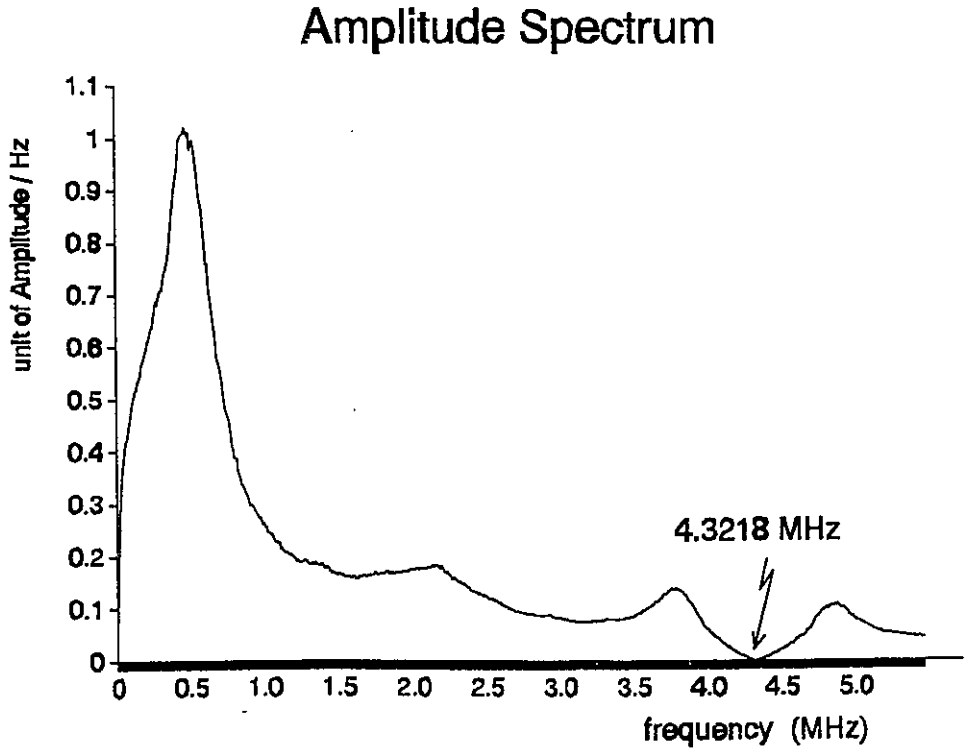

Figure 3.6 *Amplitude spectrum of the EFM modulated data in the CD system.*

an electrical high-pass filter is used to prevent interference between the data signal and the low-frequency servo control signal. The low-frequency content of the EFM signal should be small such that its quality is not affected after passing through the high-pass filter. The amplitude spectrum is zero at the integer multiples of 4.3218 MHz which is, in fact, the channel bit rate.

3.1.3 Error Correction and Concealment in the CD System

Two kinds of errors occur in the CD transmission system: random errors, and burst errors which occur in groups covering a whole symbol or a number of adjacent symbols. The burst errors occur due to dirt or scratches on the disc. These errors result in erroneous audio samples and cause unpleasant audible disturbances. So, a powerful error correction coding technique is employed in the CD system to reduce the error rate to a sufficiently low level. This error correction coding method is known as a CIRC (cross-interleaved Reed-Solomon code) [20]. CIRC is a linear nonbinary block code. In CIRC, a block of K information symbols are encoded into N code symbols; i.e., $(N - K)$ parity symbols are added to the original K symbols to form a (N,K) block code. Remember that symbols in the CD system consist of 8 bits. This is a convenient length which simplifies the required digital hardware since the prevalent existing technology is byte oriented. Interleaving is applied in CIRC to spread the effect of burst errors over a few symbols in a large number of different frames. Through interleaving, the burst errors can be treated as random errors which are easier to handle.

CIRC consists of two separate Reed-Solomon codes: DEC_1 which is a (28,24) code and DEC_2 which is a (32,28) code where each symbol corresponds to a data byte. Eight

parity symbols are then added to 24 audio symbols of each frame, and the code rate is, effectively, given by

$$R_c = \frac{24}{32} = \frac{3}{4} \ . \tag{3.12}$$

The minimum distance, d_m, for a (N,K) Reed-Solomon code [30] is

$$d_m = N - K + 1 \ , \tag{3.13}$$

and the maximum number of correctable errors per frame, t, is

$$t = \frac{d_m - 1}{2} = \frac{N-K}{2} \ . \tag{3.14}$$

In both DEC_1 and DEC_2 we have $N - K = 4$ and, so, $t = 2$. If the location of the errors (erasure locations) are known, then, the maximum number of correctable errors will be [20] equal to: $d_m - 1 = N - K$. So, 4 erasure corrections is possible in both DEC_1 and DEC_2. Interleaving is performed before DEC_1 and, also, between DEC_1 and DEC_2. DEC_1 has been designed to correct single errors and to detect up to triple errors. The probability of quadruple or higher multiple errors passing the DEC_1 without being detected is, approximately, equal to 1.9×10^{-6} [17]. Therefore, DEC_1 corrects most random and short burst errors. Those errors which are detected, but not corrected, by DEC_1 are assigned erasure flags and are passed on to DEC_2; these errors are usually due to long burst errors. DEC_2 can correct up to four errors by means of erasure decoding, but to increase its detection capability, it only corrects two errors. With this scheme, the probability of an error passing through CIRC without being detected becomes extremely small.

The detected errors which have not been corrected by CIRC, will undergo a

process known as concealment. The purpose of error concealment is to make the effect of these errors, virtually, inaudible. This is accomplished by interpolation or by muting the audio signal. This process is done slightly differently in the CD players made by different companies. As an example, we look at the procedure employed in some Philips CD decoder ICs. Interpolation means that new samples are inserted instead of unreliable ones. The interpolated samples should be such that the final result produces no audible distortion. If the sample in error has two reliable neighbouring samples, then an interpolated sample can be obtained by a linear (straight line) interpolation; i.e., the interpolated sample is, just, the arithmetic mean of the two neighbouring sample values. If a decoder delivers a sequence of wrong sample values, linear interpolation does not help, and in that case muting may have to be performed. Muting is done by rapidly turning the gain down and up again electronically. This procedure starts 32 sampling intervals before the next erroneous sample values arrive. The gain is kept at zero for the duration of errors and, then, turned up again in the following 32 sampling intervals. The gain variations follow a cosine curve to avoid the occurrence of higher frequency components. Interpolation and muting will, therefore, prevent audible clicks and, only, cause a short-lived slight increase in distortion of the audio signal. Computing the performance of CIRC becomes complicated due to interleaving performed at different stages of the encoder. A full account of CIRC and the concealment process is too lengthy to be given here. Reference [20] provides a good description of CIRC and gives some related performance measures of CIRC. Table 3.4 shows some of the specifications of CIRC as used in the CD system. From the values given in Table 3.4, we can conclude that CIRC performs quite well when BER $\leq 10^{-4}$. We will, therefore, use a BER value of 10^{-4} in our computations of the required optical power in the next chapter.

Table 3.4 Specifications of CIRC.

Aspect	Specifications
code rate	3/4
maximum completely correctable burst length	≈ 4000 data bits (i.e., ≈ 2 msec)
maximum interpolatable burst length in the worst case	≈ 12300 data bits (i.e., ≈ 6.3 msec)
sample interpolation rate	1000 samples per minute at BER = 10^{-3} one sample every 10 hours at BER = 10^{-4}
undetected error samples (clicks)	less than one every 750 hours at BER = 10^{-3} negligible at BER ≤ 10^{-4}

3.1.4 Digital-to-Analog Conversion in the CD Player

The last stage in the series of signal processing operations in the CD player is the digital-to-analog conversion [21]. The performance of the PCM modulation is limited by the quantization noise which, in turn, depends on the resolution (number of bits per sample) used in a system. For complicated signals such as speech or music where the signal fluctuates rapidly in a somewhat unpredictable manner, the quantization error can be approximately modelled [29] by a white noise process and the probability distribution of the error process is assumed to be uniform over the range of quantization error. Using this model, it can be easily shown [29] that the signal to quantization noise ratio for a linearly quantized PCM system can be expressed as

$$SNR = 6.02b + 4.8 - 20\log(\frac{x_m}{\sigma_x}) \ , \qquad (3.15)$$

where b is the number of bits per sample, x_m is the maximum amplitude of the signal and σ_x is its rms value. Equation (3.15) shows that SNR increases by 6 dB for each

additional bit. Taking $x_m/\sigma_x = 2$ for an audio signal, then, (3.15) can be written as

$$SNR = 6.02b - 1.2 \ . \tag{3.16}$$

In the CD system, each sample is represented by 16 bits. Substituting for $b = 16$ in (3.16), we get: SNR = 95.1 dB; i,e, a signal to quantization noise ratio of more than 90 dB is obtained in the CD system.

The bit stream coming from the CIRC decoder is, first, passed through a digital transversal filter as shown in Fig. 3.2. In the digital filter, the signal is oversampled at a certain rate (the oversampling rate varies with different systems) and then filtered in such a way that signals at frequencies above 20 KHz are attenuated by 50 dB after D/A conversion. This process is known as interpolation in the area of digital signal processing. Without interpolation, the required analog low-pass filter, following the D/A converter would be complex and expensive. After the digital filter, the quantization noise power has been, effectively, spread over a bandwidth a number of times larger than the original audio bandwidth (0-20 KHz), and the noise power in the audio bandwidth becomes smaller, correspondingly. Moreover, after the digital filter, a noise-shaping filter may be used to redistribute the noise power in such a way that the noise power in the audio bandwidth is reduced at the expense of an increase in the noise power outside this bandwidth.

3.2 Adapting the CD Digital Audio for the In-Theatre IR Multichannel Audio Broadcasting System

As was shown in Section 3.1, the CD system performance is very good due to the

sophisticated signal processing techniques it employs. It is desirable to make use of such a system in the in-theatre IR audio broadcasting system. Some features of the CD digital audio system such as the powerful CIRC error correction coding scheme are particularly useful for this application because they improve the performance of the system and reduce the transmitted power requirements. Although, the nature of the burst errors in the two systems are not the same, the good correction and detection capabilities of CIRC can be effective in overcoming the short burst errors caused by shadowing in the theatre environment.

On the other hand, some aspects of the CD system are far from ideal for the in-theatre audio broadcasting system. The control and display symbol which conveys information for the listener and is added as the 33rd symbol to a frame, is no longer needed and can be excluded[4]. This reduces the data bit rate by three percent. From Table 3.1, the PCM data bit rate of a CD digital audio is 1.4112 Mb/s. The CIRC error correction scheme introduces a redundancy of 4/3 and increases the data bit rate to 1.8816 Mb/s. As said before, the corresponding data of four stereo audio signals are going to be time-division multiplexed and transmitted in the intended broadcasting system. Then, the total data bit rate, B_d, will be

$$B_d = 4 * 1.8816\ Mb/s = 7.5264\ Mb/s\ . \qquad (3.17)$$

Note that B_d includes the audio bits plus the parity bits introduced by the CIRC. Since no data compression method has been used in the CD system, it seems advantageous to

[4]In the in-theatre IR audio broadcasting system, some control bits for turning on and off the lenses of the audience glasses are needed. But, since the required number of bits is extremely small compared with the data bit rate of the system, they can be ignored without affecting the generality of our work.

reduce the required bit rate by some sort of data compression scheme. A data compression technique has been reported [24] which provides an audio quality comparable to that of the CD system using a reduced bit rate of 256 Kb/s for a stereo sound signal instead of 1.4112 Mb/s. But, this technology is not easily available and is too expensive to be used in our system.

Another feature of the CD system is EFM channel coding which has been used to shape the frequency spectrum of the recorded signal to match the CD transmission channel. EFM is not necessarily the most appropriate channel code for the in-theatre environment which has a completely different channel characteristic to that of the CD recorder/playback system. As was seen in Chapter 2, the in-theatre IR transmission channel has a more or less flat frequency response. This is in contrast with the CD transmission channel which has a linearly falling characteristic as was shown, previously, in Fig. 3.3. We suggest that, when using the CD digital audio in the in-theatre audio broadcasting system, EFM should be replaced by another channel modulation method which is better suited for the in-theatre environment.

3.2.1 8B10B Channel Modulation

Channel modulation (often called channel coding or line coding) is used to match the transmitted signal to the characteristics of the transmission channel. An efficient category of channel codes are mBnB block codes where m data bits are converted into a block of n channel bits, $n > m$. Properties of several mBnB block codes have been investigated in [22], and [26]-[28]. Channel codes introduce redundancy (increased bit rate). However, at the expense of this redundancy, they can provide adequate timing and

error-monitoring information, and they may avoid baseline wander problems if the code eliminates the possibility of long strings of ones or zeros. A useful concept used for channel codes is the running digital sum (RDS) which is the cumulative difference between the number of 1 and 0 bits since the start of the transmission. It is desirable to limit the RDS variations (the difference between the maximum and minimum values of RDS) as it is known that the low frequency spectral content of the signal can be suppressed if the RDS variation is bounded; the tighter this bound will be the better will be the suppression of the low frequency content of the digital signal. Also, a bound on RDS would facilitate error monitoring by detecting the overflow of the accumulated disparity.

A well-known type of *m*B*n*B block codes is the 8B10B channel code. In 8B10B modulation, 8 data bits are translated into 10 channel bits. The resultant 10 bit blocks are transmitted in the NRZ form. Unlike EFM, no merging bits are used to combine the channel symbols. 8B10B modulation operates on 8-bit data symbols; therefore, it fits in conveniently with other parts of the CD digital audio (particularly with the CIRC error correction coding scheme), and prevents error propagation. Implementation of 8B10B modulation is much simpler than that of EFM. Also, 8B10B modulation requires a lower channel bit rate. We will see, in Chapter 4, that 8B10B modulation, due to its lower redundancy, has a superior performance to that of EFM. It is worth mentioning that 8B10B channel code is also suitable for many other applications because a symbol size of 8 is in agreement with 8-bit video samples and byte-oriented computers. In the following subsections, we will design a suitable version of 8B10B channel code, and we will give simple implementations for its encoder and decoder.

3.2.2 Designing a Code List for 8B10B Modulation

The total number of 10-bit words is $2^{10} = 1024$, but only 256 of them are needed to represent 8-bit data symbols. The task of designing the code is thus that of selecting which 10-bit codewords to use and for which 8-bit data symbols. Each 10-bit codeword can be characterized, in part, by the difference between the number of 1's and 0's in that codeword; termed the digital sum value (DSV) or disparity of the codeword. To obtain good low-frequency spectral characteristics we shall choose to minimize the RDS variations by selecting only the codewords with a DSV of 0 or ±2. Merely using codewords with small absolute disparity will not produce a bounded running digital sum. We can obtain a bounded RDS if when we assign a data symbol to a codeword with nonzero disparity, we also assign the data symbol another codeword with the opposite sign of disparity (its complement is the natural selection) and then transmit the data word using the codeword from the pair that would reduce the RDS. With codewords with 0 or ±2 disparity, we may arrange it so that the RDS after the transmission of each codeword is either 0 or +2; the zero disparity codewords do not change the RDS value, and the nonzero disparity codewords are used with an alternating disparity rule. This rule says that, the codeword with DSV of +2 is used if RDS = 0, otherwise, its complement is selected (i.e., the codeword with DSV of -2 is selected if RDS = +2). The total number of characters which can be represented by these codewords are

$$N = \binom{10}{5} + \binom{10}{6} = 252 + 210 = 462 \ , \qquad (3.18)$$

where the first term of (3.18) represents the number of codewords with a DSV of 0, and the second term is the number of codeword pairs with a DSV of ±2.

The run-length might become too large when combining the codewords. To limit the run-length, we eliminate the two zero disparity codewords with five 1's at the end or at the beginning. Similarly, two pairs of nonzero codewords with six 1's or 0's at the end or at the beginning are excluded. Then, using (3.18), we are left with a total number of codewords of

$$N = 462 - 4 = 458 \ . \tag{3.19}$$

There is still a large freedom in choosing 256 out of 458 possible combinations. We use this freedom to limit the high frequency spectral content of the signal, i.e., we choose the codewords which contain the least number of transitions. After doing this, we arrive at the final list of 8B10B channel codewords. The complete list has been shown in Table 3.5; the decimal representations of the 8-bit data symbols have been shown in the first column, and the 10-bit codewords are in the adjacent column. The first 140 (0-139) codewords are of zero disparity, i.e., they have equal number of 1's and 0's. The remaining 116 (140-255) are pairs of codewords with a disparity of ±2. The unused 10-bit words can be utilized in error detection process if the detector is able to distinguish the invalid blocks.

For frame synchronization, we have chosen a synchronization pattern of 16 bits for this particular version of 8B10B modulation. The sync word consists of three transitions with a run-length of 7 bits between each two successive transition. This pattern is unique since it never occurs with any combination of the 8B10B codewords. The sync word is 1000000011111110 if RDS = 0, and the complement of this sync word is used when RDS = +2. Some properties of the 8B10B modulation are tabulated in Table 3.6.

Table 3.5 List of codewords of 8B10B modulation.

data symbol	10-bit codeword	data symbol	10-bit codeword	data symbol	10-bit codeword
0	0111101000	41	0001110110	82	1001101100
1	0111100100	42	0001110011	83	1001100110
2	0111100010	43	1011100100	84	1001100011
3	0111100001	44	1011100010	85	1000110110
4	0011110100	45	1011100001	86	1000110011
5	0011110010	46	1001110100	87	1000011011
6	0011110001	47	1001110010	88	0000110111
7	1000111100	48	1001110001	89	1110100001
8	1000011110	49	1000111010	90	0101100011
9	0100111100	50	1000111001	91	1110010010
10	0100011110	51	1000011101	92	0100110011
11	0010111100	52	0000111011	93	0100011011
12	0010011110	53	1101110000	94	1110010001
13	0111001100	54	1100111000	95	0010110011
14	0111000110	55	1100000111	96	0010011011
15	0111000011	56	0100111001	97	1101001100
16	0011101100	57	0100011101	98	1101000110
17	0011100110	58	0110111000	99	1101000011
18	0011100011	59	0010111001	100	1100101100
19	1100011100	60	0010011101	101	1100100110
20	1100001110	61	1101100100	102	1100100011
21	0110011100	62	1101100010	103	1100010110
22	0110001110	63	1101100001	104	1100010011
23	0011011100	64	1100110100	105	1100001011
24	0011001110	65	1100110010	106	1110001001
25	0001111010	66	1100110001	107	1110000101
26	0001111001	67	1100011010	108	0110100011
27	0111010001	68	1100011001	109	1001000111
28	0000111101	69	1100001101	110	0110010011
29	0111001001	70	0110000111	111	0110001011
30	1011110000	71	0011000111	112	1000100111
31	1001111000	72	0110110001	113	0011010011
32	0011101001	73	0001101110	114	0011001011
33	0011100101	74	0110011001	115	1000010111
34	1010011100	75	0110001101	116	0100100111
35	1010001110	76	0001100111	117	0001101101
36	1001011100	77	0011011001	118	1011011000
37	1001001110	78	0011001101	119	0111110000
38	1000101110	79	1011001100	120	0011111000
39	1000001111	80	1011000110	121	0001111100
40	0101111000	81	1011000011	122	0000111110

123	1111010000
124	1111001000
125	1111000100
126	1111000010
127	1111000001
128	0100001111
129	0010001111
130	0001011110
131	0001001111
132	0000101111
133	1110110000
134	1110011000
135	1110001100
136	1110000110
137	1110000011
138	0111011000
139	0010100111
140	0001111011
141	1101111000
142	1100001111
143	0110001111
144	1010001111
145	1001001111
146	1000101111
147	1110111000
148	1110011100
149	1110001110
150	1110000111
151	0111000111
152	0011100111
153	0001110111
154	1110110010
155	1110110001
156	1110011010
157	1110011001
158	1110001101
159	0111101100
160	0111100110
161	0111100011
162	0011110110
163	0011110011
164	1100111100
165	1100011110
166	0110111100
167	0110011110
168	0011011110
169	1011000111
170	1001100111
171	1000110111
172	0101100111
173	0100110111
174	1110100110
175	1110100011
176	1110010110
177	1011110001
178	1110010011
179	1001111001
180	1000111101
181	1110001011
182	1101000111
183	1100100111
184	0111011100
185	0111001110
186	0011101110
187	1100010111
188	0111011001
189	0111001101
190	0011101101
191	1011011100
192	1011001110
193	1001101110
194	0110100111
195	0110010111
196	0111010011
197	0111001011
198	1000011111
199	0100011111
200	1101001110
201	1100101110
202	0010011111
203	1011101100
204	1011100110
205	1011100011
206	1001110110
207	1001110011
208	1000111011
209	0001011111
210	0101110011
211	0100111011
212	0111111000
213	0011111100
214	1101110010
215	1101110001
216	1100111010
217	1100111001
218	1100011101
219	0001111110
220	0110111001
221	0110011101
222	0011011101
223	1111101000
224	1111100100
225	1111100010
226	1111100001
227	0111110100
228	0111110010
229	1101101100
230	1101100110
231	1101100011
232	1100110110
233	1100110011
234	1100011011
235	0111110001
236	0110110011
237	0110011011
238	0011011011
239	0011111010
240	0011111001
241	0001111101
242	1011111000
243	1001111100
244	1000111110
245	0101111100
246	0100111110
247	0010111110
248	1111011000
249	1111001100
250	1111000110
251	1111000011
252	0011001111
253	0001101111
254	1111001001
255	1111000101

Table 3.6 Some properties of 8B10B modulation.

codeword disparity	0 or ±2
RDS at the end of each codeword	0 or +2
maximum and minimum possible RDS values after every bit	+6, -4
maximum run-length	9
proportion of unused 10-bit words	63.7%

3.2.3 8B10B Coder and Decoder

Figure 3.7 illustrates a simple coder for the proposed 8B10B modulation. It is based on 16-bit ROM of 0.5 K words which is addressed by the 8-bit data symbols and the input control function, y_1, defined by

$$y_1 = \begin{cases} 0, & \text{if } RDS = 0; \\ 1, & \text{if } RDS = +2. \end{cases} \tag{3.20}$$

The first ten output bits from the ROM are codewords with the DSV depending on the control bit, y_1, according to

$$DSV = \begin{cases} 0, +2, & \text{if } y_1 = 0; \\ 0, -2, & \text{if } y_1 = 1. \end{cases} \tag{3.21}$$

These 10-bit words are loaded to a shift register and then shifted out in a series. The output function, x_1, is defined as

$$x_1 = \begin{cases} 0, & \text{if } DSV = 0; \\ 1, & \text{if } DSV = \pm 2. \end{cases} \tag{3.22}$$

x_1 is input to a t flip-flop. The output of the flip-flop, which is y_1, switches from 0 to 1

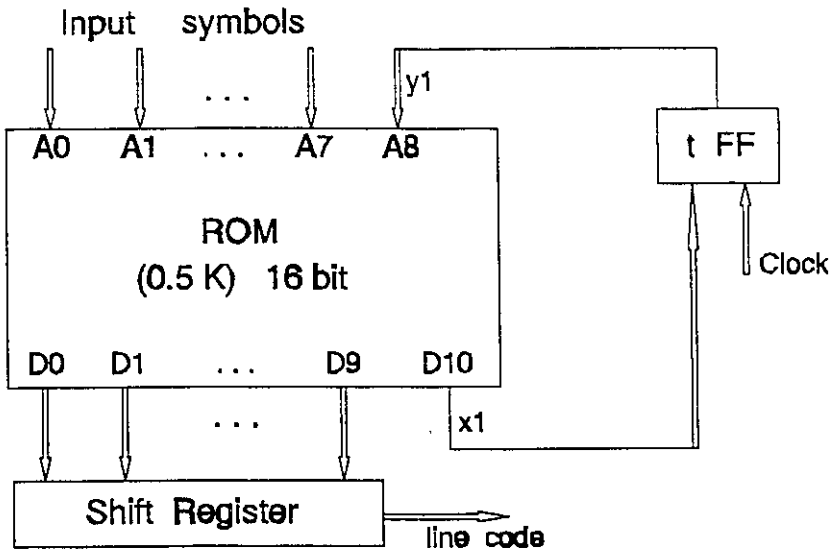

Figure 3.7 A simple implementation for the 8B10B coder.

(or from 1 to 0) when $x_1 = 1$; y_1 remains unchanged, otherwise.

The corresponding 8B10B decoder is depicted in Fig. 3.8. The decoder is somewhat more complicated since it includes the error detection logic circuitry. A 10-bit codeword from the shift register addresses a 16-bit ROM of 1 K words. The first 8 output bits are the decoded data symbol, while the other four output bits, denoted by x_2 through x_5, determine the DSV of the input codeword according to Table 3.7. Using Table 3.7 and by Karnaugh minimization, we obtained the formulae which define the logic circuit;

$$\begin{aligned} e &= x_2 + y_1 x_4 + \overline{y_1} x_5 \ , \\ y_1 &= \overline{x_2} x_4 + x_3 x_4 + \overline{y_1} x_3 + y_1 x_4 \overline{x_5} + y_1 \overline{x_2} \overline{x_4} \overline{x_5} + y_1 x_2 \overline{x_4} x_5 \ , \end{aligned} \tag{3.23}$$

where y_1 is as defined before, and e is an error flag. All invalid codewords and RDS violations are detected by the logic circuit and are given an e flag. The errors which are

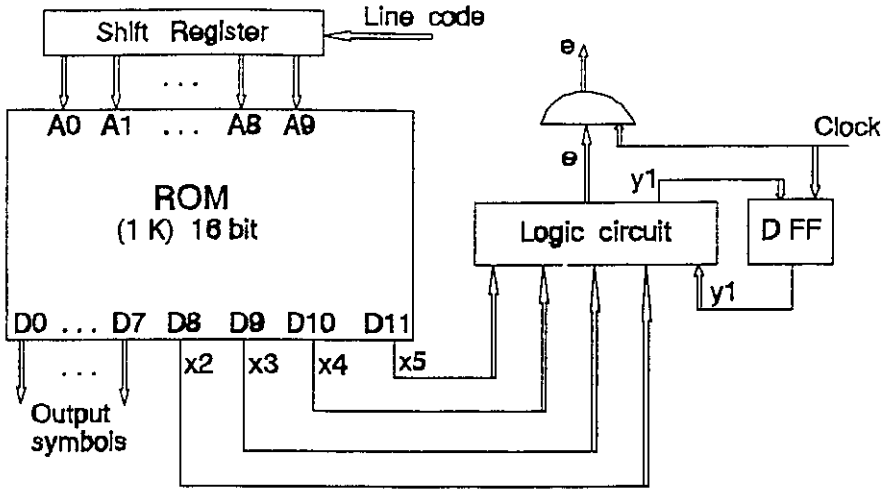

Figure 3.8 A simple implementation for the 8B10B decoder.

detected in 8B10B decoder can be corrected later by erasure method in the CIRC error correction section of the CD system.

In both the coder and the decoder, the ROM memory can be replaced by a logic circuit. In that case, the dictionary of the 8B10B codes has to be compiled such that the required logic gates is minimized.

Table 3.7 Output information of the 8B10B decoder ROM.

x_2	x_3	x_4	x_5	DSV	invalid codeword
0	0	0	0	0	No
0	0	0	1	-2	No
0	0	1	0	+2	No
1	0	0	0	< -4	Yes
1	0	0	1	-2	Yes
1	0	1	0	+2	Yes
1	0	1	1	-4	Yes
1	1	0	0	0	Yes
1	1	1	0	+4	Yes
1	1	1	1	> +4	Yes

3.2.4 A Comparison Between EFM and 8B10B Modulations

The main advantage of 8B10B modulation over EFM is that 8B10B modulation has a lower redundancy and, hence, a reduced channel bit rate. Each channel coding has an inherent redundancy because it involves the translation of a certain number of data bits to a larger number of channel bits. Moreover, a small portion of the redundancy is due to the sync pattern used in the frame format of the transmitted data. For 8B10B modulation, we consider a frame consisting of 48 symbols. The number of data bits represented by each frame is 48 × 8 = 384, while the number of channel bits per frame, including the 16-bit sync pattern, is 496. On the other hand, considering a frame of 32 symbols in EFM, the number of data bits per frame is 256 and there are 571 channel bits in each frame. So, the redundancy, r_c, for EFM and 8B10B modulations are

$$r_e = \begin{cases} \frac{496}{384} \approx 1.29 , & \textit{for 8B10B} , \\ \frac{571}{256} \approx 2.23 , & \textit{for EFM} . \end{cases} \tag{3.24}$$

Also, lower redundancy results in a higher eye-width. For a given channel modulation with a redundancy r_e, the eye-width (τ_e) is given by

$$\tau_e = \frac{T_d}{r_e} = T_c , \tag{3.25}$$

where T_d is the data bit period and T_c is the channel bit period. Different parameters of EFM and 8B10B modulations are summarized in Table 3.8. Note that we are considering four channels of CD stereo signals with a total data bit rate (PCM audio bits plus error correction coding parity bits) of 7.5264 Mb/s. The power density spectrums of these two modulations are compared in the next section.

Table 3.8 Different parameters of 8B10B and EFM modulations.

	8B10B	EFM
data bit rate (B_d) in Mb/s	7.5264	7.5264
codeword length	10 bits	17 bits
sync pattern length	16 bits	27 bits
No. of symbols per frame	48	32
frame length	496 bits	571 bits
frame rate (in frames per sec)	19600	29400
redundancy (r_c)	≈1.29	≈2.23
channel bit rate (B_c) in Mb/s	9.7216	16.7874
channel bit period (T_c) in ns	102.9	59.6
eye-width (τ_c) in ns	102.9	59.6
coder & decoder complexity	simple	relatively complex

3.3 Power Density Spectrum Estimation

The corresponding modulated symbols coming from four different audio sources are going to be time division multiplexed, interleaved, formatted in frames, and transmitted through the channel. The transmitted bit stream of a channel code such as EFM or 8B10B modulations can be characterized as a cyclostationary signal with a period equal to the frame length. To estimate the power density spectrums of EFM and 8B10B modulated signals, we take advantage of the fact that the power density spectrum of a cyclostationary process is the Fourier transform of the time-average autocorrelation function [30]; i.e., first an estimate of the autocorrelation function is obtained and then the Fourier transform of this estimate is computed.

The DC bias of the signal will be removed at the receiver by an electrical high-pass filter. Therefore, we can assume the signal to be DC free and consisting of binary digits of (+1,-1). In this case, the autocorrelation function will be the same as the autocovariance function. Now, consider a finite sequence of Q bits and let x_i be the ith bit in this sequence, $x_i \in (+1,-1)$, $i = 0,...,(Q-1)$. Also, let the discrete time-average autocovariance function and its estimate be denoted by $A_{xx}(k)$ and $\hat{A}_{xx}(k)$ respectively. Then $\hat{A}_{xx}(k)$ can be written as

$$\hat{A}_{xx}(k) = \frac{1}{Q-|k|} \sum_{i=0}^{Q-1-|k|} x_i x_{i+k} \,. \tag{3.26}$$

$\hat{A}_{xx}(k)$ is a random variable with an expected value of $A_{xx}(k)$, and a variance which gets smaller as $Q/|k|$ increases [29]. So, the estimated value will be very close to the exact value of $A_{xx}(k)$ if $Q \gg |k|$. The exact formula for the power density spectrum, $X(f)$, of the received signal [27] is

$$X(f) = \frac{1}{T_c}|G(f)|^2 \sum_{k=-\infty}^{+\infty} A_{xx}(k) e^{-j2\pi k f T_c} \,, \tag{3.27}$$

where T_c is the channel bit period and $G(f)$ is the Fourier transform of the transmitted pulse. Replacing $A_{xx}(k)$ by its estimated value and assuming that $\hat{A}_{xx}(k)$ is negligibly small for $k > M$, the power density spectrum can be approximated as

$$X(f) \approx \frac{1}{T_c}|G(f)|^2 \sum_{k=-M}^{+M} \hat{A}_{xx}(k) e^{-j2\pi k f T_c} \,. \tag{3.28}$$

Assuming a rectangular pulse, then,

$$G(f) = T_c \frac{\sin(\pi f T_c)}{\pi f T_c} \,. \tag{3.29}$$

Substituting for $G(f)$ from (3.29) in (3.28) and, also, rewriting (3.28) in an alternative

form, we get

$$X(f) \approx T_c\left(\frac{\sin(\pi f T_c)}{\pi f T_c}\right)^2 \left[\hat{A}_{xx}(0) + 2\sum_{k=1}^{M} \hat{A}_{xx}(k)\cos(2\pi k f T_c)\right]. \qquad (3.30)$$

Equation (3.30) was employed in our computations of the power density spectrums of EFM and 8B10B modulations. To satisfy the requirement of $Q > M$, we used the values of $M = 100$ and $Q = 6\times10^6$ channel bits. Fig. 3.9 illustrates the estimates of the discrete time-average autocovariance function. For the sake of comparison, the case of the unmodulated random bit stream has, also, been shown. It is seen that $\hat{A}_{xx}(k)$ falls rapidly and gets very close to zero for $k > 40$. The corresponding power density spectrums are shown in Fig. 3.10 where the x axis is the normalized frequency; the normalized frequency = frequency/data bit rate (B_d). Channel modulations have suppressed the low frequency components and have attenuated the high frequency content of the signal. An expanded view of the power density spectrums at the low frequency region is shown in Fig. 3.11. It can be seen that 8B10B modulation performs better than EFM at this region; this is due to the fact that RDS variations have been bounded more tightly in 8B10B modulation where RDS varies between +6 and -4. By recording the RDS value for a very long EFM modulated bit sequence (10^9 bits) we found that the RDS in EFM may reach values of ±36. Fig. 3.12 shows the in-band power of the two modulations. Also, the power density spectrum of the multiplexed 4-channel CD stereo signals is shown in Fig. 3.13, and the corresponding expanded view of the low frequency region is shown in Fig. 3.14. The frequency spectrum of 8B10B modulated signal is such that a high-pass filter with a cut-off frequency of 50 KHz or even 100 KHz would have a negligible effect on the frequency content of the signal. So, we can safely remove most of the low frequency

noise present in the system, without affecting the quality of the received signal.

In general, we are dealing with bit error rates of less than 10^{-4}; worst-case patterns and temporary fluctuations in the channel characteristics are largely responsible for these errors. Channel coding has to improve the worst-case patterns and make detection more reliable in the case of fluctuations in the channel characteristics. The power density spectrums, which have been found by averaging over a long bit sequence and under normal circumstances, cannot reflect an exact picture of the performance of a given channel coding. BER measurements and time-domain considerations (like step and impulse response, eye-width, etc) are more important than power spectral density functions.

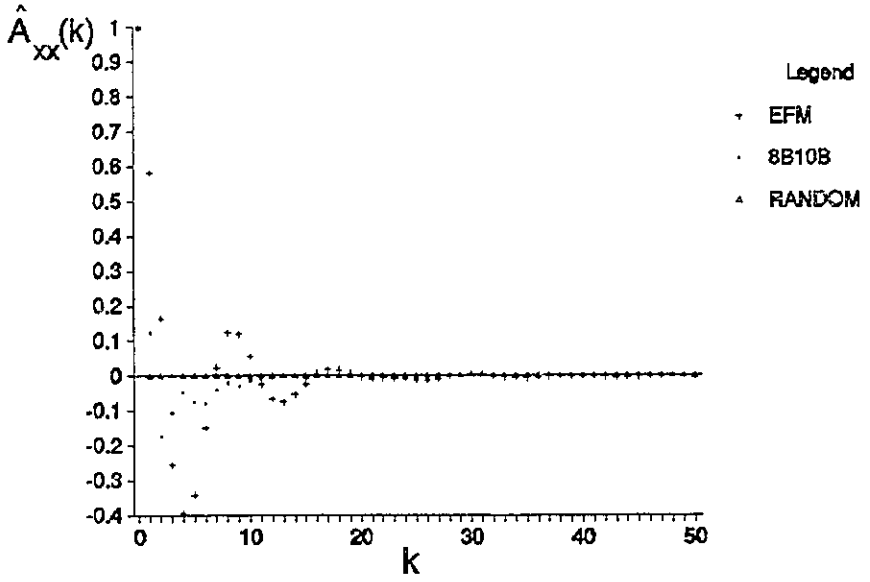

Figure 3.9 Estimates of the discrete autocovariance function for EFM and 8B10B modulations, and the unmodulated random bit stream.

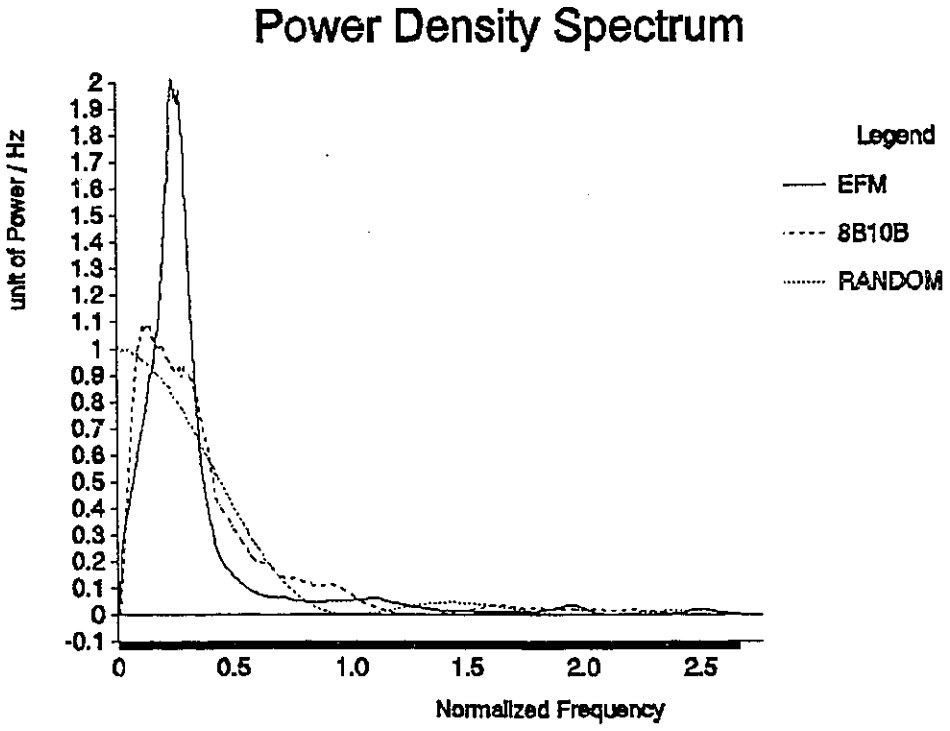

Figure 3.10 The estimated power density spectrums of EFM and 8B10B modulated signals, and the unmodulated random bit stream.

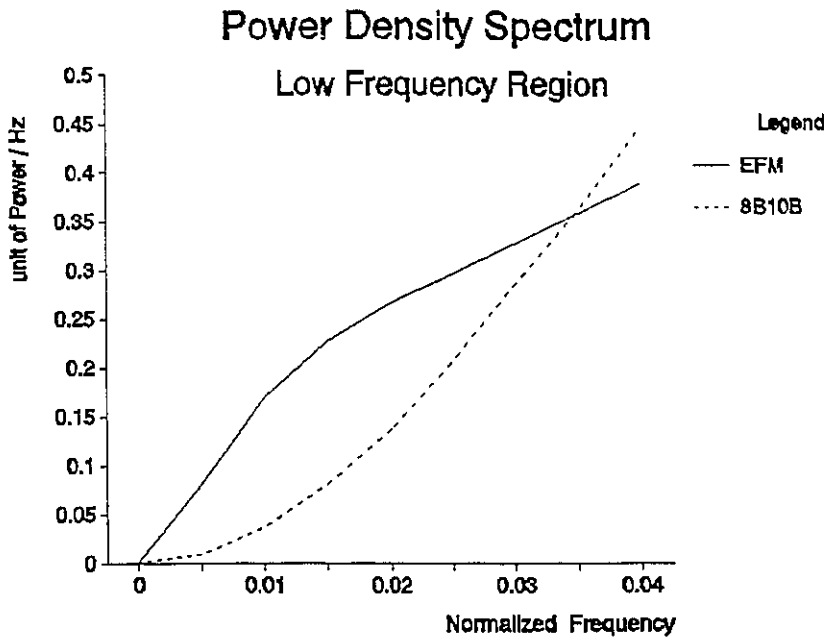

Figure 3.11 Power density spectrums of EFM and 8B10B modulated signals at the low frequency region.

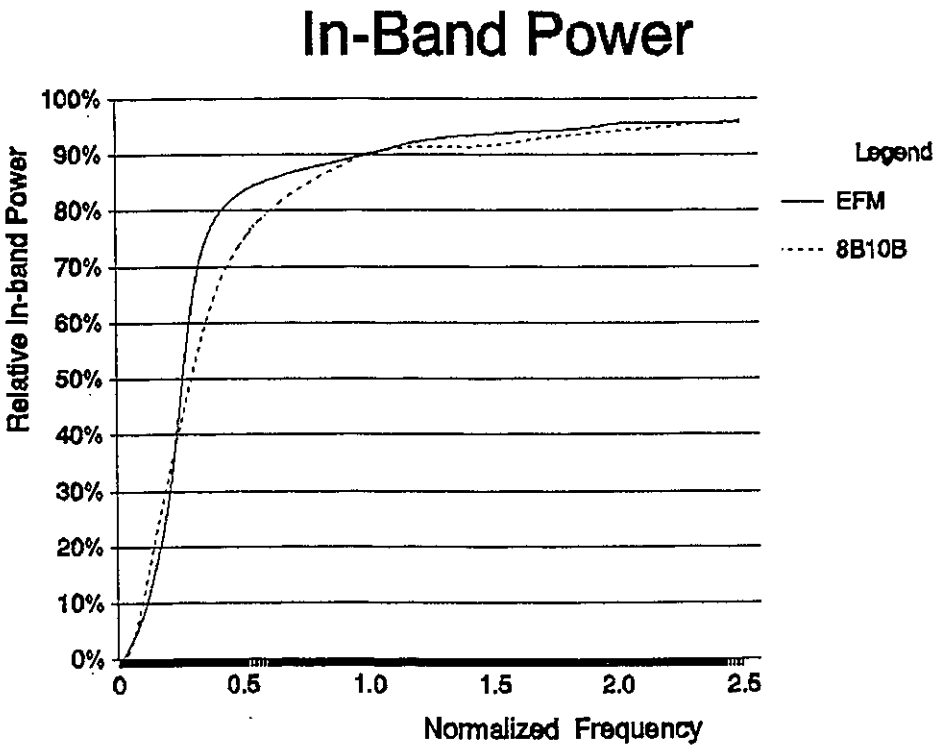

Figure 3.12 In-band power of EFM and 8B10B modulated signals.

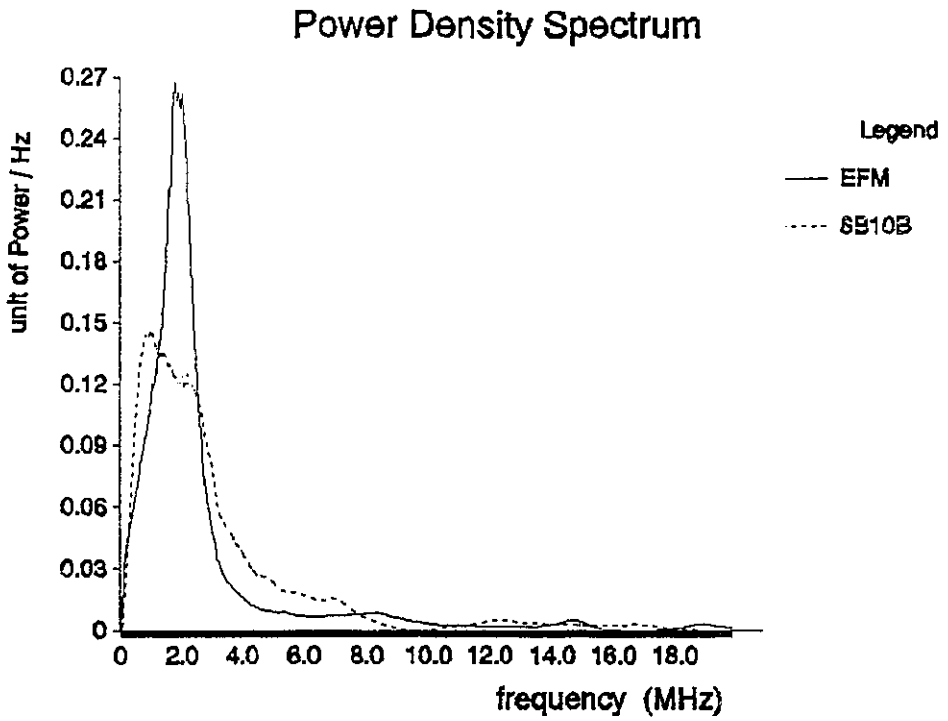

Figure 3.13 Power density spectrum of the multiplexed 4-channel CD stereo audio signal.

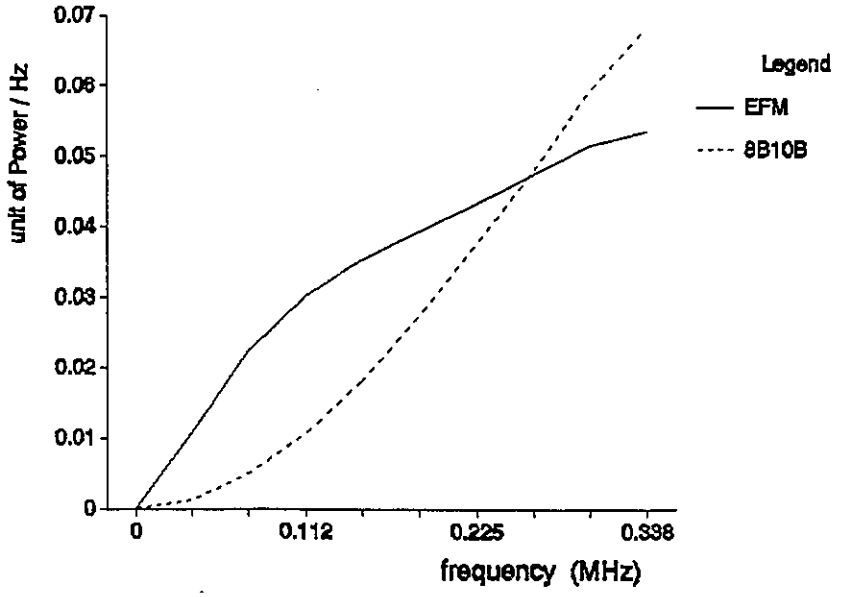

Figure 3.14 Power density spectrum of the multiplexed 4-channel CD stereo audio signal at the low frequency region.

Chapter 4

Performance Evaluation

The two causes of the degradation of the transmitted signal in our system are noise and the multipath dispersion. In addition to common electrical noises present at the receiver, the shot noise associated with the current generated in the photodetector by ambient light can be significant. In this chapter, we first look at the sources of background radiation in a theatre, and discuss how we can reduce their effects on the system. Then, a suitable receiver design is examined and a signal-to-noise ratio analysis is carried out. The receiver employed in a non-directional indoor IR transmission system is operating in an environment different from that of the optical fibre communications; we find an appropriate and simple strategy for designing the receiver so that its performance is optimized. A link power budget calculation is done to find the required transmitted optical power. For the sake of comparison, the power requirement for the case of an analog FM system is computed, as well. Finally, a simulation is performed to find the effects of the multipath dispersion on the performance of the system.

4.1 Ambient Light

In a non-directional optical transmission system, the photodetector has a wide field-of-view and is easily exposed to the ambient light. The electrical current due to the received ambient light with a constant power is accurately modelled as a constant DC term plus a zero-mean white Gaussian shot noise. The magnitude of the DC term and the shot noise power spectral density are both proportional to the incident optical power. The DC term is usually not a problem since it is removed from the signal at the receiver, but the shot noise which can be significant is added to other electrical noises present in the system.

The ambient light sources in a theatre are the projector light, tungsten-filament and fluorescent lamps. The IR radiations from any major heating element should, also, be taken into account. The power density spectrum of some common ambient light sources have been presented in [1]. The incandescent light due to tungsten-filament lamps has most of its power in the infrared region, while the light due to the fluorescent lamps is mostly concentrated in the visible range. So, as far as the noise considerations are concerned, fluorescent lamps are better suited for use in a theatre.

The ambient light can be partly blocked by an optical filter. There are two types of filters: optical interference filters with a narrow pass-band corresponding to the wavelength of the optical source, and the absorption edge filters which block only the visible part of the spectrum. The centre wavelength of the interference filter is a strong function of the angle of the incident light; i.e. they are highly directional and, therefore, are not suitable for a non-directional IR transmission system. Also, an optical filter is used at the projector to suppress the infrared portion of the projector light. As shown in

Fig. 4.1, the transmittances of the receiver infrared filter and the projector filter are such that there is little or no overlap between them; the received projector light will be strongly attenuated. Optical filters are not ideal and due to absorption or reflection of the incident light, transmittance of an optical filter in the pass-band region is less than unity. In our future link power budget calculations, we allow a typical value of 0.75 for the transmittance of the receiver infrared filter. The sensitivity of the silicon photodiode is shown in Fig. 4.1, as well. The silicon photodiode has a peak response around 800 nm wavelength; the operating wavelength should be close to this value (e.g., 820 nm).

There are, in general, fluctuations in the intensity of the ambient light. The projector light is turned on and off at around 100 times a second, and the fluorescent lamps flicker on and off at the line frequency. These fluctuations result in undesired low frequency electrical signals with harmonics which can extend up to tens of KHz. These unwanted signals can be eliminated by an electrical high-pass filter at the receiver. Fortunately, as discussed in the previous chapter, the 8B10B channel modulation allows

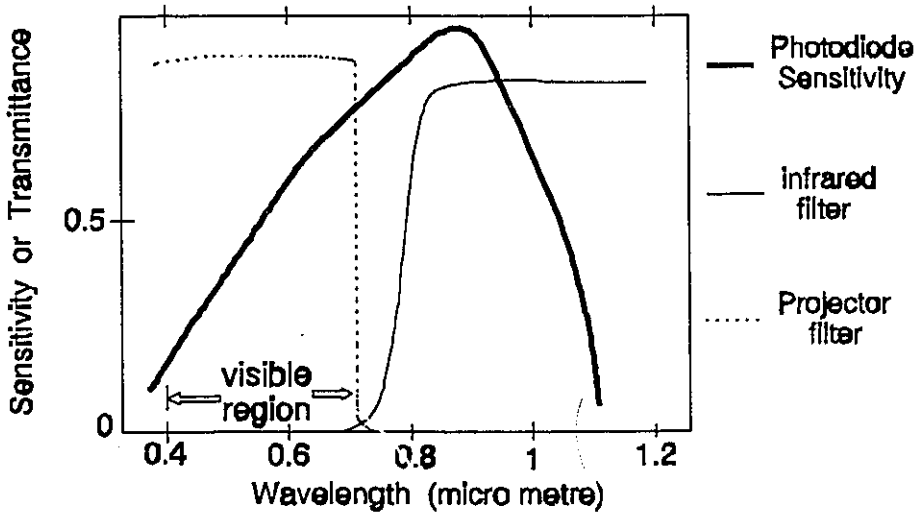

Figure 4.1 Spectral sensitivity of the silicon photodiode, and transmittances of two optical filters.

us to use a high-pass filter with a cut-off frequency of 100 KHz without affecting the quality of the received signal.

The intensity of the ambient light for several office environments and for different optical filters have been measured and reported in [1]. The received background irradiance (optical power per unit area) in an office lighted with fluorescent lamps is between 2 and 15 $\mu W/cm^2$; it is, almost, ten times larger when incandescent light is used. In our analysis, we assume a value of 50 $\mu W/cm^2$ for the received background irradiance after passing through the optical filter.

4.2 Receiver Design

There are two important differences between optical fibre communications and an indoor non-directional infrared communication system. In the latter case, the photodiode surface area is much larger and, also, we have to deal with the presence of a significant background radiation. Because of these differences, the receiver design for an indoor non-directional IR communication system requires an approach which is quite different from that commonly employed in optical fibre communications. Based on the signal-to-noise ratio analysis, we propose a simple approach for the receiver design.

4.2.1 Selection of the Photodiode and the Preamplifier Type

There are two types of photodiodes: avalanche photodiodes (APDs), and positive-negative-intrinsic (pin) photodiodes. APDs provide better sensitivity than pin photodiodes, but they require [2] high reverse bias voltages (e.g., 200 V) and, therefore, are not appropriate for use in battery-powered portable receivers in our system. The best

material for operation in the 800 to 900 nm spectral region is silicon because it has a highly-developed technology and silicon photodiodes have low dark current and high quantum efficiency. So, the photodetector chosen for the receiver in the in-theatre IR audio broadcasting system is the silicon pin photodiode. The dark current of a silicon pin photodiode is around 1 nA and its responsivity (R) is given by [33]

$$R = \frac{\eta\lambda}{1.24}, \tag{4.1}$$

where η is the quantum efficiency, λ is the operating wavelength in μm, and R is in A/W. Assuming that η = 0.76 and λ= 0.82 μm, then R = 0.5 A/W.

As seen in Chapter 2, the difference between the maximum and the minimum received optical signal power in the system can be very large; this means that a high dynamic range at the receiver is required. Transimpedance preamplifier which satisfies this requirement and, also, has a large bandwidth is suitable for our application. The transmitted bit rate in the system is less than 20 Mb/s; the silicon JFET devices which have a unity gain cut-off frequency of 100 to 200 MHz and are relatively cheaper than

Table 4.1 *Typical parameter values of a silicon JFET device.*

Transconductance (g_m)	5-10 mS
Gate-Source capacitance (c_{gs})	3-6 pF
Gate-Drain capacitance (c_{gd})	0.5-1.0 pF
Unity gain cut-off frequency	100-200 MHz
Channel noise factor (Γ)	0.7
1/*f*-noise corner frequency (f_c)	< 100 KHz
Gate leakage current	0.01-0.1 nA

other devices, can be used in the preamplifier. Typical parameter values of a silicon JFET device are Tabulated in Table 4.1.

4.2.2 Analysis of the Receiver Signal-to-Noise Ratio

In our analysis, we are neglecting the shot noise due to the received signal as well as any noise originating in the stages following the preamplifier. Also, the photodiode dark current and the silicon JFET gate leakage current are very small and are ignored. The amplifier flicker noise (or $1/f$-noise) is a low frequency noise; the $1/f$ noise corner frequency (f_c) of a silicon JFET device is less than 100 KHz. Since we are using a high-pass filter with a cut-off frequency of around 100 KHz, the flicker noise can be neglected, as well. So, we will be considering only three noises: the thermal noise due to the input resistance, the shot noise due to the received background radiation, and the FET channel noise current.

A simplified block diagram of the transimpedance receiver is shown in Fig. 4.2. The photodiode capacitance, C_d, is directly proportional to its surface area, i.e., $C_d = c_d A_d$, where c_d is the photodiode capacitance per unit area and A_d is the surface area of the photodiode. The amplifier has an open-loop voltage gain A_0, and an input capacitance C_a. The feedback resistor has been denoted by R_f. To avoid the intersymbol interference (ISI) due to the bandwidth limitation, the amplifier output is equalized to a 100% raised-cosine pulse. The equalizer can be well approximated in practice by a properly chosen low-pass filter [2]. Figure 4.3 shows the noise equivalent circuit diagram of the receiver. The thermal noise, the shot noise, and the noise due to the FET device have been denoted by i_R, i_{shot}, and i_{fet}, respectively. C_t is the total input capacitance where $C_t = C_d + C_a$, and

$R`_f$ is the equivalent input resistance where $R`_f = R_f / (A_v + 1)$. For a large size photodiode (e.g., 1 cm^2), we have $C_d \gg C_a$ and, hence, $C_t \approx C_d = c_d A_d$. The input impedance, Z_{in}, of the receiver can be written as

$$Z_{in} = \frac{R_f}{(1+A_0)+j2\pi f c_d A_d R_f}, \tag{4.2}$$

where f represents the frequency. A low-pass filter is formed at the input of the receiver

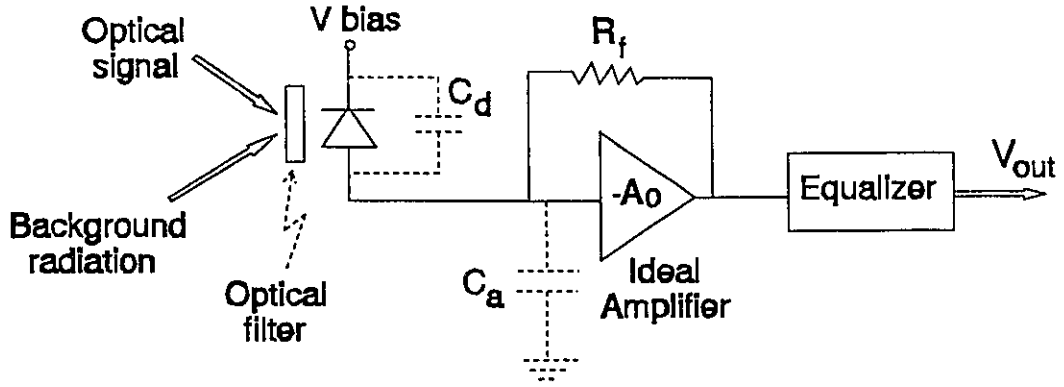

Figure 4.2 Simplified block diagram of the transimpedance receiver.

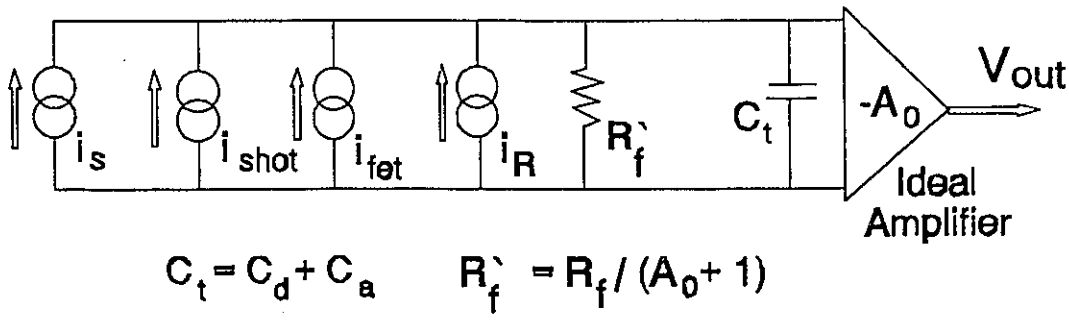

Figure 4.3 Noise equivalent circuit diagram of the receiver.

with a 3-dB bandwidth of

$$f_{3dB} = \frac{A_0 + 1}{2\pi c_d A_d R_f} . \tag{4.3}$$

The FET channel noise current is a white noise with a power spectral density of $4\Gamma kTg_m$ where k is the Boltzmann's constant, T is the absolute temperature, Γ is the FET channel noise factor and g_m is the FET transconductance. It can be easily shown that the power spectral density of this noise, when referred back to the input of the receiver, can be expressed as

$$\frac{d}{df}\langle i_{fet}^2 \rangle = \frac{4kT\Gamma}{g_m}\left[\left(\frac{A_0 + 1}{R_f}\right)^2 + (2\pi f c_d A_d)^2\right] . \tag{4.4}$$

Using (4.3), it is seen that the f^2-noise (the second term) in (4.4) is smaller than the first term when $f < f_{3dB}$, and they are equal at $f = f_{3dB}$. Assuming the postdetection filter (not shown in Fig. 4.2) has a bandwidth lower than f_{3dB}, then the f^2-noise can be ignored, and (4.4) can be rewritten as

$$\frac{d}{df}\langle i_{fet}^2 \rangle = \frac{4kT\Gamma}{g_m}\left(\frac{A_0 + 1}{R_f}\right)^2 . \tag{4.5}$$

The power spectral densities of the thermal noise and the shot are:

$$\frac{d}{df}\langle i_R^2 \rangle = \frac{4kT}{R_f} , \tag{4.6}$$

and

$$\frac{d}{df}\langle i_{shot}^2 \rangle = 2qi_{bg} = 2qI_{bg}A_d R , \tag{4.7}$$

where q is the electron charge, i_{bg} is the photocurrent due to the received background radiation, and I_{bg} is the received background irradiance. Also, the photocurrent due to the

average received optical signal is given by

$$i_s = I_s A_d R \ , \tag{4.8}$$

where I_s is the average received optical signal irradiance.

Now assuming that the 3-dB bandwidth of the receiver input low-pass filter is equal to the channel bit rate (B_c), i.e.,

$$B_c = f_{3dB} = \frac{A_0 + 1}{2\pi c_d A_d R_f} \ , \tag{4.9}$$

and combining (4.5) and (4.9), we obtain

$$\frac{d}{df}\langle i_{fet}^2 \rangle = \frac{4kT\Gamma}{g_m}(2\pi c_d A_d B_c)^2 \ . \tag{4.10}$$

An expression for the feedback resistance (R_f) is obtained by rewriting (4.9),

$$R_f = \frac{A_0 + 1}{2\pi c_d A_d B_c} \ . \tag{4.11}$$

Substituting for R_f from (4.11) in (4.6), we get

$$\frac{d}{df}\langle i_R^2 \rangle = \frac{8kT\pi c_d A_d B_c}{A_0 + 1} \ . \tag{4.12}$$

The power spectral density of the total input-referred noise current is the sum of (4.7), (4.10) and (4.12). i.e.,

$$\begin{aligned} \frac{d}{df}\langle i_{tot}^2 \rangle &= \frac{d}{df}\langle i_R^2 \rangle + \frac{d}{df}\langle i_{shot}^2 \rangle + \frac{d}{df}\langle i_{fet}^2 \rangle \\ &= \frac{8kT\pi c_d A_d B_c}{A_0 + 1} + 2qI_{bg}A_d R + \frac{4kT\Gamma}{g_m}(2\pi c_d A_d B_c)^2 \ . \end{aligned} \tag{4.13}$$

Equations (4.8) and (4.10) show that both the electrical signal power and the FET noise power are proportional to the square of the photodetector area; so, the signal-to-noise ratio

can be improved by increasing the photodetector area up to a certain point where the FET noise becomes the dominant noise, and the *SNR* will not improve significantly beyond that point. In other words, we can say that there is an optimum value for the photodetector area. Let this optimum value be where the FET noise is ten times the sum of the other two noises, i.e.,

$$\frac{d}{df}\langle i_{fet}^2\rangle = 10\left(\frac{d}{df}\langle i_R^2\rangle + \frac{d}{df}\langle i_{shot}^2\rangle\right) . \tag{4.14}$$

By combining (4.14), (4.12), (4.10), and (4.7), the optimum value of A_d is obtained which is

$$A_d = \frac{10 g_m}{8kT\Gamma\pi^2 c_d^2 B_c^2}\left[\frac{4kT\pi c_d^2 B_c^2}{A_0+1} + qRI_{bg}\right] . \tag{4.15}$$

For this value of A_d, the signal-to-noise ratio is

$$(SNR)_{opt} = \frac{10}{11}(SNR)_{max} , \tag{4.16}$$

where $(SNR)_{max}$ is the maximum achievable *SNR* for an infinitely large photodetector area.

To obtain an expression for the signal-to-noise ratio, let the transfer function of the receiver as a whole be equivalent to 100% raised-cosine filter. Then, using (4.13), the total noise power [32] can be written as

$$\langle i_{tot}^2\rangle = \left[\frac{8kT\pi c_d A_d B_c}{A_0+1} + 2qI_{bg}A_d R + \frac{4kT\Gamma}{g_m}(2\pi c_d A_d B_c)^2\right] I_2 B_c , \tag{4.17}$$

where I_2 is the noise bandwidth factor (I_2 = 0.564). The signal-to-noise ratio is

$$SNR = \frac{i_s^2}{\langle i_{tot}^2\rangle} . \tag{4.18}$$

By combining (4.18), (4.17) and (4.8), we obtain an expression for the *SNR*.

$$SNR = \frac{I_s^2 R^2 g_m}{16k\Gamma T\pi^2 c_d^2 B_c^3 I_2} \frac{A_d^2}{\left(A_d^2 + \frac{qI_{bg}Rg_m A_d}{8k\Gamma T\pi^2 c_d^2 B_c^2} + \frac{g_m}{4\Gamma R_f \pi^2 c_d^2 B_c^2}\right)} . \tag{4.19}$$

The second term in (4.19) approaches unity as A_d gets larger, and the first term is, in fact, equal to the $(SNR)_{max}$. By replacing the $(SNR)_{max}$ in (4.16) by the first term of (4.19), the corresponding expression for the $(SNR)_{opt}$ is found;

$$(SNR)_{opt} = \frac{10}{11} \frac{I_s^2 R^2 g_m}{16k\Gamma T\pi^2 c_d^2 B_c^3 I_2} . \tag{4.20}$$

From (4.20) we see that, as expected, $(SNR)_{opt}$ is independent from the thermal noise and the shot noise (i.e., it does not depend on R_f or I_{bg}). It is, also, independent from the value of the amplifier gain (A_0). But, $(SNR)_{opt}$ is inversely proportional to $c_d^2 B_c^3$; so, to achieve a higher *SNR*, we have to use a photodetector with a lower capacitance per unit area (c_d) and we have to reduce the required channel bit rate (B_c) of the system as far as possible.

The above analysis is general and can be applied to any free-space optical communication system using pin-based receivers. Based on this analysis, we propose the following simple procedure for designing the receiver:

(i) choose a convenient and modest value for the amplifier gain (A_0);

(ii) find the optimum value of the photodetector surface area (A_d) from (4.15);

(iii) find the value of the feedback resistor (R_f) from (4.11).

This analysis showed that increasing the photodetector area beyond a certain point will not improve the signal-to-noise ratio any further. But, we can achieve a 3 dB

improvement in the signal-to-noise ratio if we use two photodetectors, each followed by its own preamplifier, and combine the two resultant signals. This improvement is due to the fact that the signals add in amplitude but the noises add in power.

4.3 Link Power Budget Calculations

In this section, we apply the analysis discussed in the previous section to a typical receiver design example to find the required transmitted optical power in the in-theatre audio broadcasting system. To distinguish between different channel modulation schemes, we replace the channel bit rate (B_c) in the equations derived in the previous section by $B_d r_c$ where B_d is the data bit rate and r_c is the redundancy of the channel code. The values assumed for different variables in our example are shown in Table 4.2.

Table 4.2 Assumed values for the variables in the receiver design example.

variable	value
data bit rate (B_d)	7.5264 Mb/s
photodetector responsivity (R)	0.5 A/W
photodetector capacitance per unit area (c_d)	100 pF/cm^2
FET channel noise factor (Γ)	0.7
FET transconductance (g_m)	10 mS
absolute temperature (T)	290 K
transmittance of the receiver optical filter (T_f)	0.75
received background irradiance after the optical filter (I_{bg})	50 μW/cm^2
open-loop voltage gain of the transimpedance amplifier (A_0)	20

As shown in Table 4.2, a modest value for A_0 has been chosen: $A_0 = 20$. Following the

procedure given in the previous section, we obtain the optimum value of the photodetector surface area (A_d) and the value of the feedback resistor (R_f). These values are shown in Table 4.3. For comparison purposes, we are considering the unmodulated case in addition to EFM and 8B10B channel modulations. To refresh our memory, the value of the redundancy (r_e) is, also, shown in Table 2.3.

Table 4.3 The derived values of A_d and R_f for EFM and 8B10B modulations, and the unmodulated case.

	EFM	8B10B	Unmodulated
redundancy (r_e)	2.23	1.29	1
the optimum value of A_d (cm^2)	1.3	3.0	4.6
R_f (Ω)	1532	1146	965

To better understand the relationship between the photodetector surface area and the signal-to-noise ratio, we substitute for the corresponding values from Table 4.2 in (4.19) to obtain

$$SNR = \left[2.35 \times 10^{15} \frac{I_s^2}{r_e^3}\right] \frac{1}{1 + \frac{3.02}{r_e A_d}\left(\frac{1}{21} + \frac{0.1057}{r_e}\right)}, \qquad (4.21)$$

where I_s is in W/cm^2 and A_d is in cm^2. Similar to (4.19), it is seen that the second term in (4.21) approaches unity as A_d gets larger, and the first term (the term inside the square brackets) is equal to the $(SNR)_{max}$. For a given value of I_s and by substituting the value of r_e corresponding to different modulations in (4.21), we obtain the following normalized expressions for the signal-to-noise ratio:

$$(SNR)_{normalized} = \begin{cases} \dfrac{A_d}{A_d + 0.463}, & unmodulated\ ; \\ \dfrac{A_d}{2.155A_d + 0.652}, & 8B10B\ ; \\ \dfrac{A_d}{11.1A_d + 1.427}, & EFM\ . \end{cases} \tag{4.22}$$

The expressions of (4.22) have been normalized such that the maximum *SNR* value for the unmodulated case is equal to unity; they have been plotted in Fig. 4.4. The performance of 8B10B modulation is better than that of EFM by 7.1 dB in terms of the electrical power (or 3.55 dB in optical power); this is due to $1/r_c^3$ dependence of *SNR* as shown in the first term of (4.21). This relation between *SNR* and the redundancy (r_c) explains clearly why a low-redundant channel code like 8B10B is much more advantageous for an indoor free-space optical communication system.

We first find the transmitted power necessary to satisfy the requirements of the reference case discussed in Section 2.2 and represented by (2.7). Then, we take into account the different penalty factors present in the system, and allow for the fact that, as shown in Table 2.2, the received power is lower at other situations compared with the reference case. By replacing $(SNR)_{max}$ in (4.16) with the first term of (4.21), we obtain

$$(SNR)_{opt} = 2.136 \times 10^{15} \frac{I_s^2}{r_c^3} . \tag{4.23}$$

Using (2.7), we can write

$$I_s = 10^{-4} T_f \frac{0.4 P_t}{144\pi} , \tag{4.24}$$

where I_s is in W/cm^2 and T_f is the transmittance of the optical filter. Assuming $T_f = 0.75$

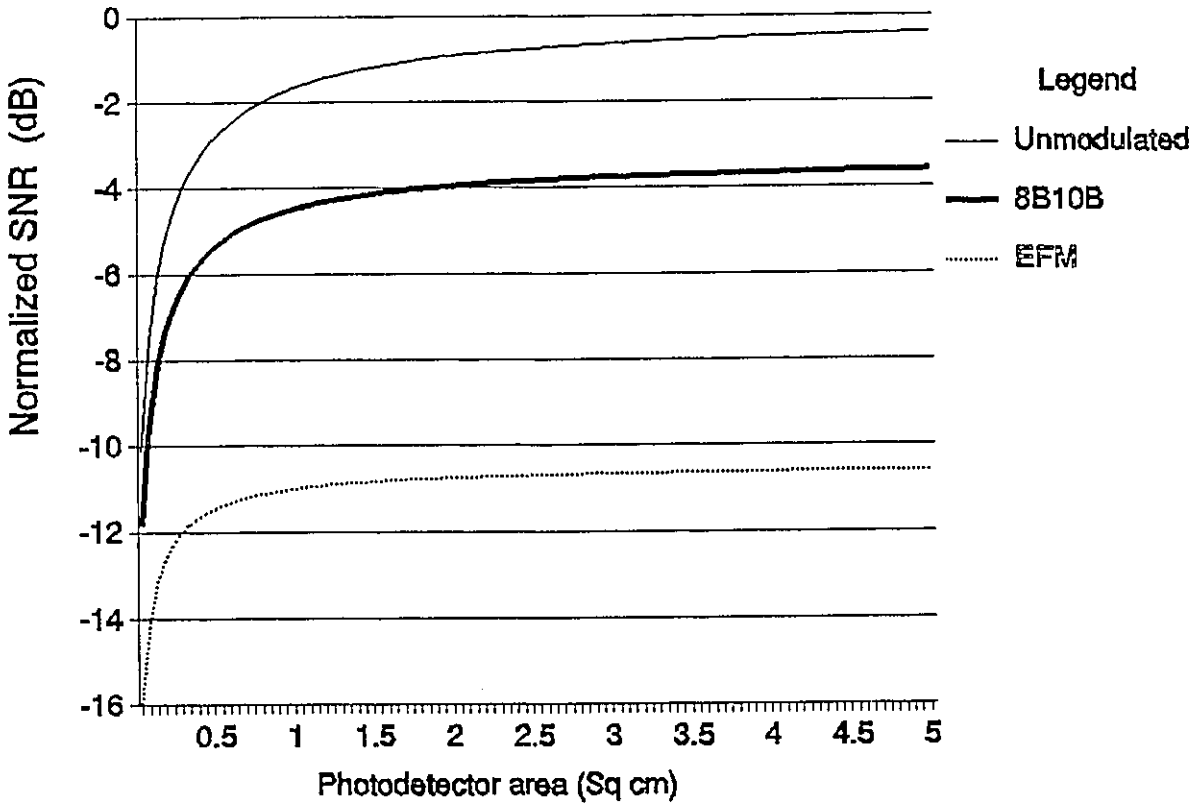

Figure 4.4 Normalized signal-to-noise ratio as a function of the photodetector area. EFM and 8B10B modulations, and the unmodulated case have been considered.

and substituting for I_r from (4.24) in (4.23), after simplification we obtain

$$(SNR)_{opt} = 9.39 \frac{P_t^2}{r_e^3} \ . \tag{4.25}$$

By rearranging (4.25), the transmitted optical power (P_t) can be expressed as

$$P_t = 0.326\, r_e^{3/2} \sqrt{(SNR)_{opt}} \ , \tag{4.26}$$

where P_t is in watts. It is known [31] that the bit error rate (BER) for this digital binary scheme is simply given by

$$BER = Q\left(\sqrt{SNR}\right) , \tag{4.27}$$

where $Q(.)$ is the well-known Q-function with numerical values tabulated in most communication text books. We saw in Section 3.1.3, that the CD system performs quite well at a BER of 10^{-4}, from the Q-function tables, we have $Q(\sqrt{13.69}) = 10^{-4}$. We can thus substitute for SNR = 13.69 in (4.26) to get

$$P_t = 1.21\, r_e^{3/2} \ . \tag{4.28}$$

Equation (4.28) gives the required transmitted optical power for the reference case. The received power in other cases such as the locations close to the edge of the audience area in the theatre or the case with a high gain screen are lower than that of the reference case. So, the transmitted power has to be increased from that given by (4.28); let us allow a 4-dB factor for this (Table 2.2 suggests that a higher value has to be chosen for this factor when a high gain screen is used). Furthermore, there are degradations in the performance of the system due to temperature, aging, laser extinction ratio, imperfect equalization (ISI), noise from post amplifier, improper sampling threshold, improper decision phase,

etc. We allow a total penalty factor of 3 dB for all these degradations. So, an overall increase of 7 dB in the transmitted optical power is required. Increasing (4.28) by 7 dB, we obtain

$$P_t = 6.06\, r_e^{3/2} \ . \tag{4.29}$$

By substituting for corresponding values of r_e from Table 4.3 in (4.29), we find the required transmitted optical power for different channel modulation schemes; this is shown in Table 4.4.

Table 4.4 The required transmitted optical power (P_t) for different channel coding schemes.

	EFM	8B10B	Unmodulated
P_t in watts	20.2	8.9	6.06

4.4 A Worked Example on an Analog FM System

To make a comparison between the analog FM and the CD-based digital scheme, we compute the required transmitted optical power for an analog FM system in this section. We consider the optical subcarrier modulation of FM signals with multiple optical sources as was shown previously in Fig. 1.3. Each stereo audio signal is FM modulated on a distinct carrier and the resultant FM signal is transmitted by a separate optical source. In our example, we assume a standard stereo audio signal of bandwidth W = 53 KHz. The FM signal [31] has a bandwidth of $2(D + 2)W$ where D is the deviation ratio. Assuming a deviation ratio of 3 (i.e., D = 3), the bandwidth of each FM

signal will be 530 KHz. After allowing a reasonable frequency separation between the neighbouring FM signals, let us assume that the combination of four FM signals occupies a bandwidth from 100 KHz to 2.5 MHz. Also, let the highest frequency component of the combined transmitted signal be denoted by B_T where B_T = 2.5 MHz in this case. Now, the 3-dB cut-off frequency (f_{3dB}) of the low-pass filter at the input of the receiver amplifier has to be at least equal to B_T. So, similar to (4.9), we can write

$$B_T = f_{3dB} = \frac{A_0 + 1}{2\pi c_d A_d R_f} , \tag{4.30}$$

and the receiver noise calculations follows in the same manner as described in Section 4.2.2; we only have to replace B_c by B_T in the corresponding equations of that section. Using (4.13), the noise power spectral density (N_0) for the receiver can be written as

$$N_0 = \frac{8kT\pi c_d A_d B_T}{A_0 + 1} + 2qI_{bg}A_d R + \frac{4kT\Gamma}{g_m}(2\pi c_d A_d B_T)^2 . \tag{4.31}$$

The transmitted optical power has been divided equally between four FM signals; so, the received electrical power (S_r) corresponding to each FM signal can be expressed as

$$S_r = \frac{1}{2}\left(\frac{I_s}{4}\right)^2 A_d^2 R^2 , \tag{4.32}$$

where 1/2 factor in (4.32) is due to the fact that the FM signal is inherently 3 dB inferior to a NRZ OOK digital signal. The signal-to-noise ratio of the detected signal [31] after the FM demodulator is given by

$$(SNR)_D = \frac{3}{2} D^2 \frac{S_r}{N_0 W} . \tag{4.33}$$

By combining (4.31), (4.32) and (4.33), we obtain

$$(SNR)_D = \frac{3D^2 I_s^2 R^2 g_m}{(1024)k\Gamma T\pi^2 c_d^2 B_T^2 W} \frac{A_d^2}{\left(A_d^2 + \frac{qI_{bg}Rg_m A_d}{8k\Gamma T\pi^2 c_d^2 B_T^2} + \frac{g_m A_d}{2\Gamma\pi c_d B_T (A_0+1)}\right)} \quad . \tag{4.34}$$

The second term of (3.14) approaches unity as A_d gets larger and the first term is the maximum achievable value of $(SNR)_D$. Similar as before, the optimum value of the photodetector area is found which is equal to 33.2 cm^2. At this optimum point, $(SNR)_D$ can be expressed as

$$(SNR)_D = \frac{10}{11} \frac{3D^2 I_s^2 R^2 g_m}{(1024)k\Gamma T\pi^2 c_d^2 B_T^2 W} \quad . \tag{4.35}$$

Equation (4.35) shows that $(SNR)_D$ is a function of D^2/B_T^2. But, B_T is somewhat proportional to D and, therefore, $(SNR)_D$ will not change much by varying the deviation ratio (D). By substituting for B_T = 2.5 MHz, W = 53 KHz, and the values of other variables from Table 4.2 in (4.35), we get

$$(SNR)_D = 2.876 \times 10^{17} I_s^2 \quad , \tag{4.36}$$

where I_s is in watts/cm^2. Now, we substitute for I_s from (4.24) in (4.36) to obtain

$$(SNR)_D = 2.876 \times 10^3 P_t^2 \quad . \tag{4.37}$$

By rearranging (4.37), P_t can be expressed as

$$P_t = 18.65 \times 10^{-2} \sqrt{(SNR)_D} \quad . \tag{4.38}$$

The analog FM system has to match the performance of the CD-based digital scheme which provides a signal-to-noise ratio of more than 90 dB. Replacing $(SNR)_D$ in (4.38) by 10^9, we get

$$P_t = 5897.65 \ watts \quad . \tag{4.39}$$

Comparing (4.39) and (4.28) shows that the CD-based digital audio system provides a very large gain (around 32 dB in optical power) over the analog FM scheme in the in-theatre audio broadcasting system.

4.5 Multipath Considerations

We carried out a simulation of the in-theatre IR digital transmission system to examine the effects of the multipath dispersion on the performance of the system. This simulation is based on the IR channel model derived in Section 2.3. The block diagram of the simulation system is shown in Fig. 4.5. Random 8-bit symbols are generated and passed to a channel modulator which could use EFM or 8B10B modulation. The modulated NRZ binary data with a rectangular pulse shape are passed through the multipath optical channel; this channel is modelled as a tapped delay line. Then, white Gaussian noise is added to the received signal, and the resultant signal is passed to a post detection filter. The post detection filter is either an RC low-pass filter or an integrate and dump (ID) filter. The bit error rate can be found by comparing the detected channel bits with the transmitted bits. As shown in Fig. 4.5, we used a sampling period of $T_c/20$ where T_c is the channel bit period.

First, as an illustrative example, we compare the eye diagrams of the EFM and the 8B10B modulated signals. Figures 4.6 and 4.7 show the corresponding eye diagrams at the SNR values of 22 dB and 10 dB, respectively. An RC low-pass filter with a 3-dB bandwidth of $0.5/T_d$ has been used, and no multipath has been introduced. It is clearly seen that the 8B10B modulated signal has a better eye diagram compared with the EFM signal. Moreover, although not shown in these two figures, we remember from Table 3.8

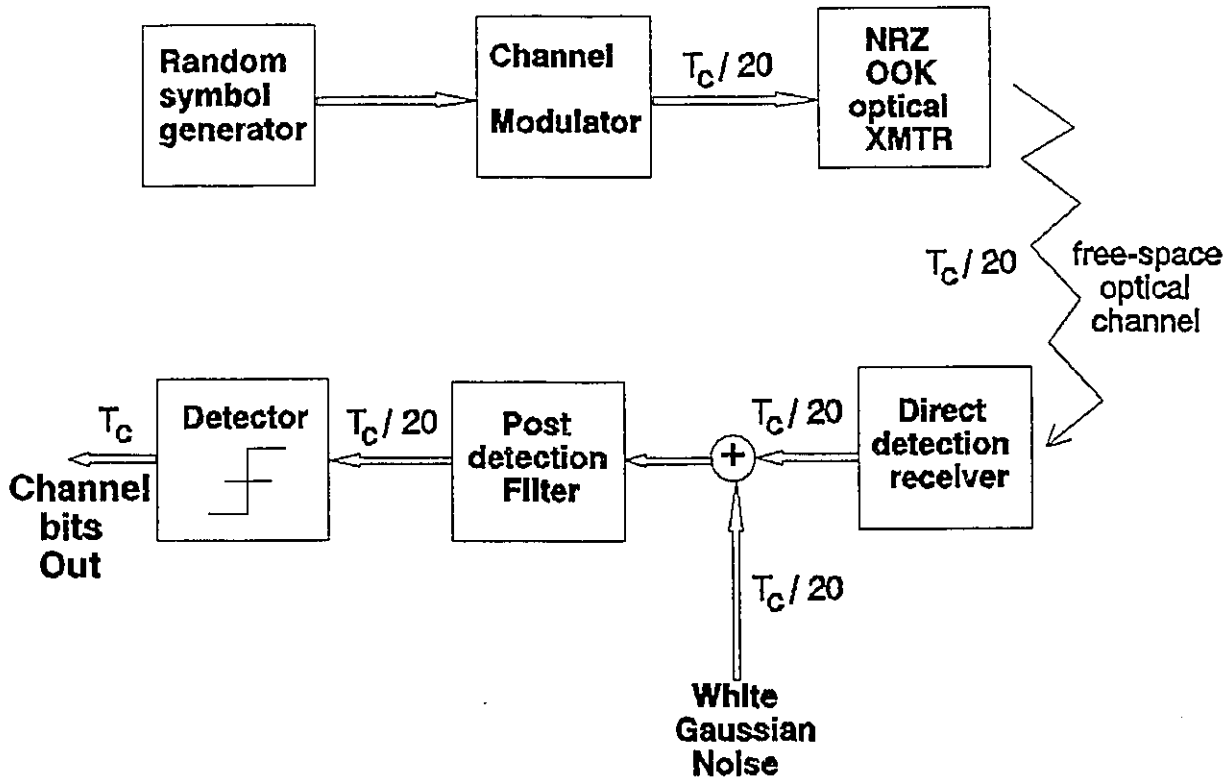

Figure 4.5 Block diagram of the simulated in-theatre infrared link.

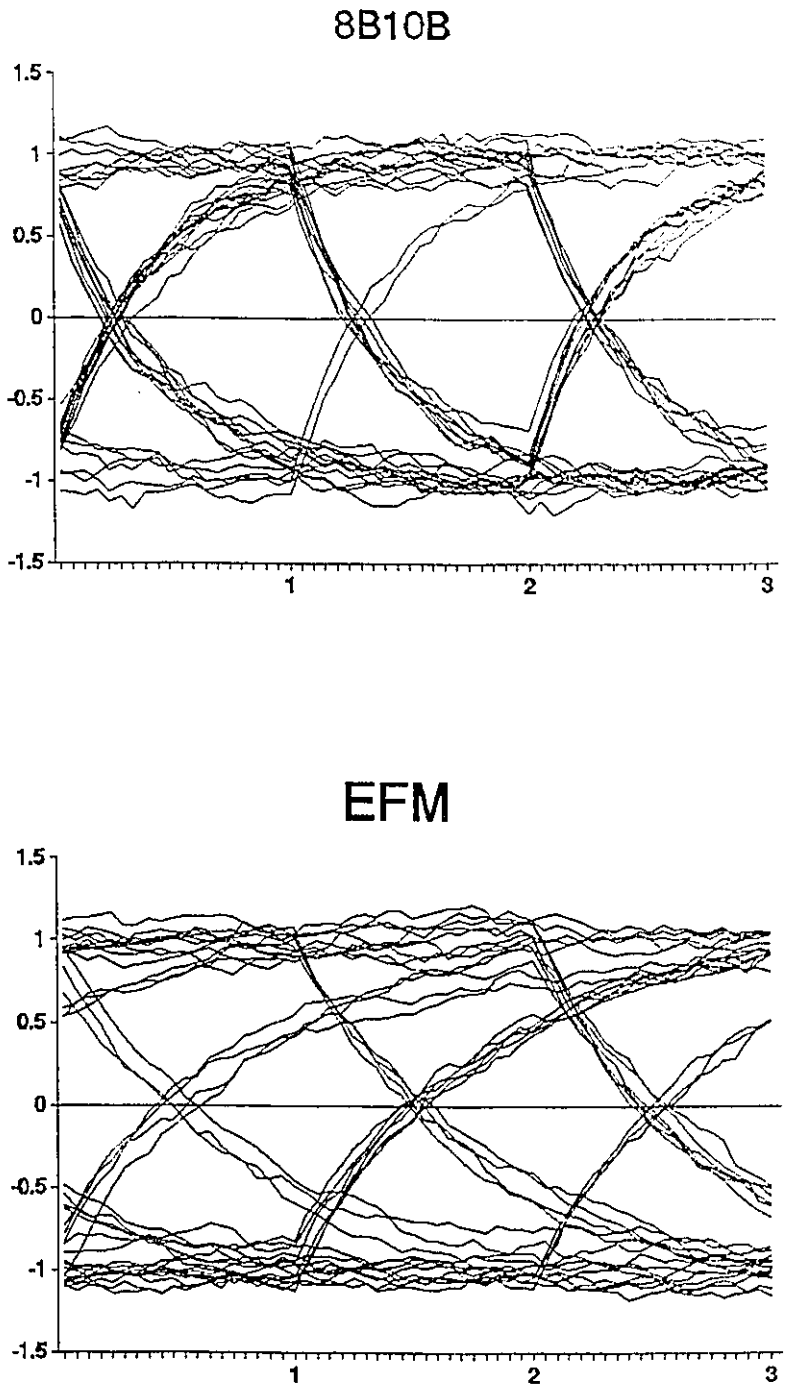

Figure 4.6 *Eye-diagram of the EFM (the bottom fig.) and the 8B10B (the top fig.) channel modulations at SNR = 22 dB, and using an RC LPF with a 3-dB bandwidth of* $0.5/T_d$.

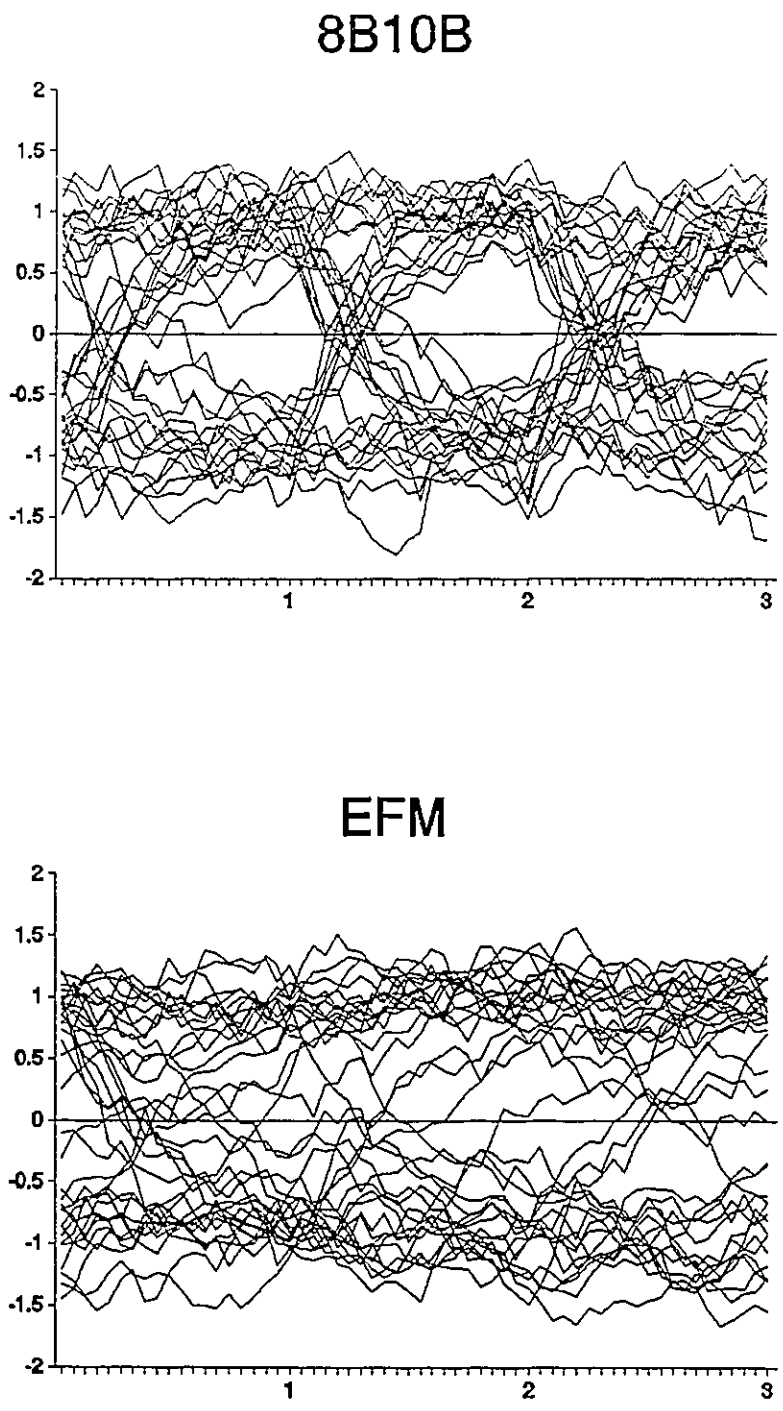

Figure 4.7 Eye-diagram of the EFM (the bottom fig.) and the 8B10B (the top fig.) channel modulations at SNR = 10 dB, and using an RC LPF with a 3-dB bandwidth of $0.5/T_d$.

that the eye-width in EFM is narrower than that of 8B10B modulation (their ratio is less than 3/5).

To find an appropriate bandwidth for the low-pass filter, we found the bit error rate (BER) at different 3-dB bandwidths of the RC low-pass filter; Figures 4.8 and 4.9 show the simulation results for EFM and 8B10B modulations respectively. For the sake of comparison, the BER with the integrate and dump (ID) filter is, also, shown in these figures. A channel with a single path has been used to obtain these results. It is observed that EFM performs best at a 3-dB bandwidth of around $0.75/T_d$ where T_d is the data bit period. The best 3-dB bandwidth for 8B10B modulation is around $0.45/T_d$ (or $0.5/T_d$). As expected, 8B10B modulation requires a smaller bandwidth than that of EFM. In other parts of the simulation, where ever the RC LPF is used, its 3-dB bandwidth is $0.75/T_d$ for EFM and $0.5/T_d$ for 8B10B.

We consider three different multipath cases in our simulation; the normalized impulse responses of the optical channel for these cases are shown in Fig. 4.10. These responses represent the optical power or equivalently the electrical amplitude. These multipath cases can be related to the IR transmission configurations with two diffusing spots on the dome as was described in Section 2.2. The cases 1 and 3 correspond to the situation where there are only two paths from the two spots and there are no reflections from the audience area. The second case can be related to a situation where there are two equal components arriving from the two spots and, also, there are two weaker components reflected from the audience area. The reflected components increase the received optical power by 1.55 dB (or 3.1 dB electrical power).

The bit error rate for different multipath cases are shown in Figures 4.11 and 4.12 for EFM and 8B10B modulation, respectively. Both the integrate and dump filter and the

RC LPF have been considered. To find out how much degradation is caused by the multipath distortions, the case with no multipath (i.e., only a single path) has also been included in the results. The integrate and dump filter is a matched filter and naturally performs better than the RC LPF when there is no multipath. But, as the multipath effects get stronger, the multipath-induced ISI dominates the total ISI and the integrate and dump filter loses its advantage over the RC LPF. At a BER of 10^{-4}, the performance of the system at the multipath case 2 is lower than that of the multipath case 1 by around 2 dB for EFM and by less than 0.5 dB for 8B10B. But, as we said before, the components reflected from the audience area in case 2 increase the received electrical power by 3.1 dB. Therefore, the reflections from the audience area in this particular case provide a net gain.

The corresponding bit error rates of EFM and 8B10B modulations with the RC LPF and at different multipath cases have been plotted in the same graph as shown in Fig. 4.13. It is observed that EFM is affected more severely by the multipath dispersion compared with 8B10B. At a BER of 10^{-4}, the difference between the worst multipath case (case 2) and the no multipath case is about 5 dB for EFM and only about 1.2 dB for 8B10B.

Finally, we used the maximum-likelihood sequence estimation (MLSE) by applying the Viterbi algorithm with soft-decision decoding on the detected symbols to find out how much such a complex scheme would improve the performance of the system. The value of the running digital sum (RDS) was chosen to represent the state at each point along the sequence. In 8B10B modulations, there are only two states because the RDS value is either 0 or +2, and the number of branches are 256 (= 2^8). The memory in the 8B10B modulated sequence is relatively short; the memory extends only to the last

symbol whose digital sum value is +2 or -2. Unfortunately, the EFM modulated sequence is much more complex mainly due to the merging bits placed between the transmitted symbols. The memory in the EFM modulated sequence is virtually infinite because the current state (the RDS value) depends on all the symbols transmitted in the past. Also, both the number of states and the number of branches are very large and state reduction, in this case, is not an easy task. So, the Viterbi algorithm was applied only on the 8B10B modulation and we did not include the EFM in this part of the simulation. Figure 4.14 shows the bit error rate for 8B10B modulation at different multipath cases, using Viterbi algorithm with soft decision decoding. The curves in this figure are very similar to the curves shown in Fig. 4.12 except that they have moved to the left by 2 dB. This is shown in Fig. 4.15 where the bit error rates with and without applying the Viterbi algorithm have been compared. The Viterbi algorithm with soft-decision decoding provides a gain of only 2 dB (or 1 dB in terms of the optical power).

In summary, the simulation results of this section show the followings:

(i) 8B10B modulation requires less bandwidth compared with EFM, ($0.5/T_d$ compared with $0.75/T_d$);

(ii) EFM is affected more severely by the multipath distortion than 8B10B modulation;

(iii) it suffices to use a simple low-pass filter as the post detection filter at the receiver;

(iv) the reflections from the audience area are not necessarily harmful and can even result in a net gain; and

(v) Viterbi soft decision decoding provides only 1 dB optical gain for 8B10B modulation and thus such a sophisticated detecting scheme is not warranted in the receivers in our system; (the receivers have to be simple and inexpensive).

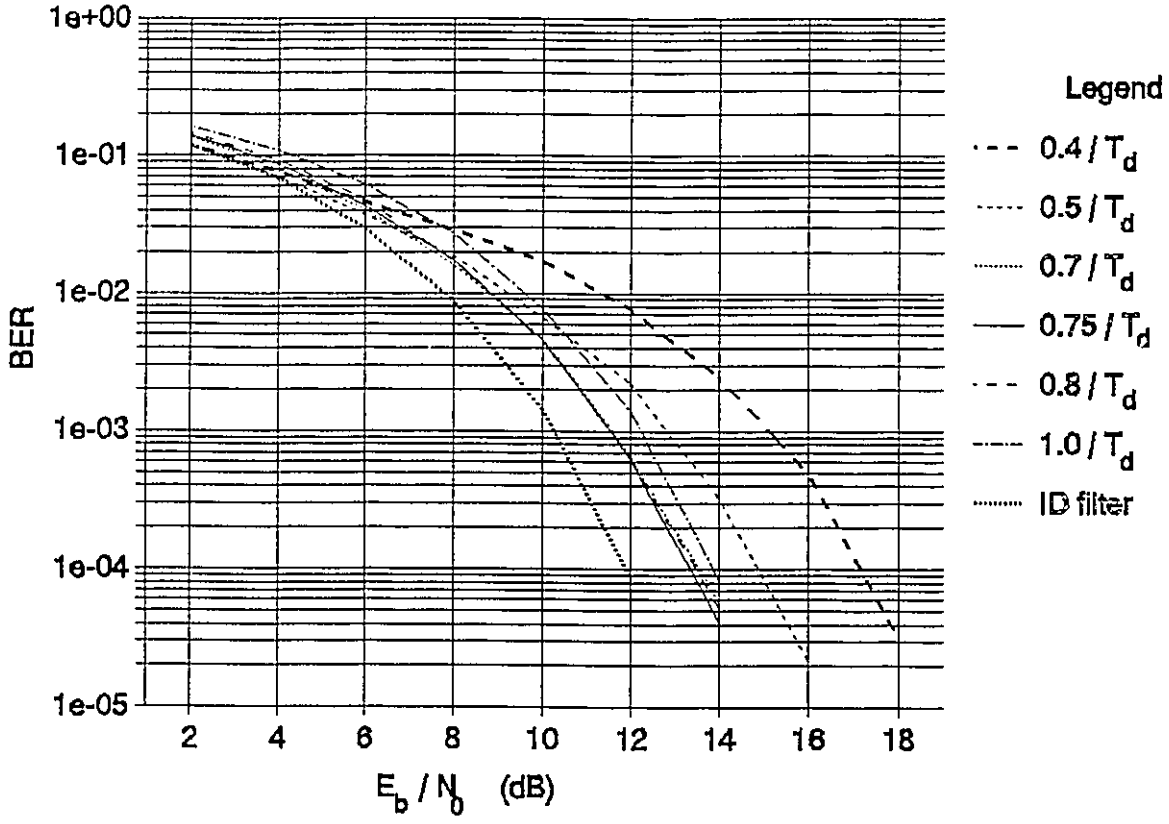

Figure 4.8 BER for EFM at different 3-dB bandwidths of the RC LPF, with a single path in the channel. The results for the integrate and dump (ID) filter have, also, been included.

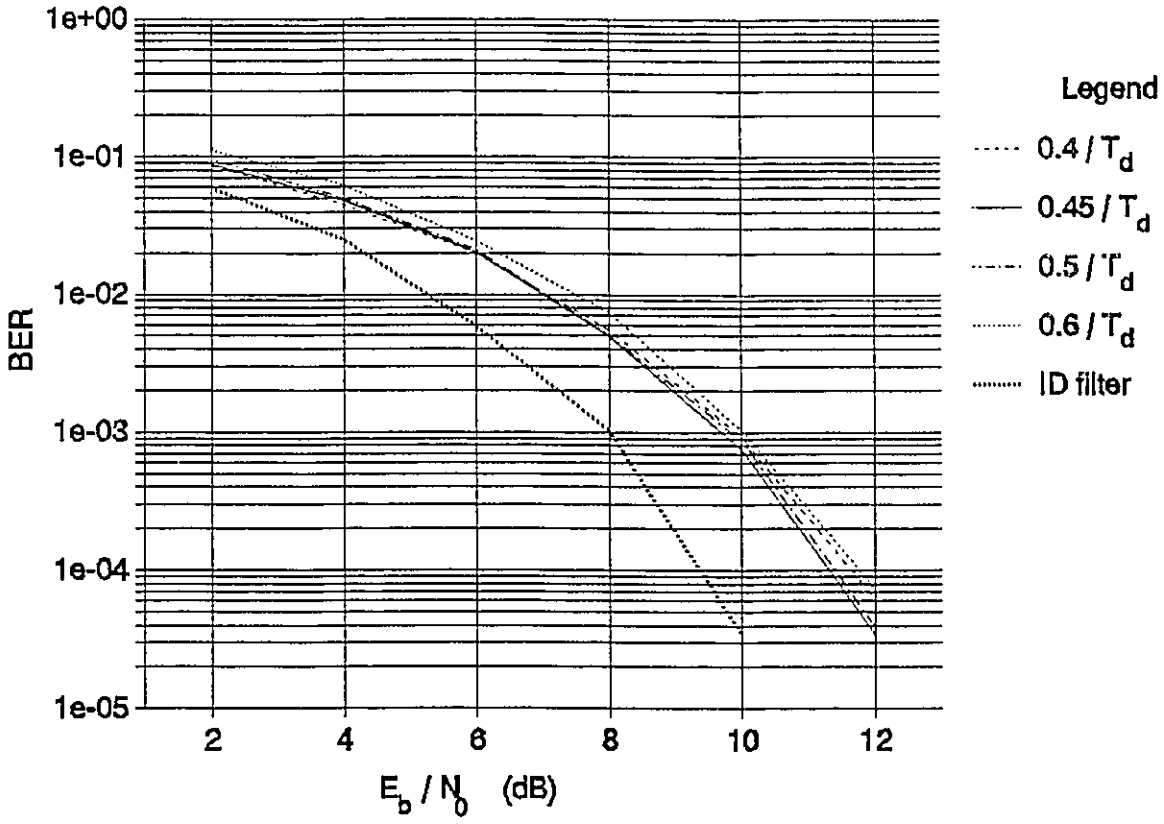

Figure 4.9 BER for 8B10B at different 3-dB bandwidths of the RC LPF, with a single path in the channel. The results for the integrate & dump (ID) filter have, also, been included.

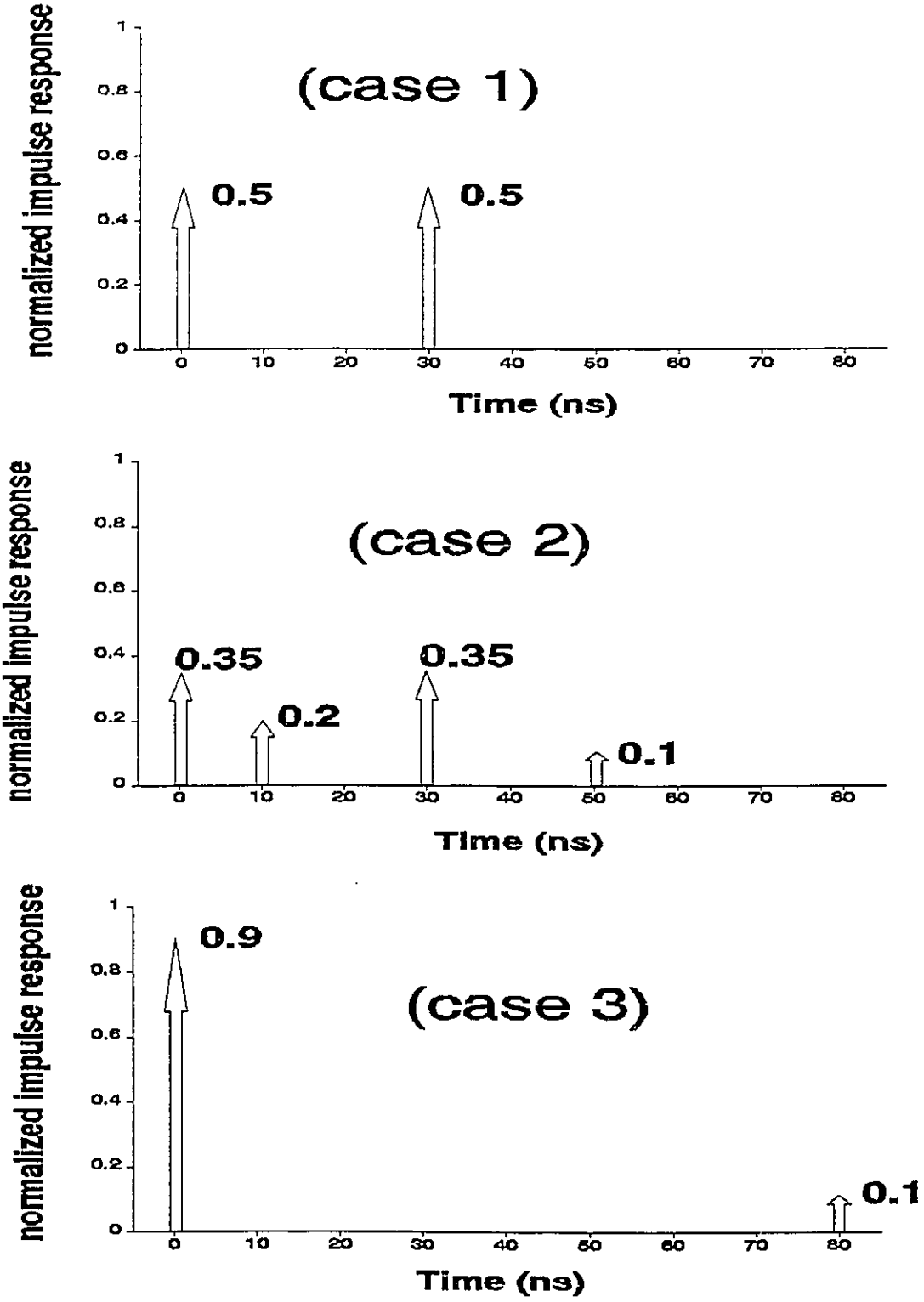

Figure 4.10 The normalized impulse response of different multipath cases considered.

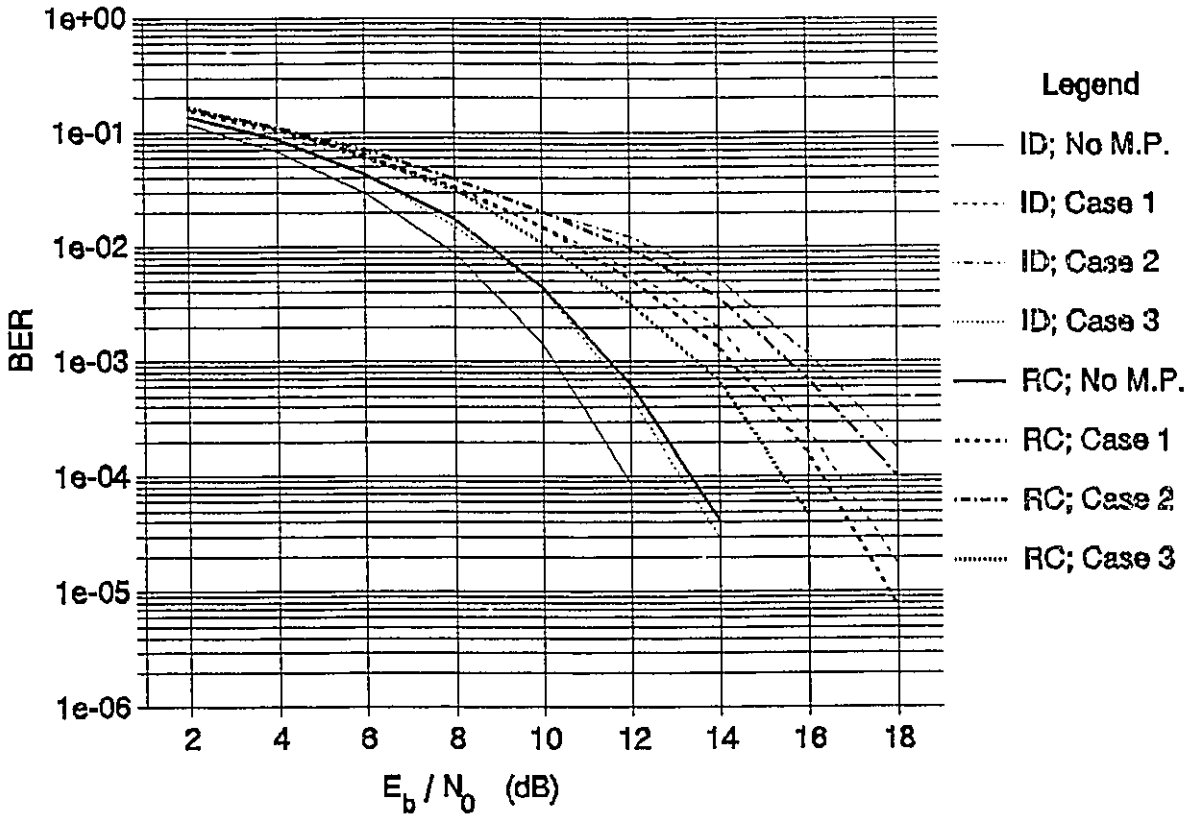

Figure 4.11 BER for EFM at different multipath cases, with the integrate and dump (ID) filter or with the RC LPF. The 3-dB bandwidth of the RC LPF is $0.75/T_d$.

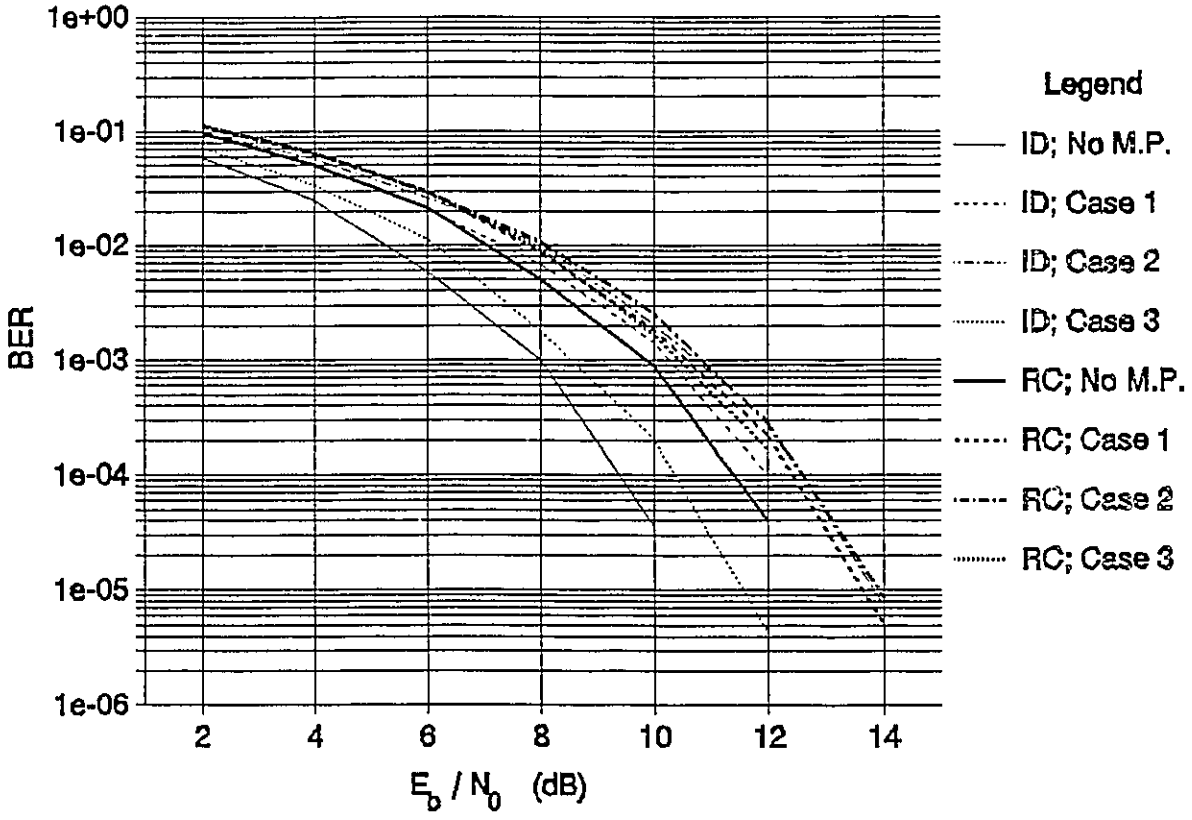

Figure 4.12 BER for 8B10B at different multipath cases, with the integrate and dump (ID) filter or with the RC LPF. The 3-dB bandwidth of the RC LPF is $0.5/T_d$.

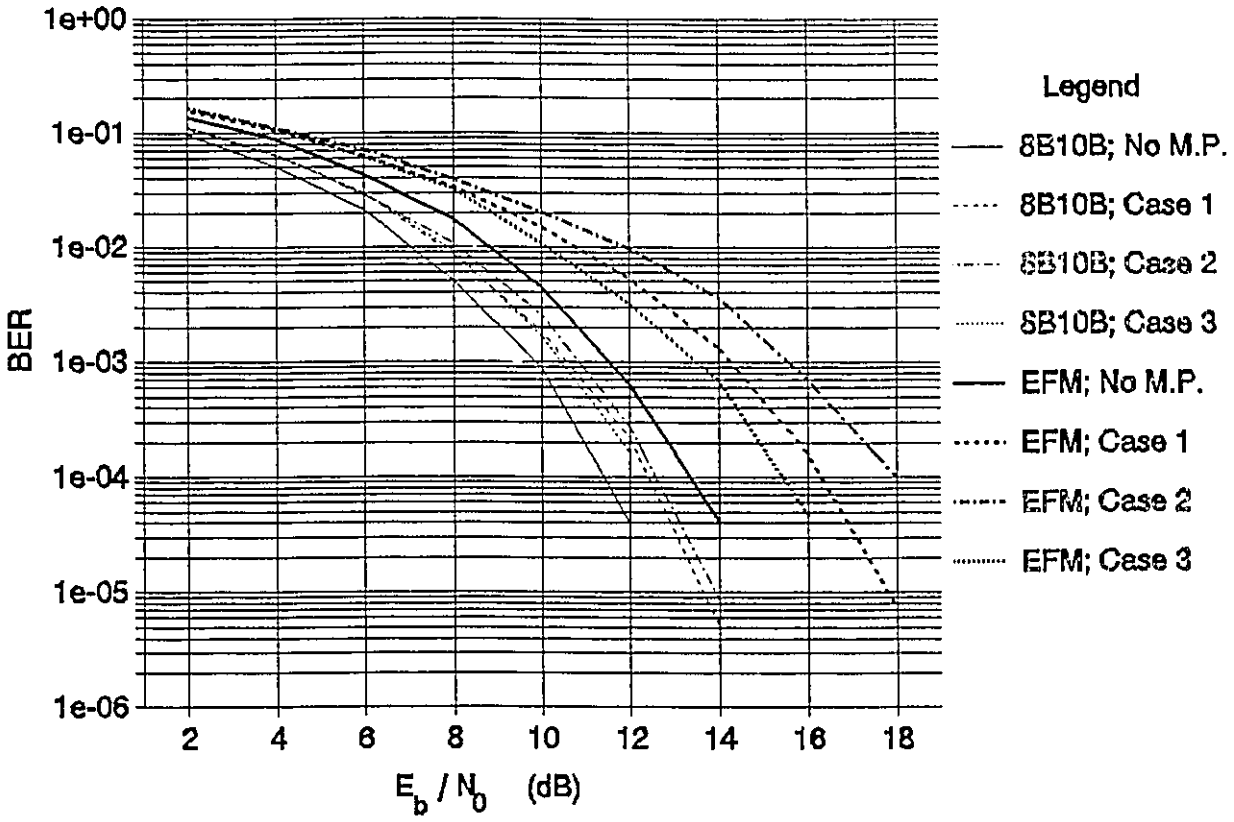

Figure 4.13 A comparison of BER for EFM and 8B10B modulations at different multipath cases; the RC LPF has been used.

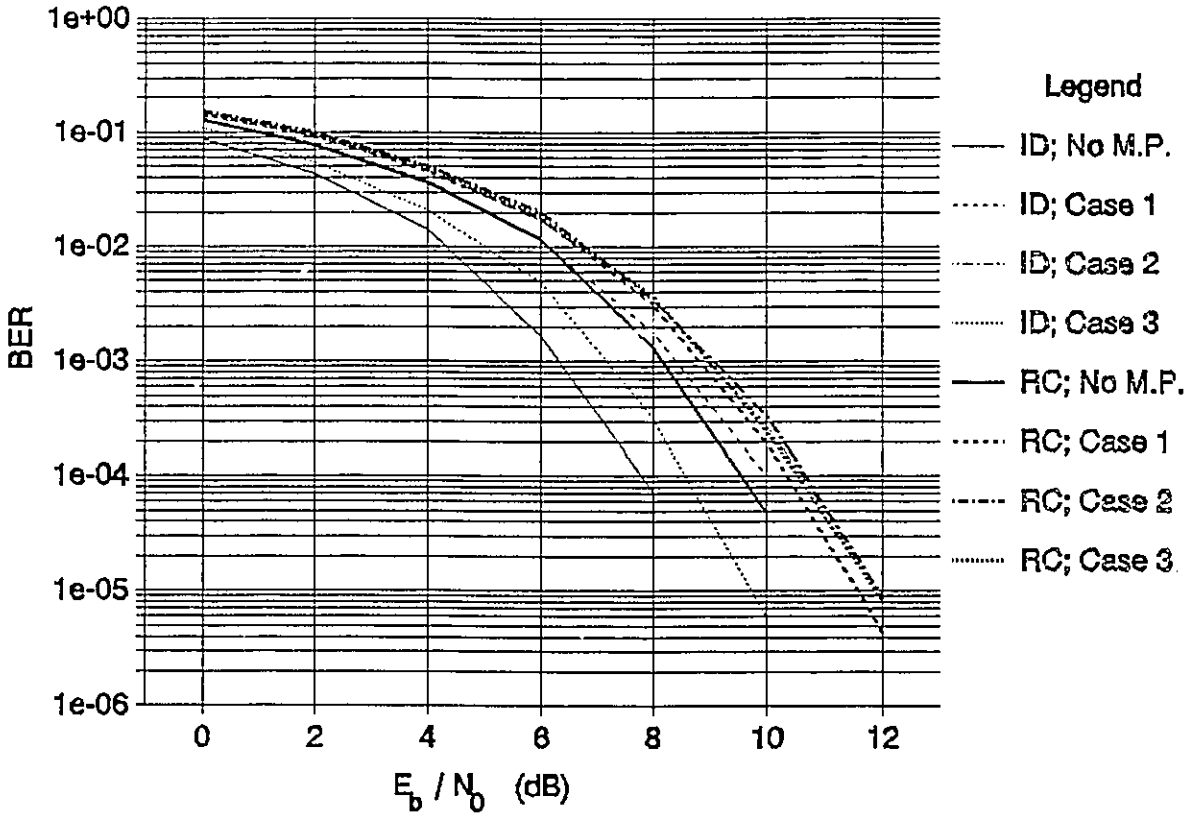

Figure 4.14 BER for 8B10B modulation using the Viterbi algorithm with soft-decision decoding. Different multipath cases and both the RC LPF and the ID filter have been included.

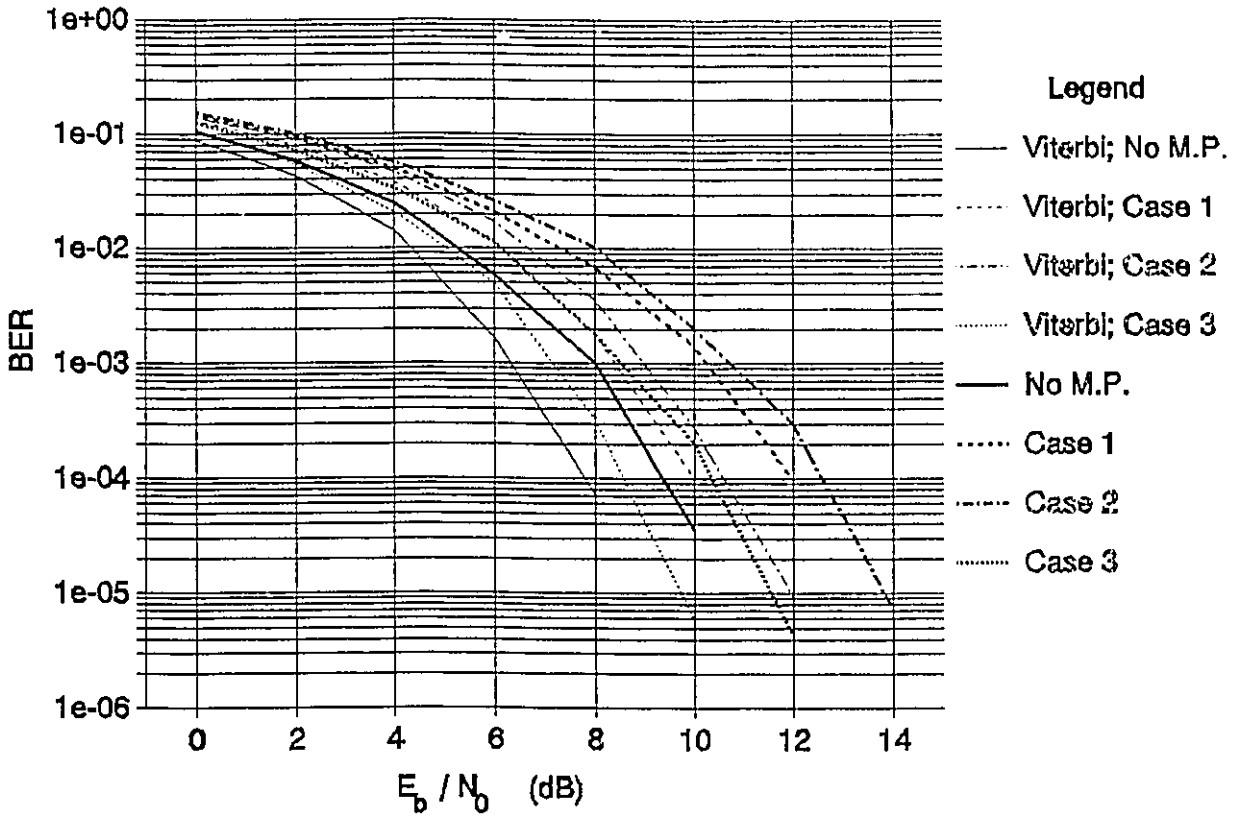

Figure 4.15 A comparison of BER for 8B10B modulation with and without applying the Viterbi algorithm. The ID filter has been used and different multipath cases have been included.

Chapter 5

Summary and Conclusions

In the previous chapters, we have looked at the various aspects of an in-theatre IR audio broadcasting system. A summary of the major material presented in this thesis, and the corresponding results are given in this section.

Infrared light has many advantages over radio frequency (RF) as the medium of transmission for an in-theatre audio broadcasting system; the most important one is that IR light is not in the regulated frequency range. A free-space IR transmission system with intensity modulation and direct detection has a particularly simple channel model. As a consequence of the fact that the photodetector area is much greater than the IR wavelength, the IR transmission channel can be replaced by an equivalent baseband transmission channel which simplifies the analysis of the system.

The diffuse infrared configuration (DIC) is power inefficient and suffers from multipath effects. For the in-theatre IR audio broadcasting system, we choose an IR transmission configuration in which a number of diffusing spots are created on the dome screen; the IR light is diffusively reflected back from these spots towards the audience

area in a theatre. It was shown that the received optical power varies greatly with position and the angular direction of the photodetector. These variations get smaller as the diffusing spots are placed further apart. So, the number of diffusing spots and their locations on the dome have to be chosen such that a compromise is made between reducing the variations of the received optical power and the effects of multipath dispersion on the performance of the system.

In the in-theatre multi-channel high-quality audio broadcasting system, the CD-based digital audio scheme has many advantages over the analog FM. A digital audio system can make use of powerful error correction coding techniques and a variety of available digital signal processing methods to improve the performance of the system. The signal-to-noise ratio and the dynamic range provided by the CD audio system are both more than 90 dB. The EFM channel coding used in the CD system performs very well in the CD optical channel which has a linearly falling characteristic. But EFM is no longer optimum for the in-theatre environment which has a different channel characteristic. EFM has a high redundancy and has to be replaced by a low redundant channel coding scheme to improve the performance of the system. The 8B10B channel modulation is a good candidate for replacing EFM because:

(i) it has a lower redundancy (1.29 vs 2.23 for EFM) and, thus, a lower transmitted channel bit rate;

(ii) it is easier to implement; and

(iii) it fits well with the other parts of the CD system.

We designed an appropriate code list of the 8B10B channel coding such that it has a small (RDS) variations and a limited high frequency content. We, also, gave simple implementations for the 8B10B coder and decoder.

The power density spectrums of the EFM and the 8B10B modulated signals were estimated. These spectrums showed that the low-frequency components of the signal in the case of 8B10B modulation is much smaller compared with EFM. A high-pass filter with a cut-off frequency of about 100 KHz has a negligible effect on the frequency content of the signal. Most of the low-frequency noise present in the system can thus be removed without affecting the quality of the received signal.

The Ambient light can produce significant shot noise at the receiver. We need to use optical filters to reduce the effects of the ambient light. An optical filter which blocks the visible part of the spectrum is used at the receiver, and another optical filter is used at the projector to attenuate the infrared portion of the projector light.

Silicon pin photodiodes are the most appropriate photodetector for use in battery-powered low-cost portable receivers in our system. Silicon photodiodes have a highly developed technology, low dark current, and high quantum efficiency.

A signal-to-noise ratio analysis for a pin-based receiver was carried out. This analysis showed that the *SNR* can be improved by increasing the photodetector area up to a certain point and the *SNR* will not change significantly beyond that point. In other words, there is an optimum value for the photodetector area. It was shown that the optimum signal-to-noise ratio, $(SNR)_{opt}$, is inversely proportional to B_c^3 where B_c is the channel bit rate. Thus, a channel coding scheme with a lower redundancy has a better performance (i.e., its transmitted optical power requirements are lower). The performance of 8B10B is better than EFM by 3.55 dB in terms of optical power (or 7.1 dB in electrical power). Based on this signal-to-noise ratio analysis, a simple procedure for choosing the receiver parameter values was proposed.

A link power budget calculation was performed to find the transmitted optical

power requirements of the in-theatre CD-based digital audio broadcasting system. For comparison purposes, the required transmitted optical power for an analog FM system was also computed. It was shown that the CD-based digital audio scheme has a large gain of around 32 dB in terms of optical power over the analog FM in the in-theatre audio broadcasting system.

Finally, a simulation was carried out to find the effects of the multipath dispersion on the performance of the system. The simulation results indicated that:

(i) 8B10B modulation requires less bandwidth compared with EFM;

(ii) the degradations due to the multipath dispersion are more severe in EFM than 8B10B modulation;

(iii) it would be sufficient to use a simple low-pass filter as the post detection filter at the receiver;

(iv) the reflections from the audience area do not necessarily result in a performance degradation; and

(v) Viterbi soft decision decoding provides only 1 dB optical gain in the case of 8B10B modulation. So, the complexity and the high-cost of the sophisticated detecting schemes can be avoided without losing much on the performance side.

5.1 Recommendations for Further Work

As a continuation of the work done in this thesis, further investigations in a number of areas could be suggested.

The optical characteristics of the theatre environment need to be looked at more carefully. For example, it would be necessary to perform some experimental measurements to find the ambient light intensity in a theatre, and to see how strong are the reflections from the audience area. An optimum IR transmission configuration was

not given in this thesis, some work would be required to optimize the number of spots and their locations on the dome.

The performance of 8B10B channel modulation in the CD-based in-theatre IR audio broadcasting system is very good because it has a low redundancy and it fits well with other parts of the CD system. A further research for finding a more suitable channel coding scheme would be interesting. There are certain channel coding schemes such as 5B6B or 16B17B which have a lower redundancy than 8B10B; but 5B6B does not operate on bytes and does not thus fit with other sections of the CD system, and the implementation of 16B17B would be complex and expensive.

As was said previously, some control bits for turning on and off the lenses of the audience glasses are required. The number of these bits is extremely small compared with the transmitted bit rate and we did not include them in our data format. Accommodating the control bits in the data format is another possible area for future work.

References

[1] F. R. Gfeller and U. Bapst, "Wireless in-house data communication via diffuse infrared radiation," *proc. IEEE*, vol. 67, no. 11, pp. 1474-1486, Nov. 1979.

[2] J. M. Kahn, J. R. Barry, M. D. Audeh, E. A. Lee and D. G. Messerschmitt, "Design of high-speed wireless links using nondirectional infrared radiation," *in Proc. Third WINLAB Workshop on Third Generation Wireless Information Networks*, East Brunswick, N.J., Apr. 1992.

[3] D. R. Pauluzzi, P. R. H. McConnell and R. L. Poulin, "Free-space undirected infrared (IR) voice and data communications with a comparison to RF systems," *in Proc. the Int. Conf. on Wireless Comm. 92*, pp. 279-285, June 1992.

[4] J. R. Barry, J. M. Kahn, E. A. Lee and D. G. Messerschmitt, "High-speed nondirective optical communication for wireless networks," *IEEE Net. Mag.*, pp. 44-54, Nov. 1991.

[5] M. D. Audeh and J. M. Kahn, "Performance simulation of baseband OOK modulation for wireless infrared LAN at 100 Mb/s," *in Proc. the Int. Conf. on Wireless Comm. 92*, pp. 271-274, June 1992.

[6] V. C. Georgopoulos and C. J. Georgopoulos, "A multiple IR/RF wireless transmission system for indoor and outdoor communications," *in IEEE Globecom'86 Conf. Rec.*, pp. 955-959, 1986.

[7] Y. Nakata, J. Kashio, T. Kojima and T. Noguchi, "In-house wireless communication system using infrared radiation," *in Proc. 7th Int. Conf. on Comp. Comm.*, Sydney, Australia, pp. 333-337, Nov. 1984.

[8] C. S. Yen and R. D. Crawford, "The use of directed optical beams in wireless computer communications," *in IEEE Globecom'85 Conf. Rec.*, New Orleans, pp. 1181-1184, Dec. 1985.

[9] T. S. Chu and M. J. Gans, "High speed infrared local wireless communications," *IEEE comm. Mag.*, pp. 4-10, Aug. 1987.

[10] A. Lessard and M. Gerla, "Wireless communications in the automated factory environment," *IEEE Net. Mag.*, pp. 64-69, 1973.

[11] H. Hashemi, G. Yun, M. Kavehrad and P. Galko, "Indoor propagation measurements at infrared optics for wireless local area networks applications," submitted for publication.

[12] G. Yun and M. Kavehrad, "Spot-Diffusing and fly-eye receivers for Indoor infrared wireless communications," *in Proc. the Int. Conf. on Wireless Comm. 92*, pp. 262-265, 1992.

[13] R. E. Patterson, J. Straus, G. Blenman and T. Witkowicz, "Linearization of multi-chanel analog optical transmitters by quasi-feedforward compensation technique," *IEEE Trans. Comm.*, vol. COM-27, no. 3, pp. 582-588, Mar. 1979.

[14] K. Asatani, "Nonlinearity and its compensation of semiconductor laser diodes for analog intensity modulation systems," *IEEE Trans. Comm.*, vol. COM-28, no. 2, pp. 297-300, Feb. 1980.

[15] K. Asatani and T. Kimura, "Analyses of LED nonlinear distortions," *IEEE Trans. Elect. Dev.*, vol. ED-25, no. 2, pp. 199-207, Feb. 1978.

[16] K. Asatani and T. Kimura, "Linearization of LED nonlinearity by predistortions," *IEEE Trans. on Elect. Dev.*, vol. ED-25, no. 2, pp. 207-212, Feb. 1978.

[17] J. B. H. Peek, "Communications aspects of the compact disc digital audio system," *IEEE Comm. Mag.*, pp. 7-15, Feb. 1985.

[18] M. G. Carasso, J. B. H. Peek and J. P. Sinjou, "The compact disc digital audio system," *Phillips Tech. Rev.*, vol. 40, pp. 151-155, 1982.

[19] J. P. J. Heemskerk and K. A. S. Immink, "Compact disc: system aspects and modulation," *Phillips Tech. Rev.*, vol. 40, pp. 157-164, 1982.

[20] H. Hoeve, J. Timmermans and L. B. Vries, "Error correction and concealment in the compact disc systems," *Phillips Tech. Rev.*, vol. 40, pp. 166-172, 1982.

[21] D. Goedhart, R. J. Van de plassche and E. F. Stikvoort, "Digital-to-analog conversion in playing a compact disc," *Phillips Tech. Rev.*, vol. 40, pp. 174-179, 1982.

[22] K. B. Benson, *Audio Engineering Handbook,* McGraw-Hill, N.Y., 1988.

[23] H. Nakajima, T. O. J. Fukura and A. Iga, *,Digital Audio Technology,* TAB Books Inc., 1983

[24] H. G. Musmann, "The ISO Audio Coding Standard," *in IEEE Globecom'90 Conf. Rec.*, vol. 1, pp. 511-517, 1990.

[25] P. S. Lidbetter, "The MADI format: Applications and Implementations in the digital studio," *Proc. AES 7th Int. Conf.*, pp. 251-261, 1989.

[26] A. X. Widmer and P. A. Franaszek, "Transmission code for high-speed fiber-optic data networks," *IEE Elect. Let.*, vol. 19, no. 6, pp. 202-203, Mar. 1983.

[27] R. Petrovic, "Low redundancy optical fiber line code," *J. Optical Comm.*, vol. 9, pp. 108-111, Sep. 1988.

[28] M. Rousseau, "Block codes for optical-fiber communications," *IEE Elect. Let.*, vol. 12, no. 18, pp. 478-479, Sep. 1976.

[29] A. V. Oppenheim and R. W. Schafer, *Discrete-Time Signal Processing*, Prentice Hall, N. J., 1989.

[30] J. G. Proakis, *Digital Communications*, McGraw-Hill, N.Y., 2nd Ed., 1989.

[31] A. B. Carlson, *Communication Systems*, McGraw-Hill, N.Y., 3rd Ed., 1986.

[32] S. D. Personik, "Receiver design for digital fiber optic communications systems, I and II," *Bell Syst. Tech. J.*, vol. 52, pp. 843-886, 1973.

[33] G. Keiser, *Optical Fiber Communications*, McGraw-Hill, N.Y., 2nd Ed., 1991.